THE ROLE OF CUTANEOUS INNERVATION IN THE SENSORY ABNORMALITIES ASSOCIATED WITH DIABETIC NEUROPATHY

By

Megan S. Johnson

Submitted to the graduate degree program in Anatomy & Cell Biology
and the Graduate Faculty of the University of Kansas in partial fulfillment of the
requirements for the degree of Doctor of Philosophy

Dissertation Committee:

_____
Douglas E. Wright, Ph.D
Committee Chairperson

_____
Ronal M. MacGregor, Ph.D

_____
Kenneth E. McCarson, Ph.D

_____
Peter G. Smith, Ph.D

_____
Michael J. Werle, Ph.D

Date defended: April 17, 2008

Table of Contents

I. Acceptance Page

The Dissertation Committee for Megan S. Johnson certifies
that this is the approved version of the following dissertation:

THE ROLE OF CUTANEOUS INNERVATION IN THE SENSORY ABNORMALITIES ASSOCIATED WITH DIABETIC NEUROPATHY

Dissertation Committee:

_____
Douglas E. Wright, Ph.D
Committee Chairperson

_____
Ronal M. MacGregor, Ph.D

_____
Kenneth E. McCarson, Ph.D

_____
Peter G. Smith, Ph.D

_____
Michael J. Werle, Ph.D

Date approved: April 30, 2008

II. Acknowledgements

My greatest debt is to Dr. Douglas E. Wright, whose mentorship and guidance have challenged me and shaped my scientific thinking. Thank you for providing the opportunity, environment, and support that allowed such autonomy and encouraged my scientific growth. Truly, this graduate school process should not have been as fun as it has been, and I am sincerely grateful to have experienced the perfect combination of freedom and excellence in education.

Each of the past and present members of the Wright lab has contributed here, not just scientifically, although their help on projects has been extensive, but also with their friendship. More space than is allowed would be required to enumerate the lessons I have been taught by each of these gifted people, but Janelle, Rohan, Susan, Neena, Melinda, and Karra, you each have meant something unique and special to me, and I am a better person for having known each of you.

Thank you as well to the members of my dissertation committee, Dr. Ronal M. MacGregor, Dr. Kenneth E. McCarson, Dr. Peter G. Smith, and Dr. Michael J. Werle, for their guidance the past five years. I value your input and insight into this work, and have appreciated your time. Thank you for treating me like a scientist.

Other acknowledgements include Dr. David Anderson for providing the original MrgD breeding pairs; Dr. Hiroshi Nishimune for microscope usage; and our collaborators in the General Clinical Reseach Center and the KU Neurology Department including Dr. Mamatha Pasnoor, Dr. Richard Barohn, and Laura Herbelin. I am also deeply appreciative of the financial and developmental support of the Madison & Lila Self Graduate Fellowship and its staff.

Finally, to my family adequate gratitude cannot be expressed. You have provided the firm foundation on which I have built my life, and all things have been made possible because of your love and legacy. Michael, Debby, Meredith, Melinda, Rod, kiddos, Kenneth, Nellie, Geraldine, and all of the Johnsons: I delight in you and treasure our times together. Grant Troy Johnson: you are my home base. My strength and clarity of mind are renewed with you. Thank you for your devotion and love, which have sustained me the last five years and been my source of joy.

III. List of Tables and Figures

Tables

Figures

IV. Abstract

Diabetes-induced nerve damage results in cutaneous denervation, nerve conduction slowing, suppressed regenerative responses, and debilitating painful or insensate sensory symptoms. The increasing prevalence of diabetic neuropathy and its persistent treatment difficulties justify continued study into the mechanisms underlying the disease and the exploration of animal models useful for assessing its complications. The purpose of this study was to elucidate the relationship between cutaneous nerve fiber density and the presence of neuropathy and its accompanying symptoms. Experiments were conducted in various animal models of diabetes and in diabetic human patients.

To explore mechanisms underlying insensate neuropathy, we evaluated behavioral responses to noxious stimuli in three animal models. Diabetic mice consistently displayed decreased sensitivity and hypoalgesia, indicative of insensate neuropathy. We also assessed peripheral innervation both indirectly, via spinal Fos expression, and directly, by quantifying footpad innervation. The diabetes-induced behavioral responses were paralleled by progressive reductions in dorsal horn activation by peripheral afferents. In contrast, direct quantification of peripheral fibers did not reveal deficits in total nerve fiber density. However, a subpopulation-specific reduction was found; peptidergic c-fibers were preferentially lost early in the diabetes progression, and their loss correlated with loss of nociceptive sensitivity. These results suggest that diabetes-induced behavioral deficits are more closely associated with the peptidergic, rather than the nonpeptidergic, subpopulation, underscoring the importance of peptidergic fibers in pain sensation.

In addition, human diabetic and nondiabetic subjects were recruited and tested for measures of sensory nerve fiber function and evaluated for cutaneous nerve fiber density. While both epidermal and dermal nerve densities were highly specific and sensitive measures for diagnosing diabetic neuropathy, correlations with sensory measures were varied, and nerve fiber density could only account for at most 60% of the variability in any given neuropathic symptom.

Collectively, results from the animal and human investigations demonstrate there are subtle disconnects in the degree to which nerve fiber density indicates pain sensitivity. Future studies should be directed toward understanding other mechanisms important in nociception during neuropathic disease. In addition, before nerve fiber density is relied upon as an outcome measure of treatment efficacy, the ability of cutaneous innervation to predict pain or lack of pain in human subjects should be addressed.

V. Chapter One:

Introduction

1. Diabetic Neuropathy

Prevalence

Diabetes mellitus is a variable, multi-system metabolic disorder caused by a combination of genetic and environmental factors and characterized by inadequate production or utilization of insulin and hyperglycemia. The International Diabetes Federation reports the total number of people with diabetes worldwide increased over the last 20 years from 30 million to 230 million. In 2005, approximately 5% of the United States population had diabetes, with an additional 2% estimated to be affected but undiagnosed (National Institute of Diabetes and Digestive and Kidney Diseases 2005). With the rapid rise of the disease, the burden of diabetes and its complications on health care systems and national economies around the world is also increasing, and in the United States an estimated $130 billion is spent in direct and indirect costs each year (Hogan et al. 2003).

Diabetes mellitus encompasses two distinct disease classifications segregated based on etiology. In both instances, normal insulin signaling as depicted in **Figure V-1** is disrupted. In type 1 diabetes, the disruption is caused by selective autoimmune destruction of pancreatic beta cells in the islets of Langerhans, resulting in deficient insulin production. Type 1 diabetes affects 5-10% of diabetic patients and generally presents at a younger age of onset (Low et al. 2004). Type 2 diabetes, accounting for 90-95% of diabetic patients, is the result of insulin resistance in peripheral tissues and inadequate compensatory insulin secretion. Mechanisms of insulin resistance include down-regulation of insulin receptors (IRs), faulty phosphorylation of insulin receptor

Figure V-1: Insulin Homeostasis

(A) Beta cells in the pancreatic islets of Langerhans release insulin in response to increased blood glucose levels. Glucose enters beta cells via the GLUT2 glucose transporter and leads to the transcription and translation of insulin mRNA. Mature insulin is synthesized from the precursor molecule proinsulin by protease cleavage of the center portion of the protein (C-peptide) by carboxypeptidase E. The remaining two polypeptides (51 amino acids in total) are bound together by disulfide bonds. Mature insulin molecules are stored in secretory vesicles until release into the bloodstream, an event also triggered by rising intracellular glucose concentrations.

(B) Insulin signaling leads to the uptake of glucose from the bloodstream into cells. The insulin receptor (IR) is composed of two extracellular alpha-domains and two transmembrane beta-domains. Insulin binding to the IR alpha-subunits leads to autophosphorylation of the IR beta-subunits and the subsequent tyrosine phosphorylation of insulin receptor substrates such as IRS-1 by the IR tyrosine kinase. IRS-1 then phosphorylates the SH2 domain of phosphatidylinositol 3-kinase (PI3K), thereby increasing the intracellular concentration of phosphatidylinositol 3-phosphate (PIP-3). This, in turn, activates phosphatidylinositol-dependent kinase 1 (PDK-1), which subsequently activates the serine/threonine kinase Akt via phosphorylation. This results in the translocation of cytoplasmic vesicles containing GLUT4 glucose transporters to the cell membrane, where they allow glucose entry into the cell. (Bevan 2001; Kido et al. 2001; Watson and Pessin 2001)

Figure V-1

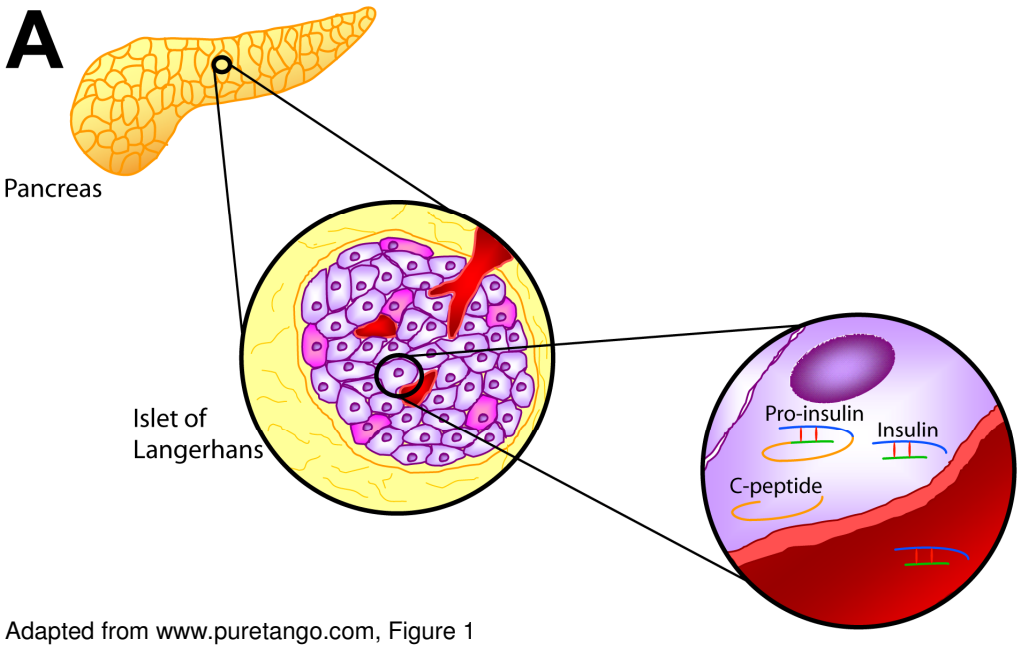

Adapted from www.puretango.com, Figure 1

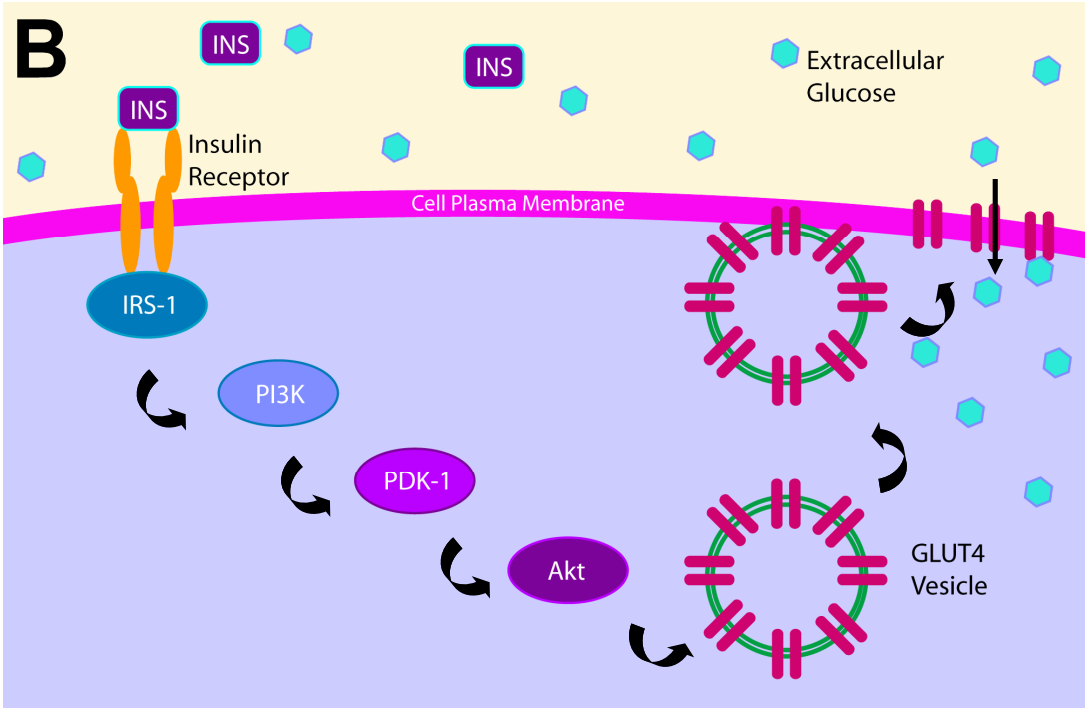

substrates (IRS; Dobretsov et al. 2007), or deficits in the translocation of the GLUT4 insulin-dependent glucose transporter (McCarthy et al. 2006; Brozinick et al. 2007). Although both types have a strong genetic component, type 2 diabetes is often associated with older age, obesity, and lack of physical activity. It is estimated that 80% of type 2 diabetes is preventable through lifestyle changes.

The rapid rise in diabetes is an alarming trend, particularly because the severity of diabetic complications is correlated with the duration of the disease. Serious complications of both types of diabetes include heart disease, nephropathy leading to kidney failure, and retinopathy with the potential for vision loss. The most common long-term complication is damage to peripheral nerves, termed neuropathy, which leads to the greatest diabetes-associated morbidity and mortality (Vinik et al. 2000) and dramatically impacts quality of life. It is estimated that anywhere from 30-100% of diabetic patients experience some form of nerve damage, ranging from mild to severely disabling (Quattrini and Tesfaye 2003; Sinnreich et al. 2005; Tesfaye and Kempler 2005). Evidence of neuropathic abnormalities has even been found in people with prediabetes, or metabolic syndrome (Singleton et al. 2001b; Smith et al. 2006; Yagihashi et al. 2007; Smith and Singleton et al. 2008).

Mechanisms

Many theories have been posited as to the exact manner in which a prolonged hyperglycemic environment contributes to nerve damage. First, for a number of reasons peripheral neurons are inherently vulnerable to metabolic disturbances such

as high blood glucose (McHugh and McHugh 2004). For example, neurons utilize an insulin-independent glucose transporter and hence do not require insulin for glucose uptake (Dobretsov et al. 2007); therefore, intracellular glucose concentrations fluctuate with glucose concentrations in the surrounding extracellular milieu. In addition, peripheral nerve fibers have a characteristic morphology that presents unique challenges for overcoming metabolic disturbances (McHugh and McHugh 2004). A vast amount of plasma membrane, proteins and cytosolic components must be maintained throughout the length of the axon by a distant cell body, located up to a meter away in the longest axons. Finally, peripheral nerves exist outside the protection of any barrier afforded to neurons in the CNS.

Mechanisms involving both direct and indirect metabolic effects of hyperglycemia on neurons have been proposed, and it is evident that both likely contribute to nerve deficits (Thomas 1999). When high levels of glucose accumulate within the neuron, glycolysis pathways (the normal fate of glucose) become overwhelmed and glucose is shunted into other pathways that lead to neurotoxicity (for comprehensive reviews, see Thomas 1999; McHugh and McHugh 2004; Vincent et al. 2004; Vincent and Feldman 2004; Pop-Busui et al. 2006; Tomlinson and Gardiner 2008). For example, excess conversion of glucose to sorbitol via the enzyme aldose reductase generates an abundance of sorbitol which presents osmotic challenges to the cell and depletion of normal corrective osmolytes. Furthermore, aldose reductase is one of many competitors for the electron donor NADPH. Its excessive use diminishes the activity of glutathione reductase and thus reduces the

production of glutathione, an important antioxidant and free radical scavenger. This is particularly problematic because free radicals, especially the superoxide ion, are generated in excess with increased glucose oxidative metabolism. Excess glucose molecules can also form advanced glycated end products (AGEs) by reacting with reactive aldehyde groups on proteins and disrupting their normal structure, function, and metabolism. Not only is the normal function of these glycated proteins lost, leading to impaired cellular function, but AGE accumulation can eventually overwhelm the cell's ability to recycle them, and signaling via the AGE receptor (RAGE) activates pro-inflammatory NFκB signaling pathways. Finally, decreased neurotrophic support may also contribute to neuronal dysregulation. Neurons depend on nerve growth factors for survival during development, and throughout adulthood these molecules provide important survival, growth, and differentiation signals. Diabetes-induced decreased expression of growth factors in target tissues, decreased expression of growth factor receptors on neuronal terminals, or decreased retrograde transport would all lead to detrimental changes in gene expression and neuronal function.

All of the aforementioned metabolic disturbances can also occur in Schwann cells, resulting in segmental demyelination and reduced nerve regeneration capacity (Jaffey and Gelman 1996; Eckersley et al. 2001; Dobrowsky et al. 2005), and cells of the endoneurial blood vessel walls, leading to reduced endoneurial blood flow and thus nutrient and oxygen deprivation (Dobretsov et al. 2007). All of the above distinct proposed mechanisms, whether primary neuronal damage or damage

secondary to glial or vasculature abnormalities, converge on the critical role of oxidative stress within the neuron as leading to loss of function (Vincent and Feldman 2004; Bitar et al. 2005; Pop-Busui et al. 2006). Eventually functional changes overcome neurons' ability to compensate and progressively lead to irreversible structural changes (Boucek 2006), and the neuron is unable to maintain its distal axons (Thomas 1999).

Presentation

Although diabetic patients are also susceptible to focal lesions of any nerve type, the nature of diabetes-induced nerve damage generally results in distal axonal degeneration in a dying-back, length-dependent fashion with relative preservation of neuronal cell bodies in the dorsal root ganglia (Thomas 1999; Said 2007). Axonal loss can also be accompanied by segmental demyelination (Jaffey and Gelman 1996) and reduced nerve regeneration capacity (Kennedy and Zochodne 2000 and 2005; Polydefkis et al. 2004). Together these structural changes can result in reduced innervation, decreased nerve conduction velocities, and reduced amplitude of nerve action potentials (Sinnreich et al. 2005), all hallmark features of clinical diabetic neuropathy. Diabetic neuropathies are generally symmetric and can impact autonomic nerves, resulting in gastroparesis, impotence, incontinence, and orthostatic hypotension; and motor nerves, leading to muscle weakness or wasting and loss of reflexes. However, the most common and best recognized form of DN is sensory

neuropathy resulting from deficits to small sensory nerve fibers (Thomas 1999; Sinnreich et al. 2005).

Interestingly, the sensory symptoms resulting from neuropathic damage to sensory fibers can manifest as insensate, painful, or both (Sorensen et al. 2002; Yagihashi et al. 2007). Sensory loss develops in the majority of affected DN patients, including both chronic numbness and insensitivity to pain or touch. Painful symptoms are only reported in up to 32% of patients with DN, are most likely to present early in the disease progression, and have a slightly higher prevalence in type 2 diabetes (Low and Dotson et al. 1998; Schmader 2002; Sorensen et al. 2002; Quattrini and Tesfaye 2003; Argoff et al. 2006). These painful symptoms can include evoked (hyperalgesia, tactile allodynia) or spontaneous (paresthesias, burning sensations, aching) manifestations (Argoff et al. 2006; Dobretsov et al. 2007). Interesting, many patients often present with both numbness and pain; in one study, ~12% of patients with insensate neuropathy also had neuropathic pain, and ~61% of patients with painful neuropathy had decreased vibration perception (Sorensen et al. 2002).

Although pain may be the most distressing symptom, it is the insensate component that leads to the morbidity associated with neuropathy (Sorensen et al. 2002; Tesfaye and Kempler 2005). The loss of protective sensation increases the risk of foot wounds (Tomlinson and Gardiner 2008); combined with slower healing rates of diabetic patients, clinical consequences can include foot ulcers, gangrene, and

amputation. The mechanisms underlying the development of either painful versus insensate symptoms remain unclear.

Treatment

Currently the most effective treatment for diabetic neuropathy is maintaining strict glycemic control, which can prevent but not restore damaged nerves (The Diabetes Control and Complications Trial Research Group 1995; Navarro et al. 1997; Boucek 2006; Sullivan et al. 2008). However, it has been reported that consistent euglycemia can only be achieved by approximately 25% of patients (Thomas 1999). Numerous drug targets are prescribed to manage painful symptoms and include opioids, gabapentin-based antiepileptics, and antidepressants (reviewed in Casellini and Vinik 2007; Chong and Hester 2007). In addition, many drugs intended to minimize the effects of hyperglycemia on peripheral nerves showed promising results in rodent models, including growth factors (VEGF, Chattopadhyay et al. 2005; NT-3, Huang et al. 2005 and Chattopadhyay et al. 2007; NGF, Apfel et al. 1994; Christianson et al. 2003a, b), antioxidants (Berryman et al. 2004; Song et al. 2005; Pitel et al. 2007), AGE inhibitors (Thomas 1999; Metz et al. 2003; Cameron et al. 2005), and aldose reductase inhibitors (Kuzumoto et al. 2006; Obrosova et al. 2007). However, to date none of these have been successful in large scale clinical trials at improving cutaneous innervation or other clinical signs of neuropathy (Thomas et al. 1999; Apfel 2000; Wellmer et al. 2001; Chalk et al. 2007; Calcutt et al. 2008; Vincent

et al. 2008). In order to develop more efficacious therapeutics, the field still requires a better understanding of the spectrum of mechanisms underlying these conditions.

2. Rodent Models of Diabetic Neuropathy

Existing animal models of diabetes vary in their presentation of neuropathy symptoms. Currently, behavioral responses to noxious stimuli are used to ascertain the somatosensory status of rodents. An increase in nocifensive responses is interpreted as hyperalgesia or allodynia, while a decrease indicates hypoalgesia, or insensitivity. Although these measures are inherently subjective, in the absence of self-report they are the best tools available for determining pain status in rodents.

Both genetic and drug-induced models exist (Calcutt 2004). Streptozotocin (STZ) is commonly used to induce diabetes in rodents because of its specific toxic effects on pancreatic beta cells (Konrad et al. 2001), thus mimicking a type 1 etiology. In several strains of rats, STZ-induced diabetes causes mechanical, thermal, and chemogenic hyperalgesia as well as tactile and thermal allodynia (Calcutt 2004). Hyperalgesia also develops in genetic rat models of type 1 and type 2 of diabetes, such as the autoimmune-initiated BioBreeding diabetic rats (Gabra et al. 2005), Zucker diabetic fatty rats (Zhuang et al. 1997; Piercy et al. 1999; Li et al. 2006), and the Otsuka Long-Evans Tokushima fatty rat (Kamenov et al. 2006). These sensory abnormalities reflect the painful aspect of human diabetic neuropathy, yet do not model the insensate symptoms suffered by the majority of human patients.

By contrast, either painful or insensate neuropathy can develop in diabetic mice, depending on the strain. STZ-treated C57BL/6 mice, a model of type 1 diabetes, display reduced sensitivity to mechanical, chemogenic, and, in some cases, thermal stimuli (Chen and Pan 2002; Christianson et al. 2003b; Walwyn et al. 2006; Johnson et al. 2007). However, we have recently shown that STZ-treated A/J mice develop increased sensitivity to the same mechanical stimulus (**Figure V-2**; unpublished observations). Similarly, non-obese diabetic (NOD) mice, a model of autoimmune type 1 diabetes, rapidly develop thermal hyperalgesia. This dichotomy is also seen in models of obesity and type 2 diabetes. While leptin knockouts (*ob/ob* mice) and the spontaneously occurring Tsumura Suzuki Obese Diabetes (TSOD) mice develop mechanical hypersensitivity (Iizuka et al. 2005; Drel et al. 2006; Vareniuk et al. 2007; unpublished observations), leptin receptor knockouts (*db/db* mice) display mechanical and chemogenic hypoalgesia (**Figure V-2**; Wright et al. 2007). Interestingly, both thermal hypoalgesia and tactile allodynia develop in normoglycemic C57BL/6 mice with impaired glucose tolerance induced by a high fat diet (Obrosova et al. 2007).

By taking advantage of the different neuropathies displayed by diabetic mouse models we can explore mechanisms underlying the development of painful versus insensate neuropathy. Rodent studies described in this work utilize the STZ-injected C57BL/6 model to investigate insensate neuropathy. By better appreciating the mechanisms underlying the development of these symptoms, we hope these results will lead to novel therapeutics for human sufferers.

Figure V-2: Insensate and painful models of type 1 and 2 diabetic neuropathy

(A,B) Behavioral responses to mechanical stimuli were evaluated weekly in nondiabetic (n = 5-6) and STZ-induced diabetic (n = 7-9) mice. **(A)** By 4 weeks post-STZ, diabetic C57Bl/6 mice responded significantly fewer times to a 1 gm monofilament than nondiabetic mice, consistent with reduced mechanical sensitivity. **(B)** STZ-induced diabetic A/J mice responded significantly more frequently to a 1 gm monofilament than their nondiabetic counterparts, consistent with tactile allodynia. Data plotted as means ± SEM. * denotes significance from vehicle-injected mice ($p < 0.05$).

(C,D) Behavioral responses to mechanical stimuli were evaluated at 12 weeks of age (after 8 weeks of chronic hyperglycemia) in nondiabetic (n = 5-6) and diabetic (n = 7-9) mice. **(C)** 12 week old *db/db* mice responded significantly fewer times to a 1 gm monofilament than their nondiabetic counterparts, consistent with mechanical insensitivity. **(D)** In contrast, diabetic *ob/ob* mice responded significantly more times to a 1 gm monofilament than did nondiabetic mice, consistent with tactile allodynia. Data plotted as means ± SEM. * denotes significant from strain-matched nondiabetic littermates ($p < 0.05$).

NOTE: Diabetic mice shown on the right in each frame.

Figure V-2

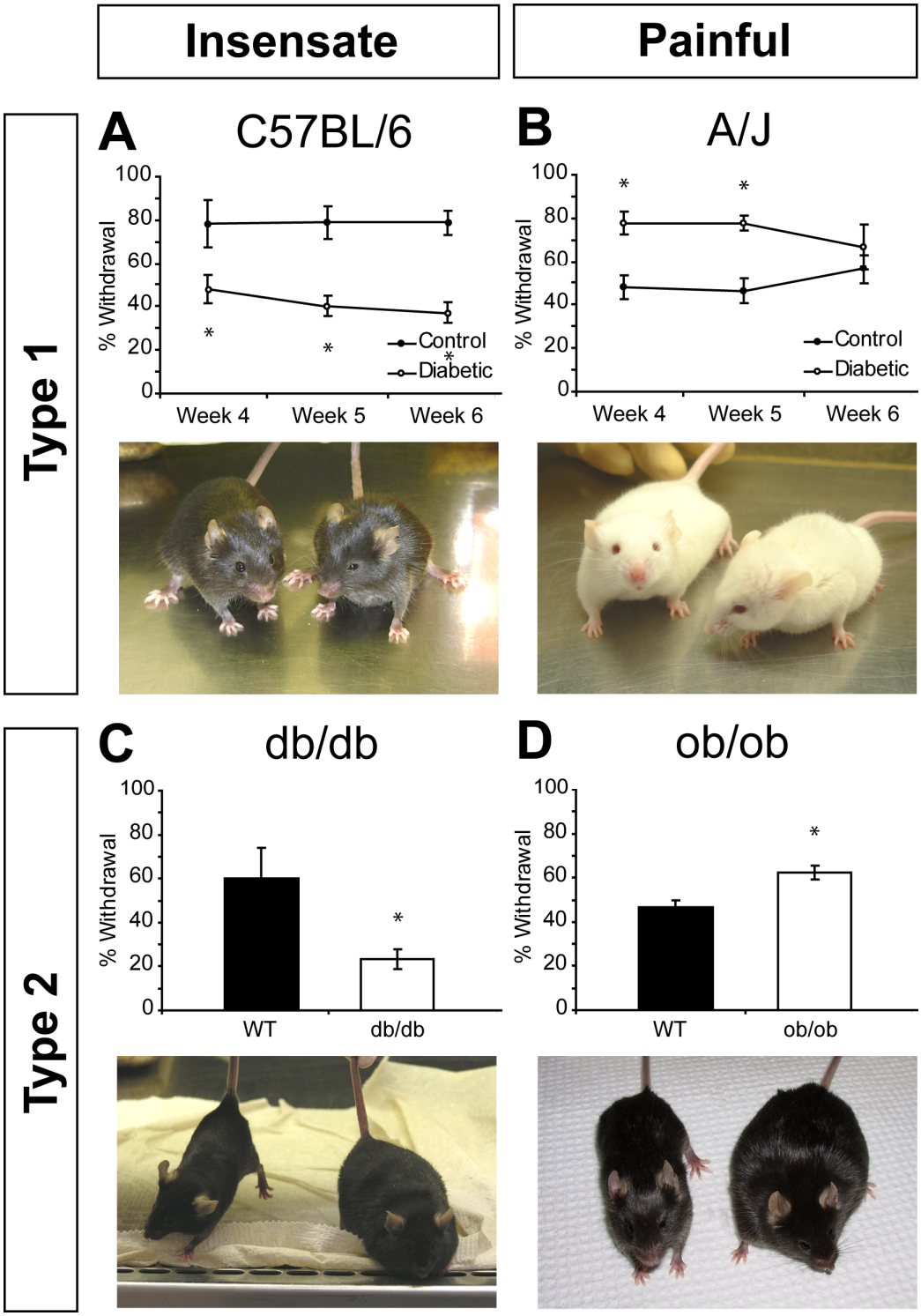
Insensate
Painful
Type 1
Type 2
A
C57BL/6
B
A/J
% Withdrawal
100
80
60
40
20
0
Week 4
Week 5
Week 6
Control
Diabetic
C
db/db
D
ob/ob
WT
db/db
ob/ob

3. Cutaneous Sensory Afferents

Cutaneous primary sensory neurons transduce our physical interactions with the external environment into electrical information, and are the first relay in the path to conscious sensations. These pseudounipolar neurons have cell bodies housed in dorsal root ganglia (DRG), central projections synapsing on second order neurons in the dorsal horn of the spinal cord, and peripheral projections terminating in target end organs. Cutaneous afferents are categorized based on their morphological, anatomical, and biochemical distinctions, as well as the modality of sensation they transmit.

Cutaneous sensory axons with the largest diameter (6-12 μm) and the greatest amount of myelin are called Aβ fibers. Because of their large diameter and heavy myelin content, these fibers transmit electrical information rapidly (35-75 m/s). Aβ fibers innervate a variety of specialized end structures called sensory receptors. The cells of the receptors together with the nerve fibers physically transduce mechanical deformations of the skin into electrical signals and subsequent neuronal action potentials. The modality of sensation transmitted depends on the location and type of end receptor. For example, Pacinian corpuscles confer upon Aβ fibers the ability to transmit deep touch and high-frequency vibration information, while Aβ fibers contacting Meissner corpuscles transmit the modality of low-frequency vibration. Other receptor types innervated by Aβ fibers include Merkel cells, which respond to light touch, and Ruffini's endings, which are sensitive to pressure and skin stretch.

Aδ fibers are smaller in diameter (1-5 μm) than Aβ fibers and are less heavily

myelinated, thus transmitting with a slower conduction speed (5-35 m/s). Aδ fibers respond to low- and high-threshold mechanical stimuli, depending on whether the fiber is associated with a hair follicle (Downy-hair fibers) or terminates as a free nerve ending, in addition to thermal and chemogenic stimuli (Traub and Mendell 1988). Aδ fibers respond to noxious stimulation, and are responsible for first, "fast" pain.

C-fibers are small in diameter (< 1.5 μm) and unmyelinated. These nociceptive neurons respond to mechanical, thermal, and chemical stimuli and are thus termed polymodal. C-fibers are responsible for the second, "slow" pain and conduct with a velocity of less than 2 m/s. These fibers are the focus of this work, so great attention will be paid in describing them here.

Two largely non-overlapping classes of C-fiber nociceptors have been identified and characterized based on their trophic factor requirements, biochemical phenotypes, and terminations (Nagy and Hunt 1982; Hunt and Rossi 1985; Molliver et al. 1997; Snider and McMahon 1998; Braz et al 2005). Peptidergic nociceptors express CGRP and substance P, neuropeptides classically considered important in pain transmission, and respond to nerve growth factor (NGF) via the expression of TrkA during development and throughout adulthood. Nonpeptidergic nociceptors are sensitive to NGF during development, but gradually downregulate TrkA beginning at post-natal day 1 (Molliver and Snider 1997) and concomitantly increase expression of Ret (Molliver et al. 1997), the GDNF receptor, thereby switching neurotrophic dependence from NGF to GDNF by post-natal day 21. GDNF-responsiveness

continues through adulthood. During adulthood, these neurons are experimentally recognized by their binding of the *Griffonia simplicifolia* lectin IB-4 and their expression of the P_2X_3 ATP receptor as well as thiamine monophosphatase (TMP), but do not express CGRP or Substance P.

Marked topographical segregation between these 2 nociceptive subpopulations exists peripherally via distinct peripheral terminations in the epidermal strata (Zylka et al. 2005); centrally with segregated spinal termination zones in the dorsal horn (Molliver et al. 1995); and at higher neural levels by engaging separate ascending pathways of pain circuitry (Braz et al. 2005; **Figure V-3**). Finally, these 2 nociceptive subpopulations also differ in their electrophysiological properties (Stucky and Lewin 1999) and neurochemical expression (Bradbury et al. 1998; Fang et al. 2006; Choi et al. 2007). Collectively, these differences argue for the existence of separate but parallel pain pathways originating from nonpeptidergic and peptidergic nociceptive neurons (Hunt and Mantyh 2001; Braz et al. 2005; Zylka et al. 2005).

The functional relevance of these parallel pain pathways has been surprisingly difficult to establish. Behavioral studies using selective knockdown approaches (Vulchanova et al. 2001, Vierck et al. 2003) have not clearly revealed modality-specific differences, although recent studies suggest that discriminative versus affective components of pain are differentially transmitted by the peptidergic and nonpeptidergic pathways, respectively (Braz et al. 2005; Zylka 2005). Only recently have studies begun to address how these populations are associated with various pain

states induced by disease or injury (Malmberg et al. 1997; Hammond et al. 2004). Furthermore, prior to this dissertation, a subpopulation-specific evaluation of the impact of diabetes in relation to symptomology had not been addressed.

4. Epidermal Innervation in Diabetic Neuropathy

Diabetic neuropathy can impact all of the aforementioned fiber types, resulting in a variety of symptoms. Deficits in cutaneous innervation are now consistently observed in rodent models of diabetes. Interestingly, this loss occurs in both painful and insensate states. For example, perhaps not unexpectedly, diabetic mice with hypoalgesia display decreased cutaneous innervation (Christianson et al. 2003b; Chattopadhyay et al. 2005; Tamura et al. 2006; Chattopadhyay et al. 2007; Christianson et al. 2007), with some studies reporting up to a 78% loss of epidermal nerve fibers (*ob/ob* mice; Drel et al. 2006; Vareniuk et al. 2007). However, reductions ranging from 33% to 47% have also been reported in diabetic rats (Bianchi et al. 2004; Lauria et al. 2005b; Obrosova et al. 2008), which develop mechanical hyperalgesia and allodynia. Proposed explanations for the seemingly incongruous presence of hyperalgesia/allodynia and reduced peripheral input in rats include diabetes-induced increased responsiveness of remaining c-fibers (Wu et al. 2001; Suzuki et al. 2002; Wu et al. 2002), sensitization of spinal neurons (Pertovaara et al. 2001; Chen and Pan 2002), and upregulation of spinal nociceptive mediators such as Substance P (Calcutt et al. 2000; Freshwater et al. 2002; Ciruela et al. 2003; Calcutt et al. 2004; Tomiyama et al. 2005; Dualhac et al. 2006).

Figure V-3: Nociceptive Subpopulations

(A) Peripheral projections of nociceptive nerve endings are topographically and morphologically separated in the epidermis. Nonpeptidergic fibers (green) predominantly course straight through underlying strata, then exhibit a tortuous, meandering pattern prior to terminating among keratinocytes of the stratum granulosum. In contrast, peptidergic fibers (red) course more directly and terminate in the stratum basalis or spinosum.

(B) Both peptidergic and nonpeptidergic fibers terminate centrally in the substantia gelatinosa of the spinal cord dorsal horn. However, the central terminals of these subpopulations are highly segregated. Peptidergic fibers synapse on second order neurons in Lamina I and outer portions of Lamina II (Lamina II_o), while nonpeptidergic neurons terminate on neurons of inner Lamina II (Lamina II_i).

(C) Peptidergic and nonpeptidergic subpopulations of nociceptors engage separate ascending pathways of pain circuitry. The central neural circuit originated by peptidergic neurons is assocated with sensory/discriminative aspects of pain and includes the parabrachial nucleus and the ventroposterolateral nucleus of the thalamus. By contrast, nonpeptidergic circuitry seems to be directed through Lamina 5 of the spinal cord to limbic brain regions associated with motivational/affective components of pain, such as the globus pallidus, amygdala, ventromedial nucleus of the hypothalamus, and bed nucleus of the stria terminalis (BNST).

Figure V-3

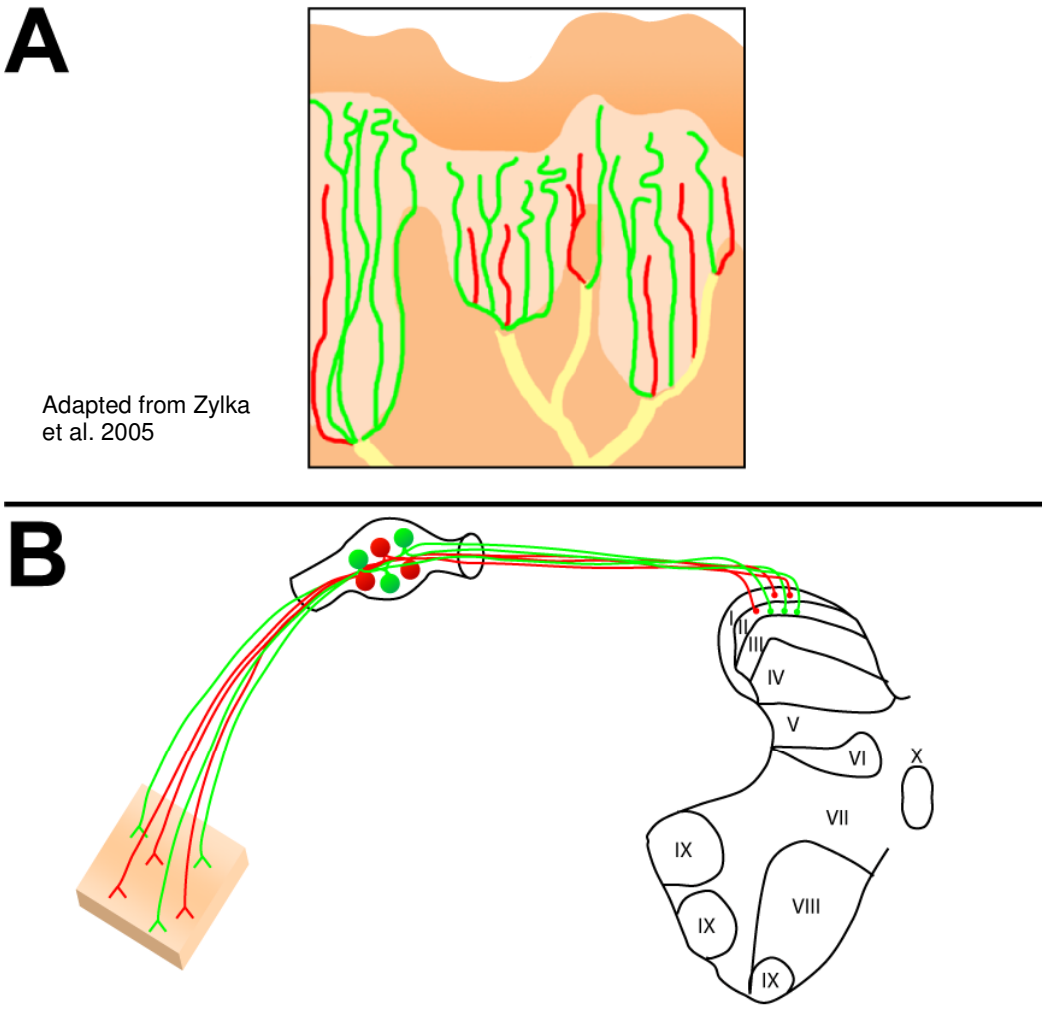

Adapted from Braz et al. (2005), Figure 4

Reduced cutaneous innervation has also been found in diabetic humans, both in those with numbness and those with painful paresthesias (Kennedy et al. 1996; Hermann et al. 1999; Hirai et al. 2000; Sumner et al. 2003; Pittenger et al. 2004; Shun et al. 2004; Sorensen et al. 2006b; Quattrini et al. 2007). Cutaneous nerve fiber density has been increasingly used clinically as a diagnostic tool for diabetic and other small fiber neuropathies (McArthur et al. 1998; Herrmann et al. 1999; Ebenezer et al. 2007; Lauria and Lombardi 2007), as it can often be the first presenting sign prior to sensory deficits or even diabetes diagnosis. However, efforts to correlate epidermal nerve fiber density with sensory symptoms have yielded limited and mixed success. For example, although Smith et al. (2006) reported that reductions in intraepidermal nerve fiber (IENF) density were the most sensitive measure of neuropathic change over electrophysiology and quantitative sensory testing, Polydefkis et al. (2004) found that IENF density was unable to distinguish between diabetic patients with and without neuropathy (Polydefkis et al. 2004). In addition, while one study reported decreased fiber densities in patients with painful neuropathy (Sorensen et al. 2006b), another study found IENF density could not distinguish between painful and painless patients (Quattrini et al. 2007). Several studies have reported successful correlations of IENF density and temperature detection thresholds, vibration detection thresholds, and electrophysiological measures (Quattrini et al. 2007), while Vlckova-Maravcova et al. (2008) have recently shown no correlation with cold detection, moderate correlation with vibration detection, and no correlation with two commonly used neuropathy scales. Perhaps most

importantly, in a Phase II clinical trial of recombinant human nerve growth factor for HIV-associated sensory neuropathy (McArthur et al. 2000), improvements in patient pain assessments were not reflected by improvements in cutaneous innervation, underscoring the disconnect between fiber density and sensory symptoms. This disconnect is further illustrated by several studies reporting the onset of cutaneous nerve fiber loss in asymptomatic patients (Herrmann et al. 2004; Shun et al. 2004; Umapathi et al. 2007). While this may indicate skin biopsies are useful for early detection of neuropathy, they may not be a perfect indicator of the somatosensory status of patients. Conversely, several studies have demonstrated an onset of behavioral deficits prior to quantifiable intraepidermal fiber loss in both diabetic rodents and humans (Chen et al. 2005; Beiswenger et al. 2007; Obrosova et al. 2007a). In order to be useful as an outcome measure for testing therapeutics, cutaneous nerve fiber density must accurately reflect what the patient is feeling, and whether it is predictive of the degree and type of neuropathy remains a question. Finally, skin biopsy studies currently focus entirely on epidermal nerve fiber density. No studies have yet addressed the association between myelinated dermal nerve fibers and sensory symptoms of DN, particularly those that may be associated with large fiber deficits.

5. Study Significance

Clearly, the impact of diabetic neuropathy on patients is great, but the disease remains difficult to treat. For that reason, a better understanding of the mechanisms

underlying neuropathy is required for the development of more efficacious therapeutics. In addition, current diagnostic tests for peripheral neuropathy have significant limitations (Lauria and Lombardi 2007). Sensory nerve conduction studies evaluate large myelinated fibers, which remain largely unaffected in small-fiber neuropathies. Quantitative sensory testing allows for modality-specific evaluations, but it requires patient report, and the degree of nerve fiber deficits may be masked by any analgesic drugs taken for painful symptoms. Finally, sural nerve biopsy, performed to visualize sensory nerve fibers, is an invasive, painful, and risky procedure.

Therefore, the goal of this study was to characterize in detail the relationship between peripheral innervation and the presence of neuropathy. As previously mentioned, cutaneous nerve fiber density is becoming a widely used indicator of neuropathy. However, its role in diabetic neuropathy must be validated before it can be used diagnostically or as a clinical outcome measure. It has been reported that intraepidermal nerve fiber quantitation has a diagnostic efficiency of 88% and a positive predictive value of 92% for sensory neuropathy (McArthur et al. 1998). But how well cutaneous nerve fiber density reflects the degree of neuropathy, and whether or not it accurately represents the sensitivity of the somatosensory system and the sensory symptoms the patient is feeling, must be ascertained. In this work, peripheral innervation was examined in diabetic mice and humans in conjuction with behavioral and sensory measures of diabetic neuropathy. Overall, these studies introduce several novel tools for the assessment of diabetic neuropathy as well as

demonstrate there are subtle disconnects in the degree to which nerve fiber density indicates pain sensitivity.

In the first study, (**"Diabetes-induced hypoalgesia is paralleled by attenuated stimulus-induced spinal Fos expression in diabetic mice"**), we examined peripheral innervation using an indirect measure, the ability of primary afferent neurons to activate second order dorsal horn neurons. This study delineated the relationship between behavioral responses to formalin injection and spinal activation as measured by Fos expression in diabetic C57BL/6 mice.

In the next two studies, we directly examined peripheral innervation by examining epidermal nerve fiber density in two diabetic mouse models. In the first, (**"Selective deficits in nocifensive behavior despite normal cutaneous axon innervation in leptin receptor null mutant (*db/db*) mice"**) we found behavioral deficits that were not reflected by changes in cutaneous innervation. One possibility for this surprising finding is a subpopulation-specific loss that was masked in the total fiber quantification. Therefore, in the next study, (**"Early loss of peptidergic intraepidermal nerve fibers in an STZ-induced mouse model of insensate diabetic neuropathy"**), we used transgenic mice to visualize specific subpopulations of epidermal c-fibers and evaluate their contribution to the total diabetes-induced fiber loss. We found a preferential decrease in peptidergic fibers early in the disease progression that mirrored the temporal appearance of reduced nociceptive sensitivity. This subpopulation-specific loss could be an important phenomenon in insensate diabetic neuropathy. Moreover, our findings that behavioral symptoms are closely

related to the losses in peptidergic epidermal fibers support the notion that peptidergic input is largely responsible for the discrimination of pain sensation, with nonpeptidergic input serving only to modulate the principal information provided by the peptidergic.

Finally, we addressed the relationship between cutaneous innervation and sensory thresholds in human patients with diabetic neuropathy in **"Quantitative sensory measures of small nerve fiber function and cutaneous nerve fiber density in patients with diabetic neuropathy".** We evaluated the sensitivity and specificity of intraepidermal nerve fiber (IENF) and myelinated dermal nerve fiber (MDNF) densities for detecting neuropathy, and also examined their correlation with various measures of sensory nerve fiber function. We found that both IENF and MDNF densities correlated with some, but not all, sensory measures. This study corroborated the validation of IENF density and introduced the utility of MDNF density in assessing diabetic neuropathy.

VI. Chapter Two:

Diabetes-induced chemogenic hypoalgesia is paralleled by attenuated stimulus-induced Fos expression in the spinal cord of diabetic mice

1. Abstract

Chronic hyperglycemia in diabetes induces abnormal nerve pathologies, resulting in diabetic neuropathy (DN). Sensory symptoms of DN can manifest as positive (painful), negative (insensate), or both. Streptozotocin (STZ)-induced diabetic C57Bl/6 mice have reduced cutaneous innervation and display reduced behavioral responses to noxious stimuli, reflecting the insensate aspect of the human syndrome. Current studies were undertaken to determine whether the diabetes-induced deficits in pain responses are reflected by changes in spinal activation in this model of DN. Nocifensive responses of nondiabetic and diabetic mice to formalin injection were measured 1, 3, 5 and 7 weeks post-STZ, and at each time point formalin-induced spinal Fos expression was quantified. Responses of diabetic mice were significantly reduced during the second phase of the formalin test beginning 3 weeks post-STZ, and during Phase 1 beginning 5 weeks post-STZ. Consistent with the behavioral responses, the number of Fos-positive cells in the dorsal horn of diabetic animals was significantly reduced beginning 3 weeks post-STZ and continuing 5 and 7 weeks post-STZ. The deficits at 5 weeks post-STZ were restored by 2-week treatments with insulin or neurotrophins. These results demonstrate that the reduced sensation occurring from progressive peripheral axon loss results in functional deficits in spinal cord activation.

2. Introduction

As described earlier, current animal models of diabetes vary in their presentation of neuropathy symptoms. STZ-treated C57BL/6 mice display reduced sensitivity to mechanical, chemogenic, and, in some cases, thermal stimuli (Christianson et al. 2003b; Chen et al. 2005; Walwyn et al. 2006). In addition, STZ-induced diabetic C57BL/6 mice display reduced dermal and epidermal innervation of the hindpaw, as well as abnormalities in the central terminals of primary nociceptive neurons (Akkina et al. 2001; Christianson et al. 2003a). Therefore, the STZ-induced diabetic C57BL/6 mouse model is well-suited for exploring abnormal peripheral nerve function associated with insensate symptoms (Christianson et al. 2003b).

However, the relationship between an animal's behavior and pain status is inherently subjective, and it is not absolute that rodent nocifensive withdrawal behaviors are directly related to the perceived stimulus intensity. Fos is an immediate-early transcription factor expressed in second order spinal neurons in response to a noxious peripheral stimulus and has been used as a surrogate for peripheral nerve activation. In response to formalin injection into the hindpaw, Fos is expressed in a temporal and spatial pattern consistent with the magnitude of nociceptive input from the hindpaw (Presley et al. 1990; Abbadie et al. 1992; Bon et al. 2002). To test the hypothesis that diabetes-induced peripheral nerve damage results in suppressed spinal activation, we compared spinal Fos expression in response to formalin injection in nondiabetic and diabetic mice during the progression of neuropathy. In addition, we tested whether insulin or neurotrophin treatments

restored Fos expression in a manner consistent with improved behavioral responses. Our results suggest that STZ-induced sensory loss in C57Bl/6 mice reduces Fos expression in the dorsal horn in a manner consistent with peripheral nerve damage and reduced primary afferent input. Moreover, treatments that improve aspects of the neuropathy can similarly improve stimulus-induced Fos expression in the spinal cord.

3. Experimental Procedures

Animals

All animal use was in accordance with NIH guidelines and conformed to the principles specified by the University of Kansas Medical Center Animal Care and Use Protocol. In all studies, 8-week-old male C57BL/6 mice (Charles River, Wilmington, MA) were housed 2-4 mice per cage on a 12:12-hour light/dark cycle under pathogen-free conditions with free access to mouse chow and water.

Experimental Design

In order to assess whether progressive behavioral deficits in diabetic mice represent true hypoalgesia, nondiabetic and diabetic mice were injected with STZ or vehicle on Day 0 and sacrificed 1, 3, 5, or 7 weeks later. Formalin testing was performed on the day of sacrifice for each separate endpoint, and formalin-induced Fos expression was evaluated. Based on these results, further experiments were performed in order to determine whether the concomitant deficits observed in behavioral responses and Fos expression could be restored. At 5 weeks post-STZ,

nondiabetic and diabetic mice treated with insulin, neurotrophins, or CSF were tested for formalin responses, sacrificed, and evaluated for Fos expression.

Diabetes Induction

Diabetes was induced by a single intraperitoneal injection of streptozotocin (Sigma, St. Louis, MO; 180 mg/kg body weight) dissolved in 10 mM sodium citrate buffer, pH 4.5 (Wang et al. 1993). Nondiabetic mice were injected with sodium citrate buffer alone. Animal weight and tail vein blood glucose levels using glucose diagnostic reagents (Sigma) were measured 1-week post-STZ and every other week thereafter to assess diabetes. Only STZ-injected mice with blood glucose levels greater than 16.0 mmol/L (288 mg/dL) were included in the diabetic groups; STZ-injected mice with blood glucose levels below that standard were not included in the study (Wang et al. 1993). Blood collection for the final time point was taken subsequent to formalin testing so that behavioral measurements would not be influenced by the blood draw. Weight and blood glucose levels were compared between nondiabetic and diabetic untreated animals using 2-way analysis of variance (ANOVA) followed by post hoc analysis using the Fisher's PLSD test. Repeated measures (RM) AVOVA was used to analyze weight and blood glucose of treated nondiabetic and diabetic animals pre- and post-treatment.

Behavioral Analysis

The formalin test was performed prior to sacrifice 1, 3, 5 and 7 weeks post-

STZ on nondiabetic and diabetic mice by an experienced experimenter blinded to the condition of the mice. After a 1 hr habituation to individual observation chambers, mice were injected subcutaneously with 20 µL of formalin (5% formaldehyde) into the dorsal surface of the right hindpaw using a 1CC insulin syringe and 28-gauge needle. The amount of time devoted to the injected foot (licking and biting) was recorded in two 10-minute windows during the acute (Phase 1; 0-10 min post-injection) and inflammatory (Phase 2; 40-50 min post-injection) phases of the formalin test. Differences in the attentive time spent to the injected foot during each phase were compared between nondiabetic and diabetic mice at each time point using unpaired t-tests.

Fos Immunohistochemistry

The expression of Fos protein was examined in the spinal cords of nondiabetic and diabetic mice. Two hours following formalin injection, when Fos protein is expressed at maximal levels (Bon et al. 2002), mice were anesthetized with Avertin (1.25% v/v tribromoethanol, Sigma; 2.5% *tert*-amyl alcohol, Sigma; 200 µL/10 g body weight) and transcardially perfused with ice cold 0.1 M phosphate-buffered saline (PBS; pH 7.4) followed by ice cold 4% paraformaldehyde in PBS. The spinal column and surrounding tissue were removed and post-fixed in the same fixative overnight at 4°C. The lumbar enlargement of the spinal cord was dissected and cryoprotected in 30% sucrose for 24 hours. Spinal segments L4/L5 were frozen in Tissue Tek (Sakura, Torrance, CA) and sectioned on a cryostat at 20 µm. Sections

were mounted on Superfrost Plus slides (Fisher Scientific, Chicago, IL) and stored at -20°C.

Following a 5 min thaw at room temperature, slide-mounted tissue was incubated under humidified conditions with 0.5% Triton-X in PBS for 20 min, 10% normal horse serum in PBS for 10 min, and with primary antibodies against c-Fos (rabbit; 1:3000; EMD Biosciences, La Jolla, CA) and NeuN (mouse; 1:1000; Chemicon) diluted in PBS for 16 hr at 4°C. For visualization, the primary antibodies were removed by three washes in PBS, and sections were incubated for 1 hr at 4°C with fluorochrome-conjugated secondary antibodies (chicken anti-rabbit Alexa 488, 1:2000; donkey anti-mouse Alexa 555, 1:2000; Molecular Probes, Eugene, OR). Sections were rinsed and coverslipped before viewing, and sections from all treatment groups and time points were included in each experiment to standardize immunocytochemical processing differences amongst all groups.

Quantification of Fos-positive neurons

The number of dorsal horn spinal neurons ipsilateral to formalin injection containing Fos-like immunofluoresence was counted live under the microscope at 20X by an experimenter blinded to the groups. Fos-positive cells were identified by strong nuclear staining, and only Fos-positive cells colabeled with NeuN, a neuronal marker, were counted. Fos-positive cells were assigned to established dorsal horn laminar regions I/II, III/IV, and V/VI. Counts from the 3 laminar regions were summed to yield the total number of Fos-positive dorsal horn cells for each section.

The sum of Fos counts represent the average of labeled dorsal horn nuclei in 10 sections, each separated by at least 60 µm, throughout the length of L4/L5 spinal segments of each cord. Differences in the total number of Fos-positive cells between nondiabetic and diabetic animals at each time point were compared using unpaired t-tests. Differences in the number of Fos-positive cells in laminar regions at each time point were analyzed using 2-way ANOVA followed by post hoc analysis using Fisher's PLSD.

Insulin Administration

Three weeks after diabetes induction, slow-release insulin pellets (13 +/- 2 mg each; 0.1 U/day/implant; LinShin Canada, Inc., Scarborough, Ontario, Canada) were implanted subcutaneously in the dorsal skin of diabetic mice (2 implants for the first 20 g body weight; 1 implant for each additional fraction of 5 g body weight) and remained for 2 weeks. After one week an additional pellet was added if blood glucose levels were not below 16 mmol/L. Weight, blood glucose levels, and symptoms of hyperglycemia were monitored as previously detailed. Sham pellets were not administered. At 5 weeks post-STZ, behavioral analysis, sacrifice, and Fos immunohistochemistry were performed and quantified as described above. Differences in the attentive time spent to the injected foot during each phase of the formalin test were compared between nondiabetic, untreated diabetic, and insulin-treated diabetic mice using 1-way ANOVA followed by post hoc analysis using Fisher's PLSD. Differences in the total number of Fos-positive cells were compared

using 1-way ANOVA followed by Fisher's PLSD. Differences in the number of Fos-positive cells in laminar regions were analyzed using 2-way ANOVA followed by Fisher's PLSD.

Neurotrophin Administration

Beginning 3 weeks after diabetes induction, diabetic and nondiabetic mice received daily intrathecal injections (50 µL; 1 µg neurotrophin) of NGF or GDNF (Chemicon International, Inc.) for 2 weeks. Growth factors were delivered intrathecally to improve delivery to the DRG, avoiding problems related to the insufficient retrograde transport of trophic factors that is known to occur in diabetic animals (Akkina et al. 2001; Christianson et al. 2003a). Individual trophic factors were dissolved in artificial cerebrospinal fluid (CSF) at a concentration of 20nM. Control mice received intrathecal injections of CSF alone as a control for the intrathecal injection paradigm. Intrathecal injections were delivered between the L6 and the S1 vertebrae using a 28-gauge insulin syringe (Hylden and Wilcox 1980). The physiological conditions of all CSF-, NGF- and GDNF-treated mice were monitored as previously detailed. At 5 weeks post-STZ, behavioral analysis, sacrifice, and Fos immunohistochemistry were performed and quantified as described above. Differences in the attentive time spent to the injected foot during each phase of the formalin test were compared between CSF-, NGF- and GDNF-treated diabetic and nondiabetic mice using 1-way ANOVA followed by post hoc analysis using the Fisher's PLSD test. Differences in the total number of Fos-positive cells were

compared using 1-way ANOVA followed by Fisher's PLSD. Differences in the number of Fos-positive cells in laminar regions were analyzed using 2-way ANOVA followed by Fisher's PLSD.

4. Results and Figures

STZ-Induced Diabetes

STZ-injected mice demonstrated symptoms typical of STZ-induced diabetes including polydipsia, polyuria, and weight loss. By 1 week post-STZ, over 90% of STZ-injected mice had significantly higher blood glucose levels compared to vehicle-injected mice; this difference was maintained throughout the study (**Table VI-1**). Nondiabetic mice increased in weight by 30.5% over the course of the study, while diabetic mice lost 14.0% of their weight in the first week following STZ injection and failed to gain weight in the remaining weeks (**Table VI-1**). Despite these differences, nondiabetic and diabetic mice were generally similar in their locomotor/grooming activity during the observation period after formalin injection, suggesting any reductions in the sensitivity to formalin were not simply due to poor health or lethargy in diabetic mice.

Diabetes-Induced Deficits in Formalin-Induced Pain Behavior

To determine the progression of diabetes-induced sensory deficits, the responsiveness to formalin injection was assessed in groups of nondiabetic and diabetic mice 1, 3, 5 and 7 weeks following STZ injection (**Figure VI-1**). In

Table VI-1. Weight and blood glucose levels of untreated nondiabetic and diabetic mice

	Week 0	Week 1	Week 3	Week 5	Week 7
Nondiabetic:					
Weight	20.5 +/- 0.95 N = 21	23.2 +/- .0.31 N = 20	24.4 +/- 0.73 N = 16	25.4 +/- 0.51 N = 11	27.8 +/- 0.91 N = 6
Glucose	NM	7.9 +/- 0.34 N = 20	8.7 +/- 0.91 N = 16	7.5 +/- 0.36 N = 11	7.4 +/- 1.80 N = 5
Diabetic:					
Weight	22.2 +/- 0.29 N = 20	19.1* +/- 0.48 N = 20	19.2* +/- 0.42 N = 15	19.3* +/- 0.90 N = 10	20.6# +/- 1.75 N = 4
Glucose	NM	25.8* +/- 0.82 N = 20	25.4* +/- 0.77 N = 15	21.3* +/- 0.82 N = 10	20.7# +/- 1.33 N = 4

Weight and blood glucose levels measured at weeks 0, 1, 3, 5 and 7 post-STZ of untreated nondiabetic and diabetic mice that underwent both formalin testing and evaluation for Fos expression. Data for each week includes values for all animals tested on that day from all time point groups. Weight is in grams; glucose levels are mmol/L. NM, not measured. Data represented as means +/- standard error of mean. * $p < 0.0001$ vs nondiabetic mice, # $p < 0.05$ vs nondiabetic mice.

Figure VI-1. The behavioral response to formalin is impaired in diabetic mice.

The behavioral responses of nondiabetic and diabetic mice to formalin injection recorded in 10 min. windows during Phase 1 and Phase 2 of the formalin test prior to sacrifice at 1 (A), 3 (B), 5 (C), and 7 (D) weeks following STZ injection. **(A)** One week post-STZ, the amount of time devoted to the injected foot did not differ between nondiabetic and diabetic mice. **(B)** At 3 weeks post-STZ, diabetic mice devoted significantly less time to the injected foot during Phase 2. **(C)** Diabetic mice displayed significantly reduced behavioral responses during both Phase 1 and 2 at 5 weeks post-STZ. **(D)** This pattern was maintained during both Phase 1 and 2 at 7 weeks post-STZ. Data plotted as means +/- standard error of mean. * $p < 0.05$ vs nondiabetic mice, # $p < 0.0001$ vs nondiabetic mice.

Figure VI-1

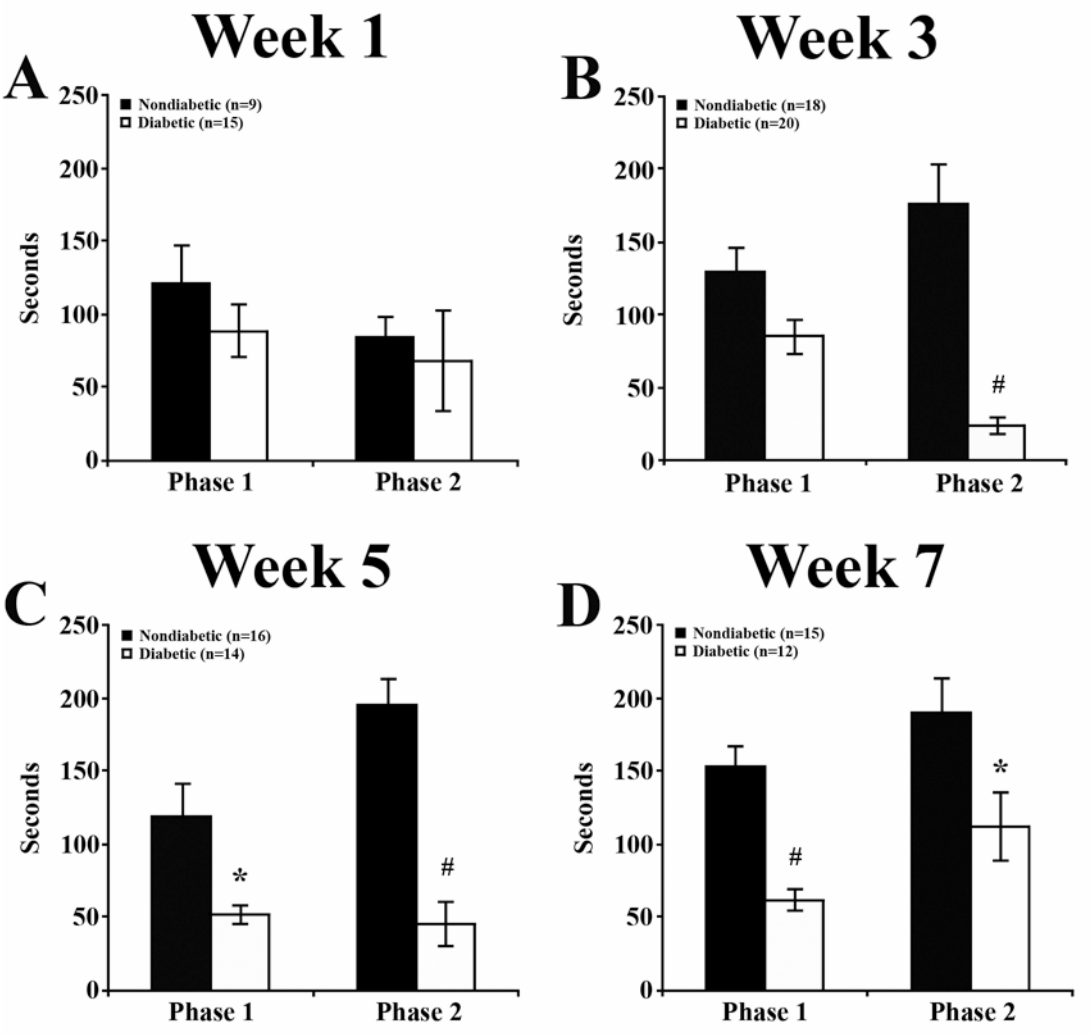
Week 1
A
Nondiabetic (n=9)
Diabetic (n=15)
Seconds
250
200
150
100
50
0
Phase 1
Phase 2
Week 3
B
Nondiabetic (n=18)
Diabetic (n=20)
#
Week 5
C
Nondiabetic (n=16)
Diabetic (n=14)
*
#
Week 7
D
Nondiabetic (n=15)
Diabetic (n=12)
#
*

nondiabetic mice, formalin injection resulted in a typical biphasic response including both an acute (Phase 1) and an inflammatory (Phase 2) phase (Murray et al. 1988). In comparison, diabetic mice gradually developed diminished responses to formalin injection during the 7 weeks following STZ-injection compared to nondiabetic mice. At 1 week post-STZ (**Figure VI-1A**), the amount of time devoted to the injected foot did not differ between nondiabetic and diabetic mice. At week 3 post-STZ (**Figure VI-1B**), diabetic mice displayed a significantly reduced Phase 2 response, responding 86.6% less than nondiabetic mice, the most severe reduction of the study. By week 5 (**Figure VI-1C**), responses during both Phase 1 and Phase 2 were significantly reduced (by 56.6% and 76.8%, respectively) in diabetic compared to nondiabetic mice. This pattern was maintained 7 weeks post-STZ (**Figure VI-1D**) when responses by diabetic mice were significantly reduced during Phase 1 and Phase 2 by 59.6% and 40.9%, respectively.

Diabetes-Induced Reductions in Spinal Fos Expression

To determine whether the diabetes-induced deficits in pain behaviors were reflected in changes in spinal activation, mice were sacrificed following the formalin test, and the expression of Fos protein was evaluated in tissue sections of L4-L5 lumbar segments of spinal cords from both nondiabetic and diabetic mice 1, 3, 5 and 7 weeks following STZ-injection. In sections from both groups of animals, Fos immunoreactivity was concentrated in the nuclei of small neurons in the superficial and neck regions of the dorsal horn ipsilateral to the formalin injection (**Figure VI-**

2A, B). Few Fos-positive neurons were observed in the contralateral dorsal horn. In spinal cord sections from diabetic animals (**Figure VI-2D, F, H, J**), the number of Fos-positive neurons was visibly decreased by week 5 (**Figure VI-2H**) compared to nondiabetic animals (**Figure VI-2G**), an effect more pronounced by week 7 (**Figure VI-2I, J**.)

In nondiabetic mice, the total number of Fos-positive neurons per 20 µm section in the dorsal horn averaged 143.1 +/- 8.65, 136.1 +/- 7.89 and 136.1 +/- 17.04 at 3, 5 and 7 weeks post-STZ, respectively (**Figure VI-2E, G, I; 3C, E, G**). At each time point, laminae I/II contained the greatest percentage of Fos-positive neurons, containing a little over half the total number of Fos-positive neurons per dorsal horn section (**Figure VI-2; 3B-E**). Laminae V/VI represented the lowest contribution to the total, never containing more than 30.0 +/- 2.03 Fos-positive neurons per section.

At 1 week post-STZ, there were no significant differences between nondiabetic and diabetic mice in the number of Fos-positive cells found in any laminar group (**Figure VI-3B**) or in total (**Figure VI-2C, D; 3A**). At 3 weeks post-STZ, although there was no significant difference in the total number of Fos-positive cells (**Figure VI-2E, F; 3C**), there were significantly fewer Fos-positive cells in laminae I/II (**Figure VI-3D**) of spinal cords from diabetic compared to nondiabetic mice. There were no differences found in the other laminar regions. By 5 weeks post-STZ, the decline in the total number of dorsal horn Fos-positive cells per section reached statistical significance (**Figure VI-2G, H; 3E**), at which time diabetic mice had 35.5% fewer than nondiabetic mice. All laminar regions appeared to contribute

Figure VI-2. Formalin-induced expression of Fos in the mouse lumbar spinal cord.

Representative images at low magnification (A, B) and high magnification (C-J) of Fos-positive neurons in the lumbar spinal cord after formalin injection. **(A, B)** Formalin-induced Fos expression was apparent predominantly on the ipsilateral side to the formalin injection in both nondiabetic and diabetic mice, albeit in fewer neurons in diabetic mice. Images were taken from mice 7 weeks post-STZ. **(C-J)** Comparisons of Fos-positive neurons were made between nondiabetic (left side) and diabetic (right side) mice. Fos expression appeared relatively normal in diabetic animals at weeks 1 (C, D) and 3 (E, F) post-STZ. However, Fos expression was visibly decreased in diabetic mice at 5 (G, H) and 7 (I, J) weeks. Scale bar, 100 μm for each image.

Figure VI-2

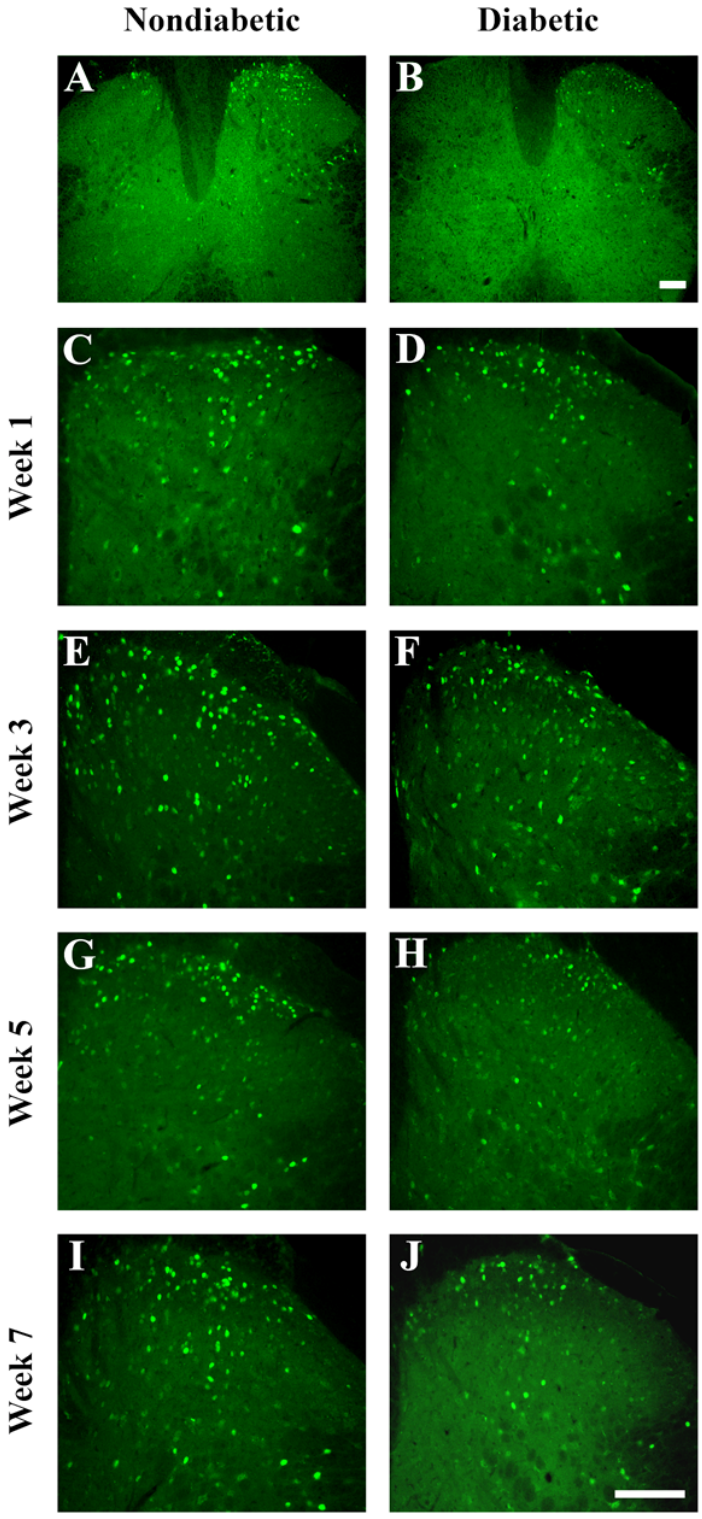

Figure VI-3. Quantification of formalin-induced Fos expression in diabetic mice.

(A, C, E, G). Quantification of total Fos expression in the dorsal horn of nondiabetic and diabetic mice. Comparisons between nondiabetic and diabetic mice revealed a significant decrease in Fos-positive neurons at weeks 5 and 7.

(B, D, F, H). Quantification of Fos expression within laminar regions. **(B)** One week post-STZ, an analysis of Fos-positive neurons within specific laminar regions revealed no significant differences between nondiabetic and diabetic animals. **(D)** In contrast, analysis at 3 weeks post-STZ revealed a significant reduction in Fos-positive neurons within laminae I/II in diabetic versus nondiabetic mice. **(F)** More severe reductions in Fos-positive neurons in diabetic mice were evident at 5 (F) and 7 (H) weeks post-STZ in all laminae, with the exception of laminae V/VI at 7 weeks. Data plotted as means +/- standard error of mean. * $p < 0.05$ vs nondiabetic mice.

Figure VI-3

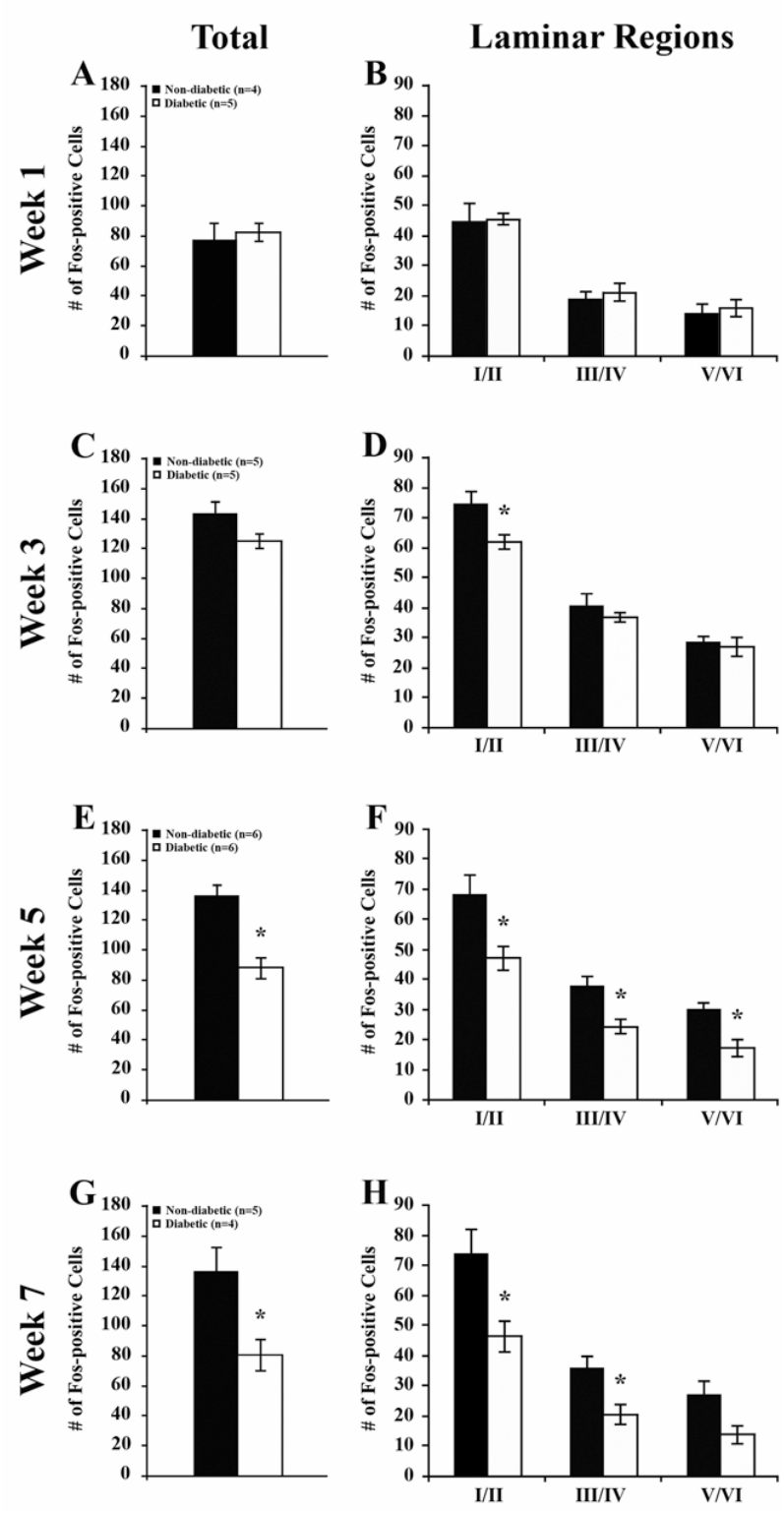
Total
Laminar Regions
Week 1
Week 3
Week 5
Week 7
A
B
C
D
E
F
G
H
# of Fos-positive Cells
Non-diabetic (n=4)
Diabetic (n=5)
Non-diabetic (n=5)
Diabetic (n=5)
Non-diabetic (n=6)
Diabetic (n=6)
Non-diabetic (n=5)
Diabetic (n=4)
I/II
III/IV
V/VI
*

to this reduction, with significant losses in laminae I/II, III/IV, and V/VI (**Figure VI-3F**). By week 7, there was a significant 40.7% reduction in the total number of Fos-positive cells (**Figure VI-2I, J, 3G**), due primarily to reductions in laminae I/II and III/IV (**Figure VI-3H**).

Insulin Effects on Diabetes-Induced Deficits in Pain Behavior and Fos Expression

To evaluate the ability of insulin to restore the diabetes-induced deficits in pain behavior and Fos expression, diabetic mice 3 weeks post-STZ received insulin from slow-release pellets for 2 weeks. At the end of the 2-week insulin treatment, insulin-treated animals had increased in body weight from 19.5 +/- 2.26 g at the start of treatment to 23.3 +/- 0.84 g ($P = 0.0987$) and significantly improved over untreated diabetic mice ($p < 0.05$). Similarly, the blood glucose levels of insulin-treated diabetic animals decreased from 22.8 +/- 1.71 mmol/L to 17.3 +/- 3.43 mmol/L at the time of sacrifice. Though this level was not significantly different from untreated diabetic animals (21.3 +/- 0.82 mmol/L at 5 weeks post-STZ; $p = 0.0902$), the insulin-treated animals improved in overall appearance and general health, and it is possible that the insulin pellets were nearly depleted by the end of the study and thus failed to maintain euglycemia throughout the entire 14-day treatment.

To determine whether insulin treatment could restore the sensory deficits induced by diabetes, the behavioral response to formalin injection of insulin-treated diabetic mice 5 weeks post-STZ was compared with that of the nondiabetic and untreated diabetic mice at the same time point. Insulin-treated mice did not devote

significantly more attentive time to the injected foot during Phase 1 of the formalin test. However, insulin restored the behavioral responses during Phase 2 to that of nondiabetic mice ($p = 0.5392$), significantly increasing the time devoted to the injected foot over untreated diabetic mice (Phase 2, $p < 0.0001$; **Figure VI-4A**). Similarly, insulin restored formalin-induced spinal Fos expression in diabetic mice, significantly increasing the number of Fos-positive dorsal horn neurons per section compared to untreated diabetic mice, both in total ($p < 0.05$, **Figure VI-4B**) and in laminae I/II ($p < 0.05$, **Figure VI-4C**).

Neurotrophin Effects on Diabetes-Induced Deficits in Pain Behavior and Fos Expression

To evaluate the ability of neurotrophins to restore the diabetes-induced deficits in pain behavior and Fos expression, diabetic mice received daily intrathecal injections of NGF, GDNF, or vehicle (CSF) 3 weeks post-STZ for a duration of 2 weeks. CSF-treated diabetic mice decreased in weight from 21.5 +/- 0.65 g at the time of STZ-injection to 18.5 +/- 1.66 g at 5 weeks post-STZ (**Table VI-2**). At the time of sacrifice blood glucose levels were 26.3 +/- 0.53 mmol/L. Diabetic mice receiving intrathecal treatment with either NGF or GDNF for 2 weeks underwent decreases in weight and continued hyperglycemia similar to CSF-diabetic mice. Statistical analysis showed there was not a significant effect of treatment on weight ($p= 0.8902$) or glucose ($p = 0.9449$) over time, suggesting NGF and GDNF intrathecal treatments had no effect on these parameters (**Table VI-2**).

Figure VI-4. Insulin increases formalin-induced pain responses and spinal Fos expression.

The behavioral responses (A) and Fos expression (B, C) of nondiabetic, untreated diabetic, and insulin-treated diabetic mice following formalin injection at 5 weeks post-STZ. Nondiabetic and untreated diabetic groups are the same mice used in **Figure VI-3 E, F**. **(A)** During Phase 1, behavioral responses of insulin-treated diabetic animals were not significantly higher than in untreated diabetic animals. During Phase 2 of the formalin test, insulin-treated diabetic mice devoted significantly more time to the injected foot than untreated diabetic mice and did not perform significantly different from nondiabetic mice. **(B)** Insulin-treated diabetic mice also had significantly greater total numbers of Fos-positive dorsal horn neurons per spinal cord section than untreated diabetic mice and were not significantly different from nondiabetic mice ($p = 0.4901$). **(C)** Insulin significantly increased the number of Fos-positive neurons per section in laminae I/II compared to untreated diabetic mice. Data plotted as means +/- standard error of mean. * $p < 0.05$ vs untreated diabetic mice, # $p < 0.0001$ vs untreated diabetic mice.

Figure VI-4

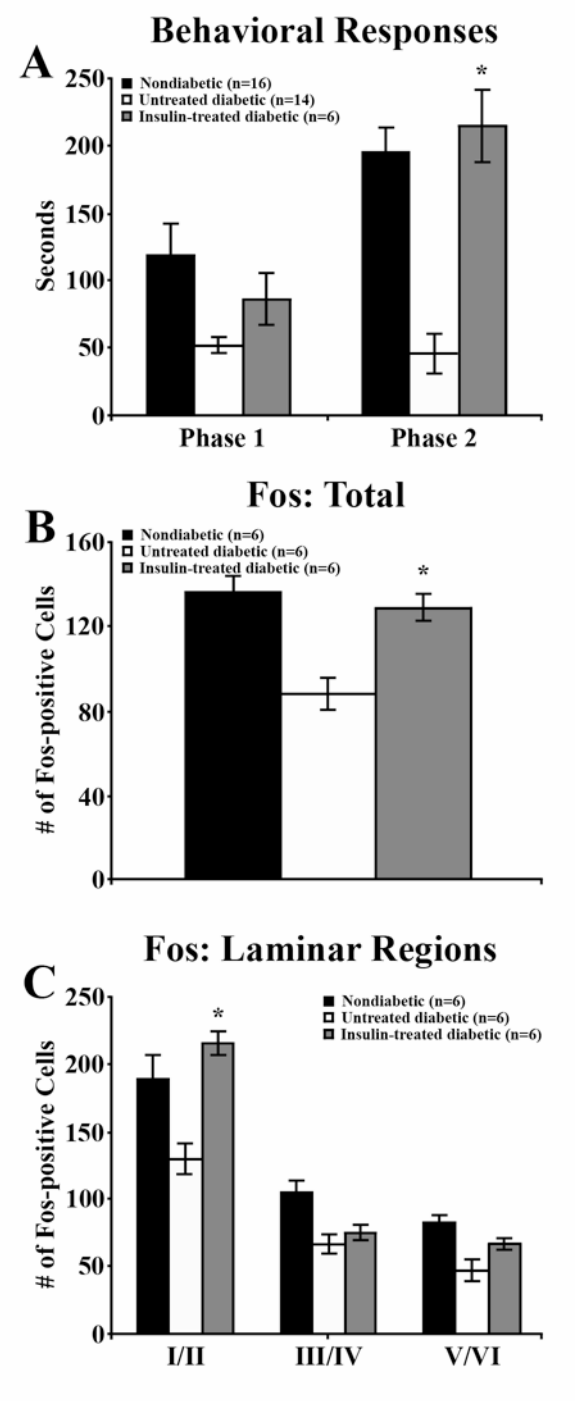
Behavioral Responses
A
Nondiabetic (n=16)
Untreated diabetic (n=14)
Insulin-treated diabetic (n=6)
Seconds
250
200
150
100
50
0
*
Phase 1
Phase 2
Fos: Total
B
Nondiabetic (n=6)
Untreated diabetic (n=6)
Insulin-treated diabetic (n=6)
# of Fos-positive Cells
160
120
80
40
0
*
Fos: Laminar Regions
C
Nondiabetic (n=6)
Untreated diabetic (n=6)
Insulin-treated diabetic (n=6)
# of Fos-positive Cells
250
200
150
100
50
0
*
I/II
III/IV
V/VI

Table VI-2. Weight and blood glucose levels of treated nondiabetic and diabetic mice

			Pre-Treatment	Post-Treatment
Diabetic				
	CSF	Weight	19.0 +/- 0.91	18.5 +/- 1.66
		Glucose	22.6 +/- 0.93	26.3 +/- 0.56
	NGF	Weight	19.3 +/- 0.42	20.3 +/- 0.97
		Glucose	24.8 +/- 0.88	26.2 +/- 0.61
	GDNF	Weight	20.0 +/- 1.00	19.3 +/- 1.20
		Glucose	23.6 +/- 0.94	26.8 +/- 0.39
Nondiabetic				
	CSF	Weight	22.5 +/- 0.65	24.5 +/- 0.50
		Glucose	8.2 +/- 0.16	8.5 +/- 0.70
	NGF	Weight	22.8 +/- 0.48	23.8 +/- 0.48
		Glucose	8.5 +/- 0.57	6.5 +/- 1.29
	GDNF	Weight	21.5 +/- 0.65	24.3 +/- 0.25
		Glucose	8.1 +/- 0.48	6.7 +/- 1.35

Weight and blood glucose levels of diabetic and nondiabetic mice receiving 2-week intrathecal treatment with CSF, NGF, or GDNF starting 3 weeks post-STZ. Weight is in grams; glucose levels are mmol/L. Data represented as means +/- standard error of mean. Statistical analysis did not reveal an effect of treatment on weight or blood glucose.

To evaluate the ability of neurotrophins to restore diabetes-induced behavioral and functional deficits, formalin responses and Fos expression were evaluated in 5-week post-STZ diabetic mice treated with CSF, NGF, or GDNF. Although not significant, the time devoted to the injected foot during Phase 1 and Phase 2 of the formalin test in NGF-treated animals was elevated (**Figure VI-5A**). GDNF failed to increase the time devoted to the injected foot during Phase I, but did produce a non-significant increase in Phase 2 (**Figure VI-5A**). It should be pointed out that the number of animals treated was only 4-7, which was lower than the N's of formalin experiments in Figure 1. Importantly, however, both NGF and GDNF treatments increased the total number of Fos-positive cells expressed in diabetic spinal cords over CSF-treated diabetic mice (NGF, $p < 0.05$; GDNF, $p = 0.0602$; **Figure VI-5B**). In NGF-treated mice, Fos expression was increased in laminae I/II ($p < 0.05$), III/IV ($p < 0.05$), and V/VI ($p < 0.05$); in GDNF-treated mice, laminae III/IV ($p = 0.0555$) and V/VI ($p < 0.05$; **Figure VI-5C**).

Neurotrophin Effects on the Pain Behavior and Fos Expression of Nondiabetic Mice

In addition to neurotrophin treatment in diabetic mice, we also treated nondiabetic mice to 2 weeks of daily intrathecal injections with CSF, NGF, or GDNF (**Figure VI-6**). Statistical analysis did not reveal a significant effect of treatment on behavioral responses to the formalin test during Phase 1 ($p = 0.9528$) or Phase 2 ($p =$

Figure VI-5. NGF and GDNF increase formalin-induced spinal Fos expression

The behavioral responses (A) and Fos expression (B, C) of diabetic mice receiving 2 weeks of daily intrathecal injections of vehicle (CSF), NGF, or GDNF. **(A)** At 5 weeks post-STZ, statistical analysis did not show an effect of treatment group on the Phase 1 or 2 behavioral responses over time. **(B)** Both NGF and GDNF treatment increased the overall number of Fos-positive neurons per section compared to CSF-treated mice. **(C)** NGF treatment significantly increased Fos-positive neurons within all laminae, while GDNF treatment increased Fos-positive neurons within laminae III/IV and V/VI. Data plotted as means +/- standard error of mean. * $p < 0.05$ versus CSF-injected diabetic mice.

Figure VI-5

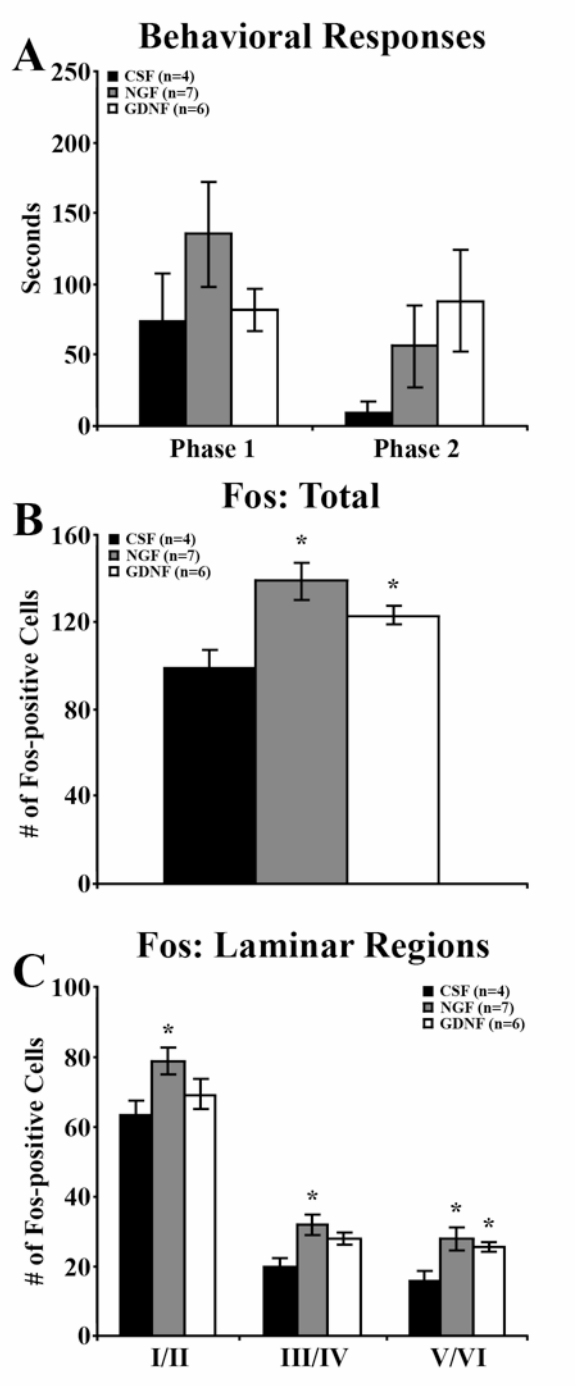
A
Behavioral Responses
CSF (n=4)
NGF (n=7)
GDNF (n=6)
Seconds
250
200
150
100
50
0
Phase 1
Phase 2
B
Fos: Total
CSF (n=4)
NGF (n=7)
GDNF (n=6)
# of Fos-positive Cells
160
120
80
40
0
*
*
C
Fos: Laminar Regions
CSF (n=4)
NGF (n=7)
GDNF (n=6)
# of Fos-positive Cells
100
80
60
40
20
0
*
*
*
*
I/II
III/IV
V/VI

Figure VI-6. NGF and GDNF did not alter formalin responses or formalin induced spinal Fos expression in nondiabetic mice

The behavioral responses (A) and Fos expression (B, C) of nondiabetic mice receiving 2 weeks of daily intrathecal injections of vehicle (CSF), NGF, or GDNF. **(A)** At 5 weeks post-STZ, statistical analysis did not show an effect of treatment group on the Phase 1 or 2 behavioral responses over time. **(B)** Neither NGF nor GDNF treatment altered the overall number of Fos-positive neurons per section compared to CSF-treated mice. **(C)** NGF and GDNF treatment did not change the number of Fos-positive neurons within any laminar region. Data plotted as means +/- standard error of mean.

Figure VI-6

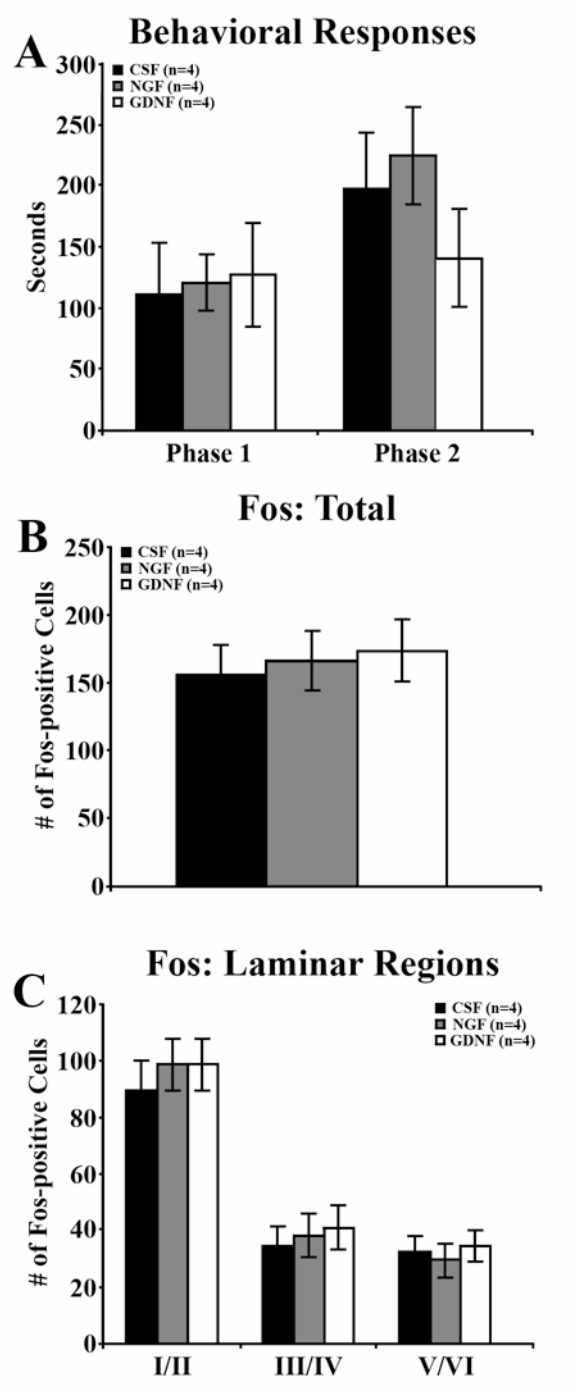
A
Behavioral Responses
CSF (n=4)
NGF (n=4)
GDNF (n=4)
Seconds
300
250
200
150
100
50
0
Phase 1
Phase 2
B
Fos: Total
CSF (n=4)
NGF (n=4)
GDNF (n=4)
# of Fos-positive Cells
250
200
150
100
50
0
C
Fos: Laminar Regions
CSF (n=4)
NGF (n=4)
GDNF (n=4)
# of Fos-positive Cells
120
100
80
60
40
20
0
I/II
III/IV
V/VI

0.3924; **Figure VI-6A**). Similarly, neurotrophin treatment did not alter total Fos expression ($p = 0.8542$; **Figure VI-6B**) or Fos expression in laminar groups ($p = 0.6640$; **Figure VI-6C**).

5. Discussion

STZ-treated C57BL/6 mice progressively develop reduced sensitivity to mechanical and noxious chemogenic stimuli (Christianson et al. 2003b), and these sensory deficits resemble the insensate symptoms experienced by most human diabetic neuropathy patients. In addition to suppressed pain responses, these diabetic mice have significant reductions in hindlimb cutaneous nerve fibers (Christianson et al. 2003a) and abnormal spinal afferent terminations (Akkina et al. 2001). Collectively, these deficits suggest that chronic hyperglycemia causes nerve damage in C57Bl/6 mice sufficient to reduce sensory input from the periphery. The present study extends these findings by delineating the relationship between behavioral responses to formalin injection and spinal activation as measured by Fos expression. Our results demonstrate the time course by which STZ-induced diabetic mice develop increasingly diminished sensitivity to chemogenic noxious stimuli. Moreover, diabetic mice display reduced Fos expression in response to formalin, and these deficits parallel the progression of the behavioral abnormalities and are consistent with known diabetes-induced changes in neural anatomy and animal behavior (Christianson et al. 2003a; Christianson et al. 2003b). These results strengthen the

view that neuropathy induced in STZ-treated C57BL/6 mice can be used to explore sensory loss as a complication of diabetes.

Chemogenic Hypoalgesia in Diabetic C57Bl/6 Mice

Formalin injection into the hindpaw is a well-established model of chemogenic pain that causes an acute and a persistent secondary pain stimulus (Murray et al. 1988; McCall et al. 1996). Thought to arise from direct activation of primary afferent fibers, the acute phase elicits robust nocifensive responses toward the injected foot. During the second phase, these responses are induced by activation of sensory fibers as a secondary response to inflammation, although central sensitization of spinal neurons has also been posited as an additive mechanism (Puig et al. 1996; Abbadie et al. 1997). We previously reported reductions in behavioral responses of C57BL/6 diabetic mice during both phases of the formalin test 9 weeks post-STZ (Christianson et al. 2003b). It is important to note that the presence of hypoalgesia versus hyperalgesia is likely dependent on the strain and species, as studies in diabetic rats have reported chemogenic hyperalgesia during both the acute and inflammatory phases (Calcutt et al. 1996; Cesena and Calcutt 1999; Calcutt et al. 2000). Similarly, studies in outbred strains of diabetic mice have reported chemogenic hyperalgesia in response to formalin (Kamei et al. 1991; Kamei et al. 1993; Takeshita et al. 1997; Kamei et al. 2001).

Here, we demonstrate that as the neuropathy progresses, reduced behavioral responses do not emerge in Phase 2 until 3 weeks post-STZ. In comparison, deficits

during Phase 1 were not apparent until 5 weeks post-STZ. The precedent loss of the Phase 2 response suggests diabetes might initially affect inflammatory-associated aspects of pain. Such aspects may include the release or function of inflammatory mediators, the delivery of those mediators to the injury site (implicating microvascular occlusion), or the response of neurons to those mediators. Another explanation could be the specific loss of the fiber subtype responsible for the Phase 2 response, namely, the peptidergic c-fibers. The Phase 1 response appeared more resistant to diabetes and may reflect the degree of cutaneous innervation. This view is supported by recent studies in a Type 2 diabetes model (*db/db* mice) in which epidermal and dermal fiber density is normal in long-term hyperglycemic mice. These mice have reduced responses to formalin in Phase 2, but Phase 1 is normal (Wright et al. 2007).

Diabetes-Induced Suppression of Spinal Fos Expression in Response to Formalin

Formalin injection induces spinal Fos expression in a temporal and spatial pattern consistent with the magnitude of nociceptive input from the hindpaw (Presley et al. 1990; Abbadie et al. 1992). Here, formalin injection induced Fos expression in both nondiabetic and diabetic mice within the superficial (laminae I/II), middle (III/IV) and neck (V/VI) regions of the ipsilateral dorsal horn. Neurons in laminae I/II are the terminal targets of primary nociceptive afferents and project to deeper laminae and higher brain regions. Formalin-induced Fos expression in these laminae is driven monosynaptically by small nociceptive primary afferents activated in the

injected paw (Presley et al. 1990). In contrast, neurons in laminae III/IV respond to input from innocuous stimuli (Hunt et al. 1987; Bon et al. 2002). Neurons in lamina V/VI also receive direct input from primary nociceptive afferents; however, a recent report suggested laminae V/VI neurons also receive projections from lamina II neurons, project to pain-related brain regions and may be an important convergence point of sensory information (Braz et al. 2005). Collectively, the overall laminar distribution of Fos expression appears to code the nature of the stimulus as well as the nociceptive intensity perceived by the animal (Hunt et al. 1987; Bon et al. 2002).

Here, decreased spinal Fos expression in STZ-injected diabetic mice paralleled the progression of deficits in nocifensive responses to formalin injection. Significant reductions in Fos expression were evident in lamina I/II 3 weeks post-STZ, concomitant with reduced behavioral responses during Phase 2 of the formalin test. By weeks 5 and 7, the suppressed responses of Phase 1 and 2 were manifested in reduced Fos expression in all laminae. It is plausible that chronic hyperglycemia may directly attenuate Fos expression in the cord. Indeed, several studies have reported that diabetes reduces the expression of a wide range of genes in neural tissues (Purves and Tomlinson 2002). However, recent studies in rats report increased Fos expression in diabetic rats with pain, suggesting that Fos expression likely remains a reliable indicator of peripheral nerve input (Morgado and Tavares 2007).

As mentioned above, STZ-induced diabetic rats display increased sensitivity to thermal, tactile, and chemical stimuli. It has been proposed that the occurrence of hyperalgesia and allodynia in the seemingly incongruous presence of reduced

peripheral input (evidenced by reductions in intraepidermal nerve fiber density and diminished substance P release centrally) is the result of aberrant information processing at higher levels (Calcutt et al. 2000; Calcutt 2004; Lauria et al. 2005). Calcutt (2004) has suggested that studies showing an upregulation of spinal nociceptive mediators (Freshwater et al. 2002; Ciruela et al. 2003; Tomiyama et al. 2005; Dualhac et al. 2006) and increased electrophysiologic activity (Pertovaara et al. 2001; Chen and Pan 2002) in spinal neurons of diabetic rats support this hypothesis and imply an enhancement of spinal nociceptive processing (Calcutt 2004). However, our results demonstrating decreased Fos expression in the dorsal horn show this not to be the case in diabetic C57Bl/6 mice. Rather, our evidence suggests the reduced peripheral input in STZ-treated C57BL/6 mice results in decreased activation of the spinal cord by peripheral afferents and thus diminished pain perception.

Restoration of Stimulus-Induced Behavior and Fos Expression by Insulin

The Diabetes Control and Complications Trial and the Epidemiology of Diabetes Interventions and Complications follow-up study emphasized the importance of early interventions aimed at maintaining proper glycemic control for preventing neuropathy in human patients (Genuth 2006). In diabetic mice, insulin treatment has been shown to effectively restore mechanical and chemogenic behavioral responses (Christianson et al. 2003b). Here, we administered insulin to diabetic mice to test whether the diabetes-induced deficits in formalin responses and Fos expression were reversible. Diabetic mice given insulin resumed weight gain and

improved blood glucose levels. Although insulin-treated diabetic mice did not reach euglycemia, tail vein blood was collected without prior removal of mouse feed, and the high metabolic rate and frequent feeding behaviors of mice may have increased the variability of measurements and resulted in higher levels. Despite the lack of euglycemia at sacrifice, insulin-treated diabetic mice responded normally during Phase 2 of the formalin test, significantly improving over untreated diabetic mice. This improvement was also reflected in spinal Fos expression. Insulin administration increased the total number of dorsal horn Fos-positive cells, specifically in laminae I/II, which suggests insulin prevented the diabetes-induced reduction in Fos expression in response to formalin. The ability of insulin to restore the sensory deficits in diabetic mice is supportive of the view that these deficits are specific to the chronic hyperglycemia, although direct actions of insulin cannot be ruled out (Leinninger and Feldman 2005).

Neurotrophin Treatment Improves Stimulus-Induced Fos Expression

Neurotrophic support has long been thought to play a role in the progression of diabetic neuropathy, and as treatments neurotrophins have shown sporadic but encouraging effects on improving sensory deficits in diabetic neuropathy (Zochodne 1996; Leinninger et al. 2004). Our previous studies have utilized both NGF and GDNF in a number of settings to test their actions on sensory deficits in diabetic C57Bl/6 mice (Akkina et al. 2001; Christianson et al. 2003a; Christianson et al. 2003b). For example, intrathecal NGF treatment to diabetic mice increases

behavioral responses to mechanical and chemogenic stimuli, but had no effect on increasing peripheral innervation of the hindpaw. The increased behavior in the absence of effects on peripheral innervation may be explained by NGF's ability to sensitize afferents, leading to increased central input. Here, NGF again had a non-significant but positive effect on chemogenic hypoalgesia and increased the Fos-positive neurons in all laminae. If NGF's actions are indeed via peripheral sensitization, the increase in Fos expression in diabetic mice suggests NGF can sensitize afferents sufficiently to increase central activation and pain behavior.

In contrast to NGF, we have reported that GDNF treatment of diabetic mice restores pain behaviors, increases axonal density in skin, and improves staining of terminals in the dorsal horn (Akkina et al. 2001; Christianson et al. 2003a; Christianson et al. 2003b). Consistent with these actions, GDNF increased stimulus-induced Fos expression in the spinal cord, particularly in the deeper laminae. These effects are consistent with improved sensory innervation and function, leading to improved spinal activation and responses to painful stimuli. These results suggest both NGF and GDNF can influence spinal activation in response to peripheral stimulation. Accessing signaling pathways related to these neurotrophins may lead to increased sensation in patients with insensate symptoms.

Our results show that although there is a good correlation between behavior and Fos expression, there are subtle disconnects in the degree to which different measures of rodent somatosensation indicate pain sensitivity. Fos may be a more direct measure of afferent drive in response to a painful stimulus, whereas behavioral

responses to an injured limb are a sum of peripheral and central processing. Our studies suggest multiple measures should be performed to acquire the best evaluation of pain sensation.

VII. Chapter Three:

Selective deficits in nocifensive behavior despite normal cutaneous axon innervation in leptin receptor null mutant (*db/db*) mice.

1. Abstract

Much of our understanding of the effects of diabetes on the peripheral nervous system is derived from models induced by streptozotocin (STZ) in which hyperglycemia is rapidly caused by pancreatic beta cell destruction. Here, we quantified sensory impairments over time in leptin receptor (leptr) null mutant (-/-) mice, a type 2 model of diabetes in which the absence of leptin receptor signaling leads to obesity and chronic hyperglycemia by 4 weeks of age. To assess these mice as a model for peripheral neuropathy, we quantified the responsiveness of leptr (-/-) mice to noxious mechanical, thermal and chemogenic stimuli, as well as epidermal and dermal innervation of the hind paw. Compared to wildtype (+/+) and heterozygous (+/-) mice, leptr (-/-) mice displayed reduced sensitivity to mechanical stimuli by 6 weeks of age; however, responses to noxious heat were normal. Leptr (-/-) also devoted less activity to their injected paw during the 2nd phase following formalin administration. However, epidermal and dermal innervation of leptr (-/-) mice was not different from that of leptr (+/+) and (+/-) mice even after 10 weeks of hyperglycemia, suggesting that cutaneous innervation is resistant to chronic hyperglycemia in these mice. These results suggest that certain rodent nocifensive behaviors may be linked to the abundance of cutaneous innervation, while others are not. Finally, these results reveal that the leptr (-/-) mice may not be useful to study neuropathy associated with distal axonal degeneration, but may be better suited for studies of hyperglycemia-induced sensory neuron dysfunction without distal nerve loss.

2. Introduction

In the previous study, the integrity of peripheral afferents and their connections with dorsal horn neurons was assessed using an indirect measure: spinal Fos expression. We found it to be a reliable indicator of peripheral nerve function in an STZ-induced type 1 diabetes model. However, this surrogate is not only dependent upon the presence and function of primary afferents, but also on their ability to activate second order neurons and indeed on the ability of second order neurons to upregulate Fos expression. Therefore, we adopted a more direct approach for the next set of experiments and directly evaluated cutaneous innervation by peripheral afferents.

The prevailing approach in modeling diabetic neuropathy in rodents has been STZ-injection, as we used in the previous study. However, the vast majority of the diabetes population is associated with type 2, which involves slower disease progression and obesity (Vinik et al. 2006). *Db/db* mice are well known for their presentation of hyperglycemia and obesity, and these mice have been used to assess diabetes complications (Ktorza et al. 1997; Dong and Ren 2007; Belmadani et al. 2008; Kolavennu et al. 2008). It is now known that the phenotype in *db/db* mice is due to miscoding in the leptin receptor (leptr; Chen et al., 1996; Chua et al., 1996). In terms of neuropathic complications, studies report nerve conduction velocity deficits, morphological and metabolic changes, and behavioral changes suggestive of nerve damage (Sima and Robertson 1978; Carson et al. 1980; Norido et al. 1984; Vitadello et al. 1985; Berti-Mattera and Eichberg 1988; Bianchi et al. 1990; Walwyn et al.

2006). However, many of these pathologies suggest damage to primarily larger sensory and motor fibers (Sima and Robertson 1978).

In humans, significant attention has been focused on degenerative changes in cutaneous innervation. Skin biopsy analysis has shown correlations between neuropathy and reduced epidermal innervation, leading to the use of epidermal quantification from skin biopsies as a common diagnostic tool (Kennedy et al. 1996; Herrmann et al. 1999; Lauria et al. 2005). Indeed, reductions in intraepidermal nerve fiber (IENF) density appear early in the diabetes progression (Smith and Singleton 2006), suggesting this approach may be favorable to electrophysiological assessments that focus on large fiber deficits and often fail to uncover small fiber damage.

In the current study, we assessed the behavioral responses of leptr null mutant (-/-) mice to a variety of sensory stimuli and evaluated epidermal and dermal innervation. Our results demonstrate that leptr (-/-) mice develop modality-specific behavioral deficits despite the lack of demonstrable axon loss in the epidermis and dermis. These results suggest this model may be favorable to study hyperglycemia-induced sensory neuron dysfunction without peripheral nerve loss.

3. Experimental Procedures

Leptr Null Mutant Mice (db/db mice)

All animal use was in accordance with NIH guidelines and conformed to the principles specified by the University of Kansas Medical Center Animal Care and Use Protocol. Male and female leptr mice (Strain Name: BKS.Cg-*m* +/+ *Lepr*^{db}/J)

were purchased from the Jackson Laboratory and housed in the Laboratory Animal Resources Facility at the University of Kansas Medical Center under pathogen-free conditions. A breeding colony was established to generate animals with each genotype, and mice were maintained on an 8604 Harlan Teklad Rodent diet. Mice were housed 2-4 mice per cage on a 12:12-hour light/dark cycle with free access to mouse chow and water. Genotypes for leptr (+/+), (+/-), and (-/-) mice were confirmed using polymerase chain reaction analysis from tail DNA. Mice were weighed at weekly intervals and blood glucose levels were measured using glucose diagnostic reagents (Sigma, St. Louis, MO). All homozygous mice displayed obesity, polydipsia, and polyuria. Weight and blood glucose levels were compared between leptr (+/+), (+/-), and (-/-) mice using repeated measures analysis of variance (RM ANOVA) followed by post hoc analysis using the Fisher's protected least significant differences (PLSD) test.

Behavioral Assessments

Behavioral experiments could not be performed blindly due to the vastly different appearance of the leptr (-/-) mice compared with leptr (+/-) and (+/+) mice. However, all behavioral measurements were performed randomly among anaimals of all genotypes to reduce bias among groups.

Mechanical

All genotypic groups were tested weekly for behavioral responses to mechanical stimuli using calibrated von Frey monofilaments (Stoelting, Wood Dale,

IL). All mice were acclimated for 1 hour to the behavior room, the VonFrey testing table, and the procedure two times prior to the first testing day. Morever, mice were placed in the testing room for 1 hour before each testing session. Mice were placed under clear plastic chambers (3 X 8 X 12 cm) atop of a wire mesh-top table and allowed to habituate for 30 minutes. Responses to a single monofilament were recorded for each animal using a 1 g von Frey monofilament applied to the middle plantar surface of the hind paw, and trials alternated between right and left paws. Previous studies have demonstrated that a 1.4 gm monofilament results in withdrawals approximately 30-60% of the time (Christianson et al. 2003b; Gandhi et al. 2004). The percent response was obtained by determining the number of withdrawals in response to six separate monofilament applications. Comparisons were made between test groups using RM ANOVA and Fisher's PLSD.

In addition, mechanical sensitivity of additional groups of mice was measured using a dynamic plantar aesthesiometer (Ugo Basile 37400; Stoelting). These measurements were performed by placing the plantar aesthesiometer beneath the hind paw and allow the actuator filament (0.5 mm diameter) to advance and exert increasing force during a 6 s interval. The maximum force elicited was 8 g. Mechanical sensitivity was measured as the force that elicited a paw withdrawal. The mean force necessary to elicit a response was obtained by determining the number of withdrawals in response to three separate applications to alternating paws, and the average for each genotypic group was compared using RM ANOVA decomposed with Fisher's PLSD.

Radiant Heat

Mice were tested weekly for behavioral responses to thermal stimuli using a radiant heat source applied to the plantar surface of the hind paw. Similar to vonFrey testing, mice were acclimated to the room and testing procedure two times prior to the initial testing. All mice were placed under plastic chambers on a heated glass surface of a Hargreaves' apparatus (UARDG, University of California) and allowed to habituate for 15 minutes. An acute thermal stimulus from a high-intensity projector lamp bulb (Eiko CXL/CXR, 8V, 50W, Japan) was focused to the plantar surface of the hind paw from beneath the glass surface. The stimulus lamp intensity was calibrated to 4.75 amperes of current, and paw withdrawal latency was measured to the nearest 0.01sec. This current level produces a heating rate of 1.6°C/sec, which is appropriate for activating C-fibers (Yeomans et al. 1996; Dirig et al. 1997). Tests were performed in triplicate, alternating between right and left paws to allow skin temperature to normalize prior to the next test. The average latency from both feet was quantified for each animal, and the average for each genotypic group was compared using RM ANOVA and Fisher's PLSD.

Chemogenic

Formalin tests were performed just prior to sacrifice on 16-week old mice. Twenty microliters of formalin (5%, diluted in saline) was injected subcutaneously in the dorsal surface of the right hind paw using a 1cc insulin syringe and 28-gauge needle. The amount of time spent licking or biting the injected paw or leg was visually measured in 5-minute intervals for one hour (Murray et al. 1988).

Differences in the time devoted to the inflamed foot were compared between genotypic groups using RM ANOVA and Fisher's PLSD. Additionally, the amount of time devoted to the injected foot was also summed in two windows during the acute (Phase 1; 0-15 min post-injection) and inflammatory (Phase 2; 30-50 min post-injection) phases of the formalin test. Differences between groups during Phase 1 and 2 were compared using two-way ANOVA followed by Fisher's PLSD.

Hind paw Cutaneous Innervation

Tissue Collection

Following the formalin test, mice were deeply anesthetized with Avertin (1/25% v/v tribromoethanol, 2.5% tert-amyl alcohol, Sigma, St. Louis, MO; 200 µL/10g body weight). The plantar surface of the left hind paw was dissected and lightly post-fixed for 1 hour in Zamboni's fixative (4% paraformaldehyde, 14% saturated picric acid, 0.1 M phosphate buffered saline [PBS]; pH 7.4; 4°C), rinsed in PBS for 24 h, then immersed overnight in 30% sucrose at 4°C. Tissue was frozen in OCT and sectioned on a cryostat at 30 µm. Sections were mounted on Superfrost Plus slides (Fisher Scientific, Chicago, IL) and stored at -20°C until immunostaining. Tissue sections from different animals were coded to blind the experimenter during the analysis of epidermal and dermal fiber density.

Immunohistochemistry

After thawing 5 min. at room temperature, slide-mounted tissue was circled with a Pap Pen to create a hydrophobic ring (Research Products International).

Tissues sections were then covered with a blocking solution (0.5% porcine gelatin, 1/5% normal goat serum, 0.5% Triton-X, Superblock buffer [Pierce, Rockford, IL]) for 1 hr. at room temperature. For epidermal innervation, a rabbit anti-PGP 9.5 primary antibody (1:400; Ultraclone Cambridge, UK) and a goat anti-rabbit secondary antibody (Alexa 555; 1:2000; Molecular Probes, Eugene, OR) were used to label all axons in the skin. For myelinated dermal innervation, a rabbit anti-NF-H primary antibody (#AB1991, 1:500; Chemicon, Temecula, CA) and a donkey anti-rabbit secondary antibody (Alexa 488; 1:2000; Molecular Probes) were used to visualize all myelinated axons in the dermis. The polyclonal anti-NF-H primary antibody is not affected by the level of neurofilament phosphorylation. Primary antibodies were diluted in blocking solution, and sections were incubated overnight at 4°C in a humidified tray. For visualization, sections were washed 3 x 5 min. with PBS followed by incubation for 1 hr. with secondary antibodies diluted in PBS. Following three washes with PBS, slides were coverslipped and stored at 4°C.

Epidermal Axon Quantification

Intraepidermal nerve fiber (IENF) density was quantified according to recently published guidelines (Lauria et al. 2005). Six randomly chosen tissue sections were quantified from each animal. For each section, three frames of view at 40X magnification were randomly chosen for quantification, and the length of the dermal/epidermal junction in each frame was measured using NIH ImageJ. Only single PGP 9.5+ axons crossing the dermal-epidermal junction were counted, excluding secondary branching and nerve fragments not crossing the dermal-

epidermal junction. The number of IENF/mm in each of three frames of view was averaged for each section, and the average of 6 sections yielded the mean IENF density for each animal. Comparisons between groups were made using a one-way ANOVA.

Dermal Myelinated Axon Quantification

Six randomly chosen tissue sections were quantified from each animal, with at least 150 µm between sections. For each section, three frames of view at 20X magnification were randomly chosen for quantification. The dermal area occupied by NF-H+ immunoreactivity within 100 µm of the dermal-epidermal junction was calculated as a percent of the total area measured using ImageJ (NIH). The percent area occupied by NF-H+ immunoreactivity in each of three frames of view was averaged for each section, and the average of six sections yielded the mean percent area for each animal. Comparisons between groups were made using a one-way ANOVA.

4. Results and Figures

Obesity and hyperglycemia in leptr (-/-) mice

As a consequence of mutations in the leptin receptor, leptr (-/-) mice develop severe obesity and chronic hyperglycemia beginning at 3-4 weeks of age. Here, examination of 8 week old mice leptr (-/-), (+/-), and (+/+) revealed that leptr (-/-) mice had already developed substantial weight gain and hyperglycemia compared to both leptr (+/+) and (+/-) counterparts (**Figure VII-1A, B**; $p < 0.05$). The leptr (-/-)

Figure VII-1. Blood Glucose and Weights of Leptr Mice

Weight and blood glucose levels of leptr (+/+, n = 5), (+/-, n = 5), and (-/-, n = 5) mice from 9-16 weeks of age. **(A)** Obesity has already developed in leptr (-/-) mice by 9 weeks of age. **(B)** Similarly, leptr (-/-) mice have already developed persistent hyperglycemia. Weight is in grams, glucose levels are mmol/L. Data plotted as means ± SEM. * denotes significant difference between (+/+) and (-/-) mice ($p < 0.05$).

Figure VII-1

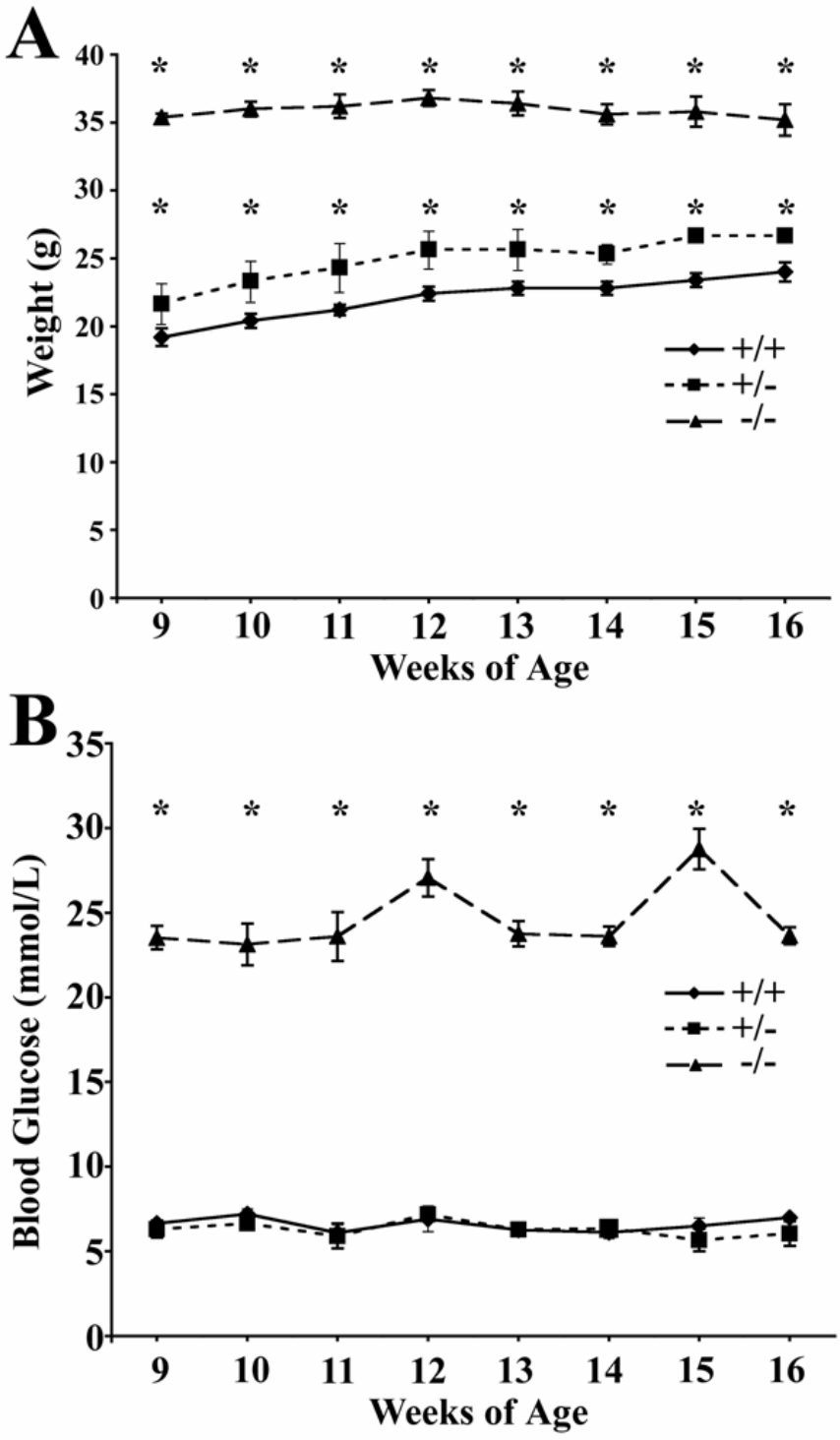
A
Weight (g)
40
35
30
25
20
15
10
5
0
9
10
11
12
13
14
15
16
Weeks of Age
+/+
+/-
-/-
B
Blood Glucose (mmol/L)
35
30
25
20
15
10
5
0
9
10
11
12
13
14
15
16
Weeks of Age
+/+
+/-
-/-

mice approached 35 grams and their weight was maintained at this level until sacrificed at 16 weeks of age. In comparison, the leptr (+/-) mice slowly gained weight during the study similar to the leptr (+/+) mice. Neither the leptr (+/-) nor or (+/+) mice reached above 25 grams, typical of normal healthy mice (**Figure VII-1A**). However, the weights of leptr (+/-) mice were significantly different from those of leptr (+/+) mice ($p < 0.05$).

Similar to weight, leptr (-/-) mice already displayed significant hyperglycemia by 8 weeks of age (**Figure VII-1B**). Blood glucose levels in leptr (-/-) mice consistently ranged from 23-38 mmol/L, which is well above the normal 16 mmol/L standard for diabetes. Blood glucose levels of leptr (+/-) mice were not significantly different from those of their wildtype counterparts ($p > 0.05$).

Behavioral responses to sensory stimulation of the hind paw

Withdrawal to noxious radiant heating of the paw was tested weekly beginning at 9 weeks of age (**Figure VII-2A).** Throughout the testing period, no significant differences were detected in response latencies among leptr (+/+), (+/-), and (-/-) mice.

In contrast to thermal responses, behavioral responses to mechanical stimuli were significantly different in leptr (-/-) mice (**Figure VII-2B**). At 9 weeks of age, leptr (-/-) mice already displayed significantly fewer withdrawal responses to a 1 gm von Frey monofilament applied to the plantar surface the hind paw, suggesting tactile hypoalgesia. Because the reduced tactile responses were present at the onset of

Figure VII-2: Behavioral responses of leptr mice to noxious thermal and mechanical stimulation.

(A) Behavioral responses to radiant noxious heat stimuli were evaluated weekly in leptr (+/+, n = 7), (+/-, n = 5), and (-/-, n = 6) mice from 9 to 16 weeks of age. Leptr (-/-) mice displayed similar latencies to paw withdrawal as leptin (+/+) and (+/-) mice, suggesting no overt changes in thermal thresholds during these ages.

(B) Behavioral responses to a 1 g von Frey monofilament were evaluated weekly in leptr (+/+, n = 7), (+/-, n = 5), and (-/-, n = 6) mice from 9 to 16 weeks of age. Overall, leptr (-/-) mice displayed significantly reduced withdrawal responses to a monofilament applied to the plantar surface the hind paw. Data plotted as means ± SEM. * denotes significant difference between (+/+) and (-/-) mice ($p < 0.05$).

Figure VII-2

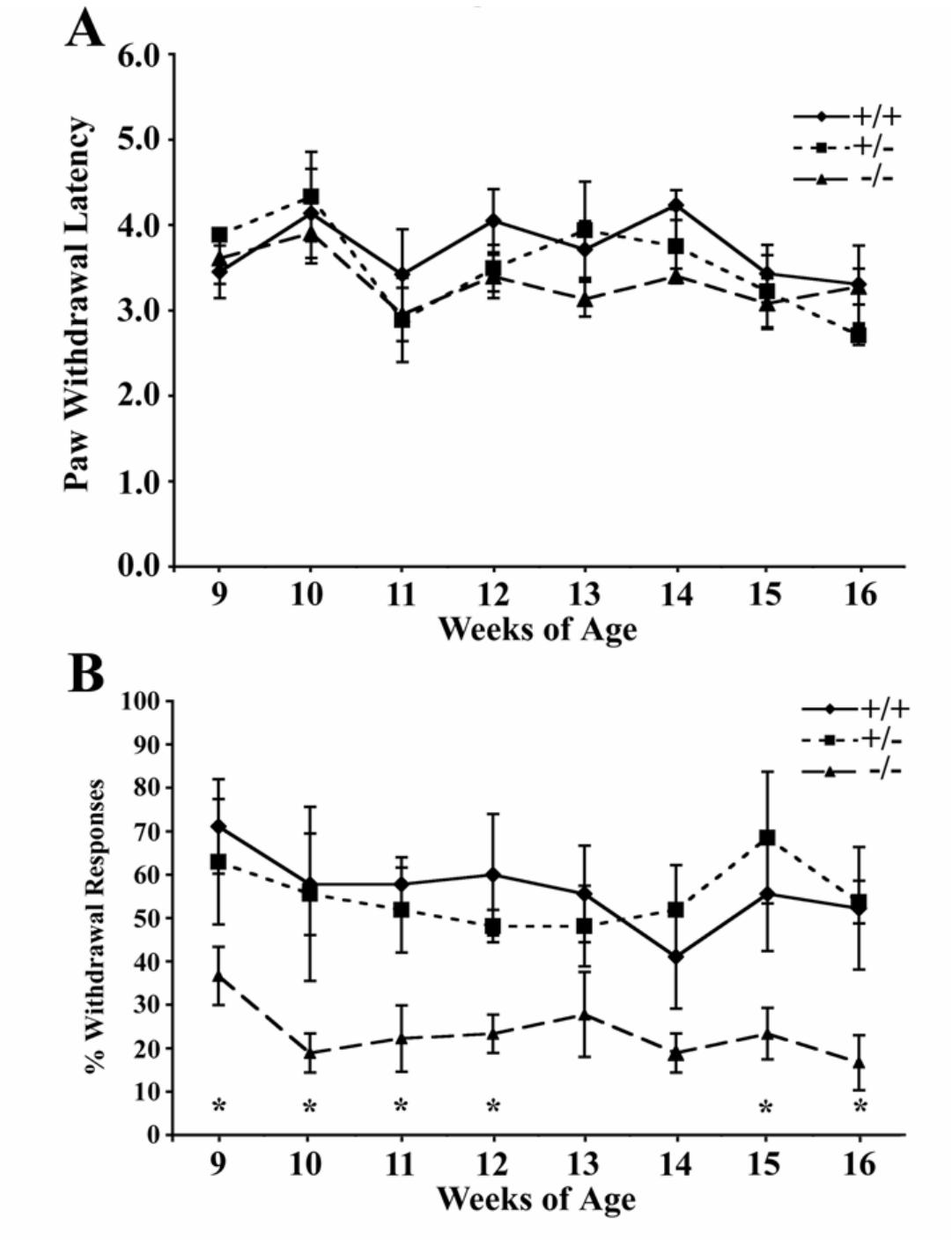
A
Paw Withdrawal Latency
6.0
5.0
4.0
3.0
2.0
1.0
0.0
+/+
+/-
-/-
9
10
11
12
13
14
15
16
Weeks of Age
B
% Withdrawal Responses
100
90
80
70
60
50
40
30
20
10
0
+/+
+/-
-/-
*
*
*
*
*
*
9
10
11
12
13
14
15
16
Weeks of Age

testing, additional groups of mice were tested beginning at 4 weeks of ages using a dynamic plantar aesthesiometer (**Figure VII-3A**). At 4 weeks of age, all 3 genotypes were identical in their responses to tactile stimulation. By 6 weeks of age, leptin (-/-) mice began to display much higher thresholds than leptr (+/-) and (+/+) littermates. This tactile hypoalgesia generally continued as long as the animals were tested (16 weeks). The blood glucose measurements and weights of the specifics groups tested are shown in **Figure VII-3B** and **C**, revealing concomitant increases in weight and blood glucose during these early ages (Fig. 3B, C). Importantly, tactile allodynia was never observed in leptr (-/-) mice.

Leptr (-/-) mice display abnormal responses in phase II of the formalin test.

Behavioral responses to 5% formalin injected into the right hindpaw were evaluated in leptr (+/+), (+/-), and (-/-) mice at 16 weeks of age (**Figure VII-4A**). Leptr (+/+) mice displayed the typical responses to formalin in a biphasic manner. Phase 1 begins immediately after injection and lasts for roughly 15 minutes, followed by a lull in activity, and then followed by an increase in activity in phase II. Phase I is proposed to be driven by direct activation of C- and Aδ-fibers, while phase II is thought to be caused by inflammation-driven C-fiber input and by central sensitization (Murray et al. 1988). Leptr (+/-) mice were not different from leptr (+/+) mice in either stage. Leptr (-/-) mice displayed a similar response to formalin injection during Phase I (**Figure VII-4A, B**). However, leptr (-/-) mice displayed substantially reduced responses to formalin in Phase II (**Figure VII-4A, B**).

Figure VII-3: Leptr (-/-) mice display reduced responsiveness to mechanical stimuli by six weeks of age.

Behavioral responses to mechanical stimuli were evaluated weekly in leptr (+/+), (+/-), and (-/-) mice during periods when obesity and hyperglycemia were developing. By 6 weeks of age, leptr (-/-) mice begin to display reduced responses to mechanical stimulation of the hindpaw. Quantification of mechanical sensitivity was measured using a plantar aesthesiometer that elicits an increasing force to the plantar surface of the paw. Latencies to paw withdrawal were significantly longer in leptr (-/-) mice after 6 weeks of age. Data plotted as means ± SEM. * denotes significant difference between (+/+) and (-/-) mice ($p < 0.05$).

Figure VII-3

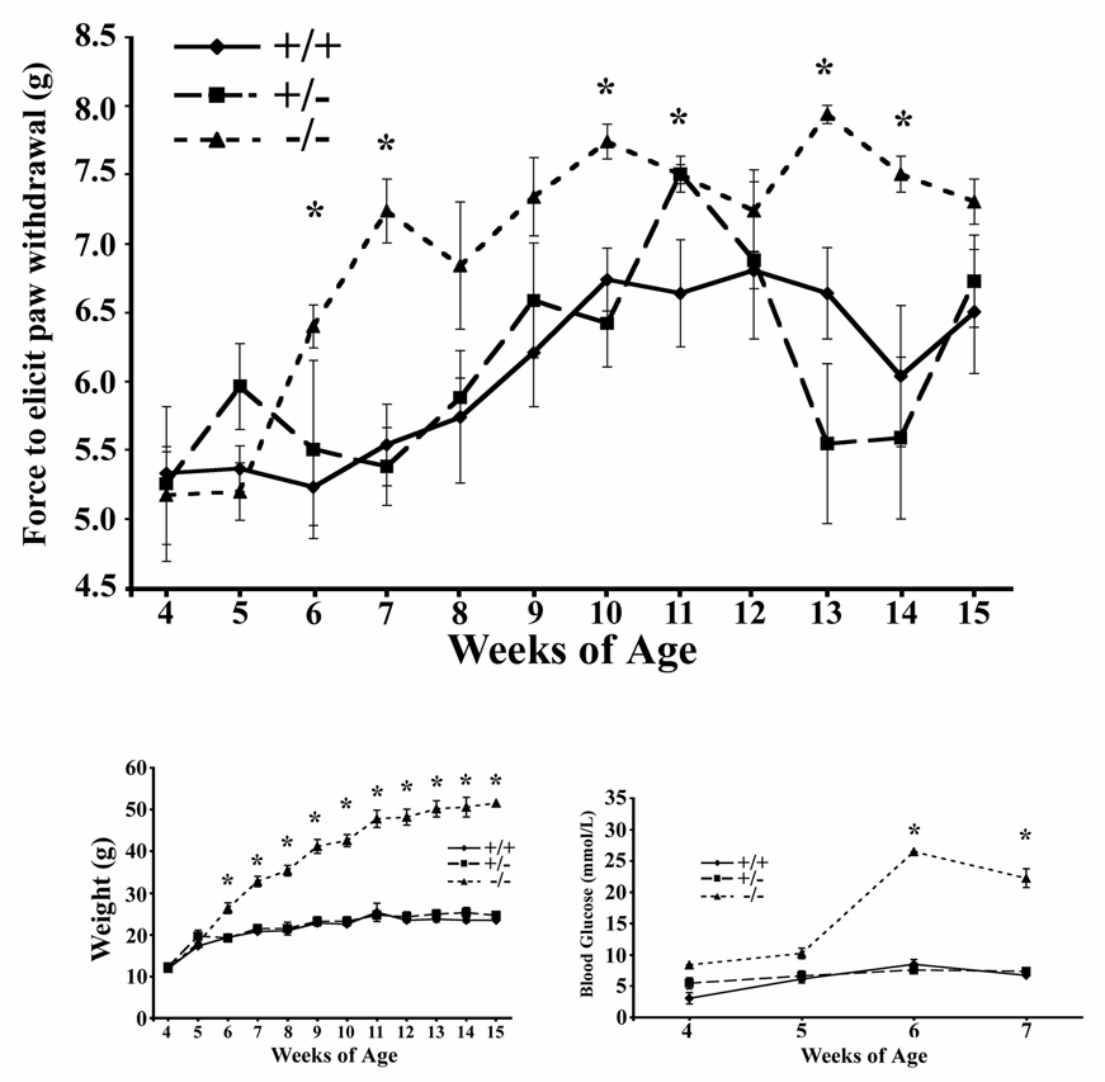
Force to elicit paw withdrawal (g)
8.5
8.0
7.5
7.0
6.5
6.0
5.5
5.0
4.5
+/+
+/-
-/-
4 5 6 7 8 9 10 11 12 13 14 15
Weeks of Age
Weight (g)
60
50
40
30
20
10
0
+/+
+/-
-/-
4 5 6 7 8 9 10 11 12 13 14 15
Weeks of Age
Blood Glucose (mmol/L)
35
30
25
20
15
10
5
0
+/+
+/-
-/-
4 5 6 7
Weeks of Age

Figure VII-4: Leptin (-/-) mice display abnormal responses during Phase 2 of the formalin test.

(A) Behavioral responses to 5% formalin injected into the right hindpaw were evaluated in leptr (+/+), (+/-), and (-/-) mice at 16 weeks of age. Compared to leptr (+/+) and (+/-) mice, leptr (-/-) mice devoted similar amounts of time to the injected foot during Phase I compared to leptr (+/+) and (+/-) mice. In contrast, leptin (-/-) mice displayed significantly reduced responses to formalin during Phase 2.

(B) Data plotted for Phase 1 consists of the total time devoted to the injected foot during the first 15 (0-15) minutes, while activity within Phase 1 was pooled from 30-50 minutes. Leptr (-/-) mice only showed significant deficits in Phase 2. Data plotted as means ± SEM. * denotes significant differences between (+/+) and (-/-) mice ($p < 0.05$).

Figure VII-4

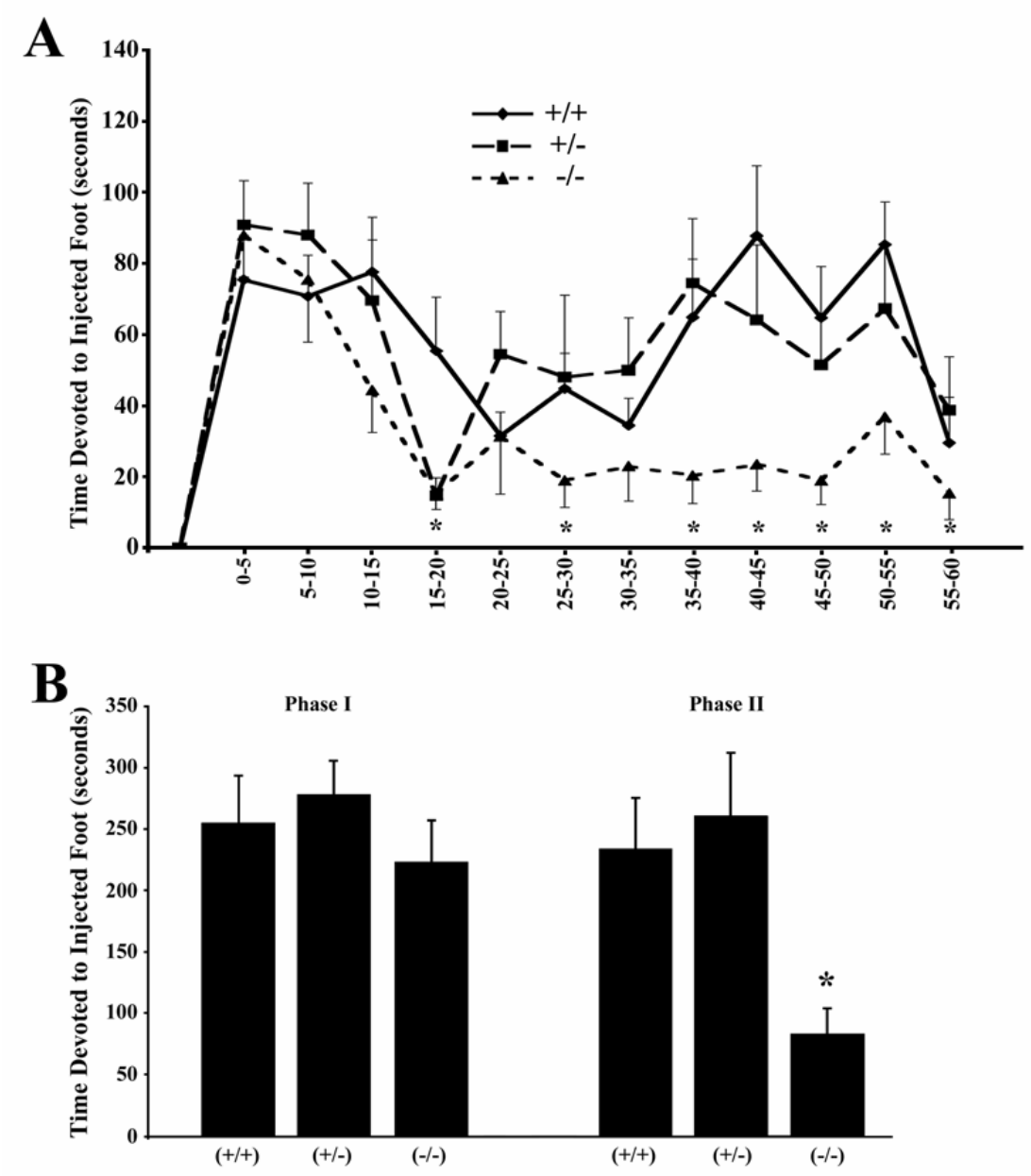
A
Time Devoted to Injected Foot (seconds)
140
120
100
80
60
40
20
0
+/+
+/-
-/-
*
0-5
5-10
10-15
15-20
20-25
25-30
30-35
35-40
40-45
45-50
50-55
55-60
B
Time Devoted to Injected Foot (seconds)
350
300
250
200
150
100
50
0
Phase I
Phase II
*
(+/+)
(+/-)
(-/-)
(+/+)
(+/-)
(-/-)

Cutaneous axon abundance in the hind paw is normal in leptr (-/-) mice.

To address if the behavioral responses to sensory stimulation were associated with reduced cutaneous innervation, sections of hind paw skin were processed for immunohistochemistry to quantify epidermal and dermal innervation in mice 16 weeks of age (**Figure VII-5, 6**). PGP 9.5 ubiquitously labels all axons, and we used PGP 9.5 to quantify axon density within the epidermis (**Figure VII-5A, C, E**). Analysis of the epidermis in leptr (+/+) mice revealed typical patterns of innervation of the mouse paw, with individual axons penetrating the epidermis and coursing to the outer layers (**Figure VII-5A**). Surprisingly, similar axonal distributions and epidermal fiber counts were evident in leptr (+/-) and (-/-) mice (**Figure VII-5C, E**, $p > 0.05$).

A major sensory deficit displayed by leptr (-/-) mice was reduced mechanical responsiveness. Mechanical sensitivity involves myelinated Aβ fiber input from dermal sensory receptors, we hypothesized that the content of myelinated fibers within the dermis may be abnormal in leptr (-/-) mice. Immunohistochemistry using antibodies to the heavy chain of neurofilament H were used to label all myelinated axons terminating in the dermis of the hind paw (**Figure VII-5B, D, F**). Myelinated fibers in the dermis course along within fascicles and then extend superficially as small fascicles or individual fibers, many of which terminate at the dermal/epidermal border. Similar to unmyelinated fibers in the epidermis, the abundance of myelinated fibers in leptr (+/+), (+/-) and (-/-) mice was not significantly different (**Figure VII-5B, D, F; Figure VII-6B**, $p > 0.05$).

Figure VII-5: Epidermal and myelinated dermal axons appear normal in leptr (-/-) mice.

(A, C, E) Immunohistochemical labeling of PGP 9.5+ axons in glabrous skin from the footpad of (A) leptr (+/+), (C) leptr (+/-), and (E) leptr (-/-) mice. PGP 9.5+ axons penetrate into the epidermis and extend out to the superficial layers. Individual axons were evident (horizontal arrows) in the epidermis of all three genotypes.

(B, D, F) Immunohistochemical labeling of NF-H+ axons in the dermis of the footpad of (B) leptr (+/+), (D) leptr (+/-), and (F) leptr (-/-) mice. NF-H+ axons course through the dermis in small to medium fascicles and then terminate as punctate endings associated with Merkel cells or Meissner's corpuscles (angled arrows). The profile of NF-H+ myelinated axons in the dermis appeared similar in all three genotypes. Scale bar = 50 µm for panels (A, C, and E); 100µm for panels (B, D, and F).

Figure VII-5

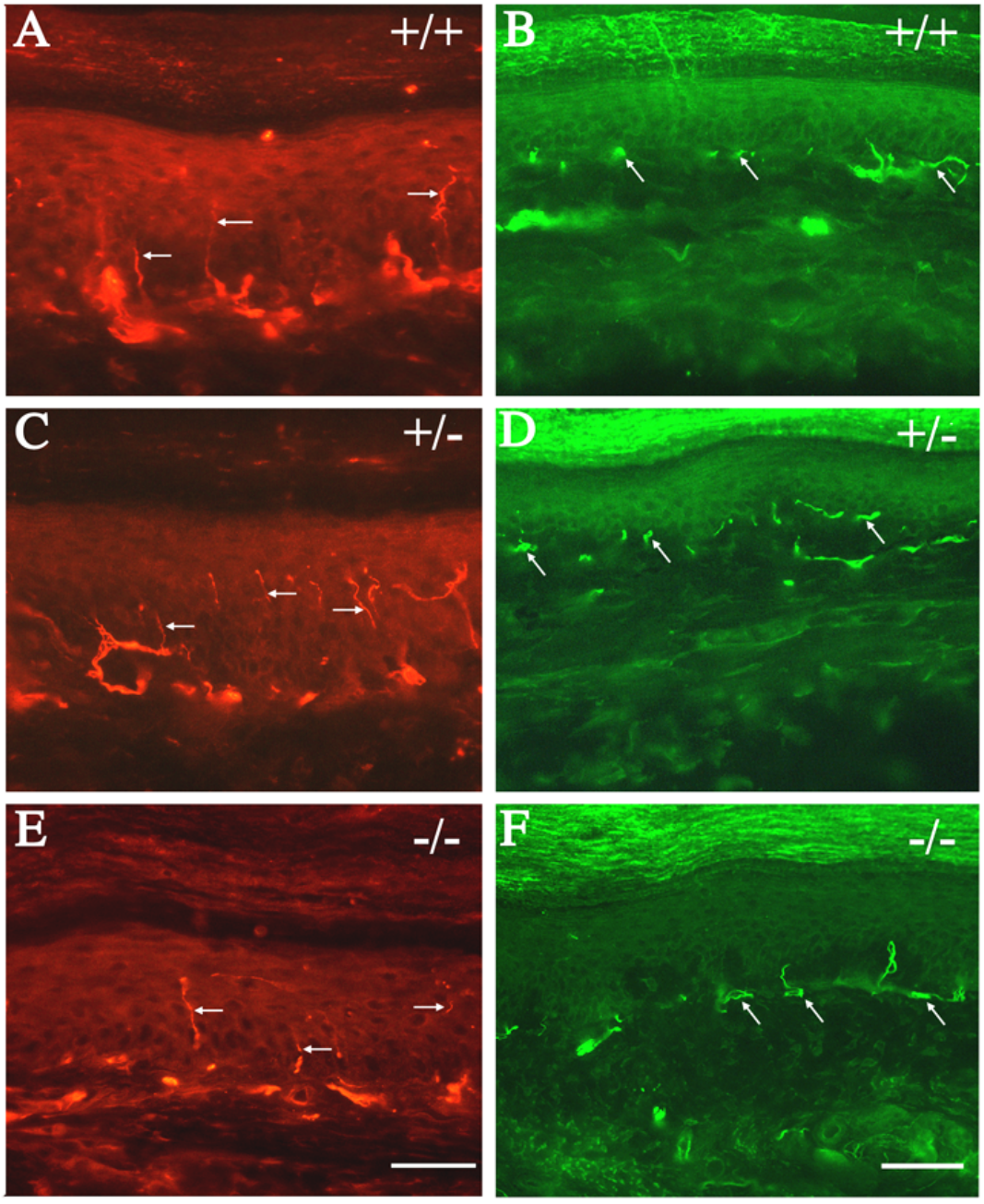

Figure VII-6: Quantification of axon abundance in the epidermis and dermis of leptr mice.

(A) Intraepidermal axon abundance was determined according to criteria outlined for human IENF quantification (Lauria et al., 2005). No significant differences were detected among leptr (+/+), (+/-), or (-/-) mice ($p > 0.05$).

(B) The abundance of NF-H+ myelinated axons in the dermis was determined using NIH ImageJ by measuring the amount of dermal area occupied by NF-H+ axons. Again, no significant differences were detected among leptr (+/+), (+/-), or (-/-) mice ($p > 0.05$).

Figure VII-6

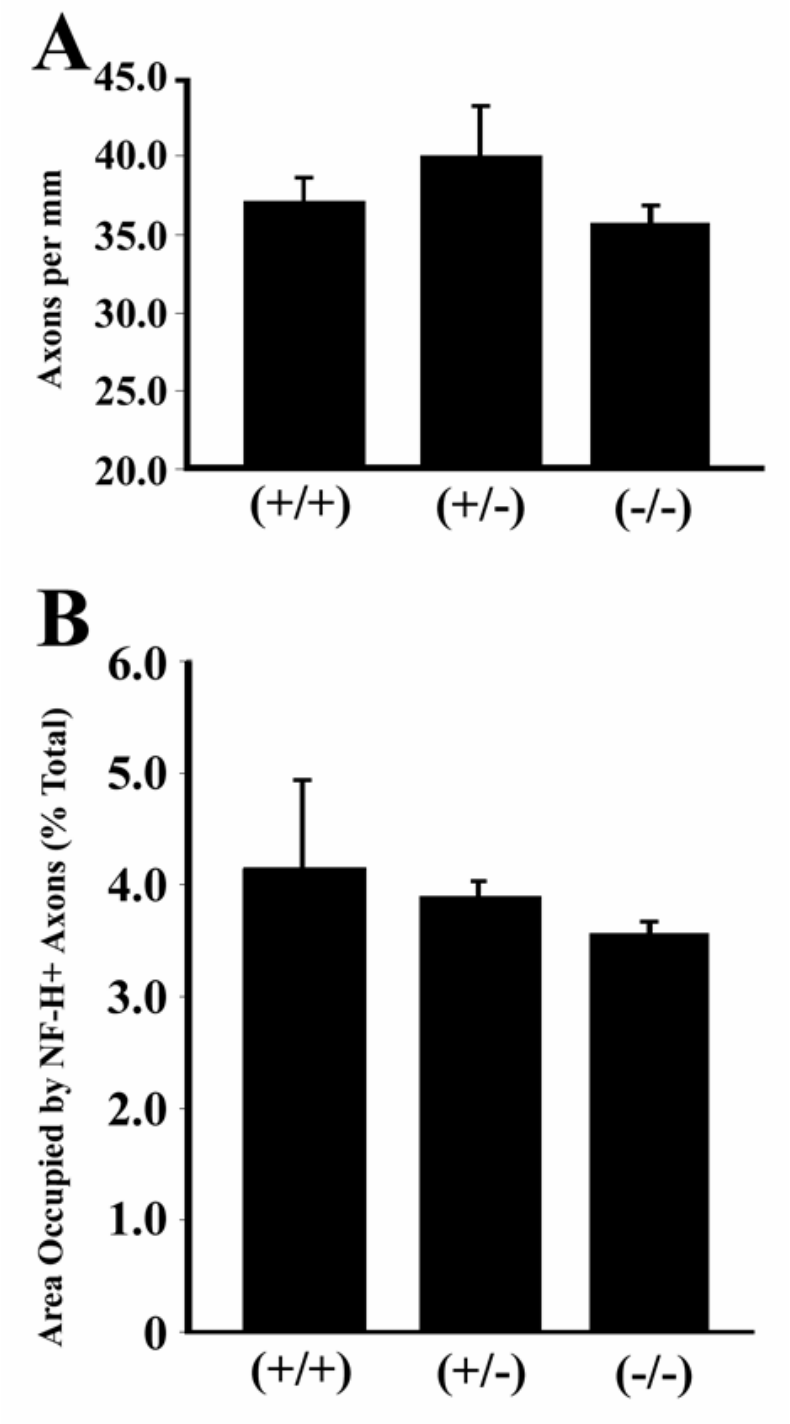
A
45.0
40.0
35.0
30.0
25.0
20.0
Axons per mm
(+/+)
(+/-)
(-/-)
B
6.0
5.0
4.0
3.0
2.0
1.0
0
Area Occupied by NF-H+ Axons (% Total)
(+/+)
(+/-)
(-/-)

5. Discussion

The incidence of neuropathy in patients with diabetes is rapidly increasing, and accurately mimicking sensory deficits in humans using rodent models has proven problematic. This issue is complicated by the diversity of symptoms displayed by humans, including large- versus small-fiber (or both) and painful versus insensate (or both). Here, we examined leptr null mutant mice, with particular attention to sensory deficits and the innervation of the plantar surface of the hind paw. As a model of type 2 diabetes, leptr (-/-) mice develop obesity and hyperglycemia after 4 weeks of age. Behaviorally, leptr (-/-) mice display reduced responsiveness to von Frey stimulation and the second stage of formalin, which may be related to impaired inflammatory responses and/or central sensitization. Surprisingly, however, leptr (-/-) mice show no quantitative deficits in epidermal or dermal innervation at 16 weeks of age, despite the presence of the behavioral abnormalities in response to mechanical and chemogenic stimuli. Collectively, these findings suggest that as a model of type 2 diabetes, the neuropathological complications are selective, and behavioral changes can exist in the absence of overt axonal loss.

Leptr (-/-) mice as a model of type 2 diabetes

The leptr (-/-) or *db/db* mice have been studied as a model of obesity-induced diabetes for nearly 30 years. These animals are obese, hyperglycemic, and hyperinsulemic (Garris and Garris 2005). Neural complications have been reported in these mice, including impaired nerve conduction velocity, large-fiber axonal atrophy,

impaired axonal transport, and thermal hypoalgesia. Many of these pathological problems have been detected in mice 6 months or older, consistent with the view that many of the neural complications in the leptr (-/-) mice are subtle and require longer time periods to develop (Sima and Robinson 1978).

Recently, neural complications have been reported in leptin null mutant mice (*ob/ob* mice, Drel et al. 2006). In these mice, leptin is not produced and these mice develop obesity. Although these mice are hyperinsulinemic, they appear to have somewhat lower blood glucose levels than the leptr (-/-) mice (Drel et al. 2006). However, neural complications seem to appear more severe at earlier ages in *ob/ob* mice compared to the leptr mice studied here. By 11 weeks of age, the *ob/ob* mice had already developed sensory and motor nerve conduction velocity deficits, thermal hypoalgesia, tactile hyperalgesia, and substantial loss of nerve fibers in the epidermis of the hindpaw (Drel et al. 2006). The thermal hypoalgesia, tactile hyperalgesia and reduced epidermal innervation in the *ob/ob* mice differ from our observations in the leptr (-/-) mice, and these differences will be discussed below.

Thermal Sensitivity

Throughout the testing period, the leptr (-/-) never displayed altered thermal thresholds compared to leptr (+/+) or (+/-) mice, suggesting the sensitivity to noxious heat was normal during these early stages of chronic hyperglycemia. Previous studies have demonstrated thermal hypoalgesia in leptr (-/-) mice, but these changes only become detectable after 6 months of age (Walwyn et al. 2006). Because thermal

sensitivity is mediated by small C-fibers, it shouldn't be surprising that thermal thresholds were not altered in light of normal epidermal innervation in the leptr (-/-) mice, and it is reasonable to suggest that diabetes-induced abnormal thermal thresholds best reflect C-fiber damage. This view is supported by the presence of thermal hypoalgesia in the *ob/ob* mice that undergo severe epidermal loss, as well as by studies in human patients that report strong correlations between abnormal thermal sensitivity and reduced IENF densities (Pan et al. 2001; Pan et al. 2003; Chiang et al. 2002; Pittenger et al. 2004; Shun et al. 2004; Drel et al. 2006). Finally, because the leptr (-/-) were so corpulent, we were concerned that their size may actually impede their ability to perform an appropriate hind limb withdrawal. However, their normal withdrawals from noxious thermal stimuli revealed they were capable of normal hind limb movements.

Mechanical Sensitivity

The reported responses of diabetic rodents to tactile stimulation are quite mixed but shound not be surprising in light of the variability displayed by human patients with neuropathy. In humans, mechanical sensitivity ranges from no sensation to severe tactile allodynia. Here, leptr (-/-) mice consistently displayed reduced responsiveness to mechanical stimuli and never displayed increased sensitivity. This reduction appeared at about 6 weeks of age, lagging just behind overt hyperglycemia and obesity. We have previously reported that, using both the up-down method and percent withdrawal, STZ-induced diabetic C57BL/6mice

displayed reduced sensitivity to mechanical stimulation 4-5 weeks after diabetes induction (Christianson et al. 2003b). In STZ-induced rats, increased mechanical sensitivity has predominantly been observed. In contrast, *ob/ob* mice were reported to display increased sensitivity to mechanical stimulation. In our own hands, we have tested multiple different inbred strains of STZ-induced diabetic mice, and several of these strains displayed normal or slightly heightened responses to mechanical stimulation despite long-term hyperglycemia (unpublished observations).

Collectively, the variability in mechanical sensitivity suggests that the response to tactile stimulation is under complex regulation. Mechanical sensitivity is conveyed by a range of cutaneous fiber types, including mechanosensitive C-fibers, myelinated Aδ-fibers, and larger myelinated Aβ fibers (Koltzenburg et al. 1997; Cain et al. 2001). Additionally, tactile allodynia in STZ-induced rats is suggested to strongly involve central sensitization in the spinal cord, suggesting paw withdrawal to tactile stimulation is subject to modulation by the central nervous system (Wang et al. 2007). If similar mechanisms are at work in human patients, it is not unreasonable to expect that diabetic humans may develop very different problems associated with tactile sensation depending on the axonal fiber types undergoing damage, insulin levels, and the impact on central modulatory circuits.

Chemogenic Sensitivity

Formalin is a commonly used noxious chemogenic agent used to elicit acute pain in rodents (Murray et al. 1988)). Quantification of the responses of leptr (-/-)

mice revealed relatively little change in the initial response to formalin compared to leptr (+/+) and (+/-) mice. This first phase is due to direct activation of C and Aδ-fibers, and the response of the leptr (-/-) mice is consistent with the normal numbers of C-fibers in the epidermis. For example, STZ-induced diabetic C57BL/6 mice have demonstrable decreases in epidermal innervation in addition to attenuated Phase I responses that are associated with reduced spinal Fos expression (Christianson et al. 2003a; 2003b; Johnson et al. 2007). Thus, it is plausible to suggest that, like thermal thresholds, initial responses to formalin by diabetic rodents generally reflect C-fiber status in the epidermis. It could be predicted that diabetic rodents like the *ob/ob* mice with severe epidermal loss would have little to no initial response to formalin.

In contrast to Phase 1, leptr (-/-) mice displayed attenuated responses to formalin in Phase 2. It is interesting to note that all diabetic mice we have tested exhibit a suppressed response during the second phase, suggesting the abnormalities involving Phase 2 are consistent across models (Christianson et al. 2003b; unpublished observations). Additionally, in the previous study delineating the time course of concomitant behavioral deficits and spinal Fos expression, Phase 2 deficits were the first to appear at 3 weeks post-STZ, while Phase 1 deficits did not appear until 5 weeks post-STZ. Behavioral responses to Phase 2 are driven by inflammation induced by formalin but also involve central sensitization with the spinal cord. It is not clear whether the suppressed Phase 2 response in leptr (-/-) mice is due to altered inflammatory reactions or central sensitization; both likely play a role. One intriguing explanation for the early Phase 2 deficits could be a selective loss of the

fiber subpopulation responsible for driving the Phase 2 neurogenic inflammation response, namely, the peptidergic subpopulation.

Resistance of cutaneous fibers to chronic hyperglycemia

One surprising aspect of this analysis is that the number of fibers present in the epidermis and superficial dermis was similar in all three genotypes. At the time of the analysis (16 weeks of age), the leptr (-/-) mice were exposed to over 10 weeks of uncontrolled hyperglycemia, yet the abundance and general morphology of epidermal and dermal fibers were normal. In comparison, our studies in STZ-induced C57BL/6 mice revealed significant reductions in epidermal and dermal innervation only 6-7 weeks after STZ treatment (Christianson et al. 2003a; Christianson et al. 2007). Moreover, the *ob/ob* mice display severe epidermal losses at 11 weeks of age (Drel et al. 2006). These results suggest that distal fiber degeneration is not only due to high circulating levels of glucose. Other factors including insulin levels, trophic factor production, diet, and genetic background likely play important roles in the rate at which distal axons degenerate (Christianson et al. 2003a; Romanovsky et al. 2006; Toth et al. 2006).

Although the prevalence of fibers appeared unaffected in the leptr (-/-), our analysis doesn't address directly any electrophysiological evidence of damage to sensory axons. The two behavioral tests related to C-fiber function (thermal, formalin-Phase 1) suggest that C-fiber function is intact. However, the abnormal mechanical sensitivity may suggest that although dermal fibers are present, they may

have some functional deficits that may be related to metabolic dysfunction rather than to axonal degeneration. This idea would be consistent with impaired nerve conduction velocities in the leptr (-/-) mice, which is measure of larger fiber dysfunction rather than C-fibers (Sima and Roberston 1978; Norido et al. 1984).

It should be pointed out that another group has reported reduced epidermal innervation in leptr (-/-) mice (Underwood et al. 2001; Gibran et al. 2002). These studies used computer-assisted image analysis to quantitate epidermal and dermal innervation in trunk regions of 8- to 12-week old leptr (-/-) mice. Similar to our results, these authors reported no differences in dermal innervation. Possible differences between the studies include the body regions studied, technical approaches used to quantitate axonal innervation, and the age of the mice.

In conclusion, analysis of leptr (-/-) mice has revealed distinct behavioral deficits in response to varied sensory stimulation, despite normal numbers of epidermal and dermal axons in the hind paw. These results suggest that as a model, the leptr (-/-) mice may be useful for examining certain aspects of large fiber function related to impaired physiological function and reflex activity but may not be a model to address the pathogenesis of axon degeneration in distal targets. In addition, the striking differences between *ob/ob* and leptr (-/-) models should provide an opportunity for direct comparisons of parameters relevant to the development of neuropathic complications, including insulin levels, pancreatic destruction, inflammation, and peripheral nerve degeneration. For example, two papers report hyperinsulinemia in both *ob/ob* mice (nine-fold increase in 12-week-old mice using

radioimmunoassay; Dong et al. 2006) and leptr (-/-) mice (four-fold increase in 10-week-old mice using enzyme-linked immunosorbant assay; Greer et al. 2006). Thus, both models appear to be hyperinsulemic, but perhaps very high insulin levels in the *ob/ob* mice are detrimental, while moderate hyperinsulinemia in leptr (-/-) mice are protective. Using these two type 2 models, future studies should be directed toward parsing out relationships between glycemic, insulinemic, and inflammatory states related to the development of peripheral nerve damage.

VIII. Chapter Four:

Early loss of peptidergic intraepidermal nerve fibers in an STZ-induced mouse model of insensate diabetic neuropathy.

1. Abstract

Peptidergic and nonpeptidergic nociceptive neurons represent parallel yet distinct pathways of pain transmission, but the functional consequences of such specificity are not fully understood. Here, we quantified the progression of peptidergic and nonpeptidergic axon loss within the epidermis in the setting of a dying-back neuropathy induced by diabetes. STZ-induced diabetic MrgD mice heterozygous for green fluorescent protein (GFP) in nonpeptidergic DRG neurons were evaluated for sensitivity to noxious mechanical, thermal, and chemogenic stimuli 4 or 8 weeks post-STZ. Using GFP expression in conjunction with PGP9.5 staining, nonpeptidergic (PGP+/GFP+) and peptidergic (PGP+/GFP-) intraepidermal nerve fibers (IENFs) were quantified at each time point. At 4 weeks post-STZ, nonpeptidergic epidermal innervation remained unchanged while peptidergic innervation was reduced by 40.6% in diabetic mice. By 8 weeks post-STZ, both nonpeptidergic and peptidergic innervation was reduced in diabetic mice by 34.1% and 43.8%, respectively, resulting in a 36.5% reduction in total epidermal IENFs. Behavioral deficits in mechanical, thermal, and chemogenic sensitivity were present 4 weeks post-STZ, concomitant with the reduction in peptidergic IENFs, but did not worsen over the next 4 weeks as nonpeptidergic fibers were lost, suggesting the early reduction in peptidergic fibers may be an important driving force in the loss of cutaneous sensitivity. Furthermore, behavioral responses were correlated at the 4 week time point with peptidergic, but not nonpeptidergic, innervation. These results reveal that peptidergic and nonpeptidergic nociceptive neurons are differentially

damaged by diabetes, and behavioral symptoms are more closely related to the losses in peptidergic epidermal fibers.

2. Introduction

Pain is mediated by small-diameter, unmyelinated or lightly-myelinated nociceptive neurons responding to mechanical, thermal, and chemical stimuli. Two largely non-overlapping classes of C-fiber nociceptors, the peptidergic and nonpeptidergic subpopulations, have been identified and characterized based on their trophic factor requirements, biochemical phenotypes, and terminations (Nagy and Hunt 1982; Hunt and Rossi 1985; Molliver et al. 1997; Snider and McMahon 1998; Braz et al 2005). Collectively, the differences between these subpopulations argue for the existence of separate but parallel pain pathways (Hunt and Mantyh 2001; Braz et al. 2005; Zylka et al. 2005). The functional relevance of these parallel pain pathways has been surprisingly difficult to establish. In addition, only recently have studies begun to address how these populations are associated with various pain states induced by disease or injury (Malmberg et al. 1997; Hammond et al. 2004).

In the previous study, sensory neuron dysfunction in *db/db* mice was evidenced by selective modality-specific deficits in cutaneous sensitivity but did not lead to quantifiable axon loss. Sixteen weeks of age could be early to look for such deficits in this slowly-progressing model, or other mechanisms (insulin, hyperleptinemia, etc.) may protect nerve fibers in these mice. However, another possibility is that a small, subpopulation-specific loss affects behavioral sensitivity

but is masked in the overall total innervation. Indeed, nonpeptidergic and peptidergic neurons have been shown to differ in their vulnerability to and recovery from spinal nerve ligation (Hammond et al. 2004) and dorsal rhizotomy (Belyantseva and Lewin 1999). Particularly in light of the selective deficits in the Phase 2 formalin response, the peptidergic fibers are an intriguing candidate for subpopulation-specific loss induced by diabetes.

Currently, it is unknown whether nociceptive subpopulations contribute equally to the loss of cutaneous innervation that is consistently seen in human patients and rodent models of diabetic neuropathy (Kennedy et al. 1996; Hermann et al. 1999; Christianson et al. 2003a; Christianson et al. 2007; Shun et al. 2004; Paré et al. 2007). In the current study, we returned to the STZ insensate model in order to utilize genetically modified mice expressing green fluorescent protein (GFP) only in nonpeptidergic cutaneous afferents (Zylka et al. 2005). The goal was to determine the extent to which peptidergic and nonpeptidergic axons were affected during the progressive loss of epidermal axons, and how their respective loss contributes to the gradual decline in behavioral responses. Our results demonstrate that peptidergic axons are preferentially lost in the mouse epidermis during the emergence of behavioral deficits, suggesting that these two populations are differentially damaged by diabetes and that behavioral symptoms may be more closely tied to damage within the peptidergic population.

3. Experimental Procedures

MrgD Mice

MrgD is a member of the Mas-related G protein-coupled receptor family, and its expression identifies a distinct neuronal subpopulation (55). The MrgD mouse line was generated using a construct that replaced amino acids 20 to 315 of the 321 amino acid MrgD coding region with an in-frame fusion of farnesylated enhanced green fluorescent protein (GFP), so that GFP is expressed in MrgD-expressing neurons. Wildtype (MrgD+/+) mice have two full copies of the MrgD gene, while MrgD+/- mice are heterozygous for the GFP gene-deleting allele expressed from the MrgD promoter (see Ref. 55 for more details). Zylka et al. (55) reported that GFP+ neurons in MrgD+/- mice peripherally project exclusively to skin, terminating as free nerve endings in the epidermis, and do not innervate any other body tissue examined. By coimmunostaining for a cocktail of antibodies including CGRP, Zylka et al. also demonstrated that virtually all epidermal fibers can be accounted for by either MrgD or CGRP, and that MrgD neurons "likely constitute all nonpeptidergic innervation of the epidermis." MrgD neurons in MrgD+/- and -/- mice are similar in GFP expression and projection profiles.

Heterozygous MrgD mice (MrgD+/-) mice backcrossed to C57BL/6 mice for 5 generations were kindly provided by D. Anderson (California Institute of Technology). Upon receipt, backcrossing of MrgD+/- mice to C57BL/6 mice (Charles River, Wilmington, MA) continued; all mice used in the following experiments were backcrossed for a total of 10 to 13 generations. Mice were housed 2 to 4 per cage on a

12:12-hour light/dark cycle under pathogen-free conditions with free access to water and mouse chow (Harlan Teklad 8604, 4% kcal derived from fat). MrgD+/+, +/-, and -/- mice were identified by polymerase chain reaction (PCR) on DNA harvested from tail snips using the following PCR primers:

5'-CTGCTCATAGTCAACATTTCTGC-3'

5'-CATGAGATGCTCTATCCATTGGG-3'

5'-GGAGAAACAGCTAAAGTGCG-3'

PCR reaction products were run on an agarose gel, and MrgD+/+ mice were identified by the presence of a single band corresponding to 960 base pairs (bp); MrgD+/- mice by the presence of bands at 960 bp and 516 bp; and MrgD-/- mice by a single 516 bp band. All animal use was in accordance with NIH guidelines and conformed to the principles specified by the University of Kansas Medical Center Animal Care and Use Protocol.

STZ-Induced Diabetes

Diabetes was induced in 8-wk old male MrgD+/+ and MrgD+/- mice following baseline behavioral testing. Mice were injected with a single intraperitoneal injection of streptozotocin (180 mg/kg body weight; Sigma, St. Louis, MO) dissolved in 10 mmol/L sodium citrate buffer, pH 4.5. Littermate controls received sodium citrate buffer alone. Food was removed from all animal cages for 5 hours prior to and 4 hours following STZ injection. Animal weight and blood glucose levels (using glucose diagnostic reagents; Sigma) were measured 2 weeks

after STZ injection and every other week thereafter. Mice were included in the diabetic group if their whole blood glucose level, tested by tail vein sampling for intermediate measures and sampling from the decapitation pool for the terminal measure, was > 16.0 mmol/L at every measure. Insulin was not provided at any time. Mice were euthanized following behavioral testing at either 4 or 8 weeks post-STZ.

Quantification of Intraepidermal Nerve Fiber (IENF) Density

Tissue Collection

Mice were anesthetized with Avertin (1/25% v/v tribromoethanol, 2.5% tert-amyl alcohol; 200 µL/10 g body weight) to areflexia. The plantar surface of the left hind paws, including all volar pads, were dissected, immersion-fixed for 1 hour in Zamboni's fixative (3% paraformaldehyde, 15% picric acid in 0.1 M phosphate buffered saline [PBS], pH 7.4) at 4°C, rinsed in PBS overnight, then placed in fresh PBS every morning for three days. Tissue was cryoprotected in 30% sucrose at 4°C for 24 hours, then frozen in Tissue Tek (Sakura, Torrance, CA) and stored at -80°C until sectioning on a cryostat at 30 µm. Sections were mounted on Superfrost Plus slides (Fisher Scientific, Chicago, IL) and stored at -20°C until immunostaining.

Immunohistochemistry

After thawing 5 min. at room temperature, slide-mounted tissue was encircled with a hydrophobic barrier using a Pap Pen (Research Products International, Mt. Prospect, IL) and treated with a blocking solution (0.5% porcine gelatin, 1.5% normal goat serum, 0.5% Triton-X in Superblock Buffer [Pierce, Rockford, IL]) for 1 hr. at

room temperature. The primary antibody (rabbit anti-PGP9.5; 1:400; Ultraclone, Isle of Wight, UK) was diluted in blocking solution and incubated with sections overnight at 4°C. For visualization, sections were washed 3 x 5 min. with PBS followed by incubation for 1 hr. with a fluorochrome-conjugated secondary antibody (goat anti-rabbit Alexa 555; 1:2000; Molecular Probes, Eugene, OR) diluted in PBS. Following three washes with PBS, slides were coverslipped and stored at 4°C until viewing.

IENF Quantification

IENF density was quantified according to recently published European Federation of Neurological Societies guidelines (Lauria et al. 2005a). Four randomly chosen tissue sections separated by at least 60 µm were quantified from each animal. For each section, four 40x frames of view were randomly chosen for quantification. Sections were counted live while viewing using a Nikon E800 fluorescent microscope. Only single IENFs crossing the dermal-epidermal junction were counted, excluding secondary branching and nerve fragments not crossing the dermal-epidermal junction. PGP9.5+/GFP+ fibers were considered nonpeptidergic, while PGP9.5+/GFP- fibers were considered peptidergic. PGP9.5+/GFP+ and PGP9.5+/GFP- fiber counts were summed to yield the total number of fibers. For each group (total, PGP9.5+/GFP+, and PGP9.5+/GFP-), the number of fibers counted in the frame of view was divided by the length of the dermal-epidermal junction in the frame of view to arrive at the IENF density measure (# of fibers/mm). IENF density in 4 frames of view was averaged to yield the IENF density per 30 µm

section, 4 sections were averaged to yield IENF density per animal, and group means were calculated. All data are reported as mean +/- standard error of the mean (SEM).

Behavioral Assessments of Cutaneous Sensitivity

Mechanical

Behavioral responses to a Von Frey monofilament (1.4 g) were assessed at baseline (8 weeks of age prior to STZ injection) and either 4 or 8 weeks post-STZ. Mice underwent a training session on the day prior to the first day of testing. On testing days, mice were placed in individual clear plastic cages (11 x 5 x 3.5 cm) on a wire mesh screen elevated 55 cm above the table and allowed to acclimate for 45 min. The combined mean percent withdrawal of three applications to each foot on two consecutive testing days was calculated for each animal, and group means were calculated.

Thermal

Thermal testing was performed using a thermal analgesiometer (UARDG, Dept. of Anest., Univ. Cal. San Diego, La Jolla, CA) on the same days as, but immediately following, mechanical testing. Mice were placed in individual clear plastic compartments (9 x 9 x 14 cm) atop a glass surface and allowed to acclimate for 1 hr. A radiant heat source (4.0 V) 40 mm from the glass floor was applied to the mid-plantar surface of 1 hind paw for a maximum of 20 seconds, and the number of seconds until paw withdrawal was recorded as the latency. Latencies were recorded three times on alternating hind paws, with at least 10 minutes separating applications

to the same hind paw. The mean withdrawal latency of 6 total applications on two consecutive testing days was calculated for each animal, and group means were calculated.

Chemogenic

To assess chemogenic nociception, the formalin test was performed prior to sacrifice on the day following the final mechanical and thermal testing day. After a 1 hr. habituation to individual observation chambers (27 x 18 x 21 cm), mice were injected with 20 µL of 5% formalin (in saline, pH 7.0) subcutaneously into the dorsal surface of the right hind paw using a 1 CC insulin syringe and a 28-gauge needle. The amount of time devoted to the injected foot (licking and biting) was recorded in two 10-minute windows during the acute (Phase 1; 0-10 min. post-injection) and inflammatory (Phase 2; 40-50 min. post-injection) phases of the formalin test.

Statistical Analysis

To test whether the MrgD-GFP transgene affected the development of diabetes or the progression of diabetes-induced behavioral deficits, comparisons were made between nondiabetic and diabetic MrgD+/+ and MrgD+/- mice at each time point using repeated measures (RM) analysis of variance (ANOVA) (weight, blood glucose) and two-way ANOVA (Von Frey, thermal, formalin Phase 1 and 2) followed by post-hoc analysis using Fisher's protected least significant differences (PLSD). Fiber subtypes in nondiabetic mice were compared between 4 and 8 weeks post-vehicle using Student's T-test. All other comparisons between MrgD+/- nondiabetic

and diabetic mice at the 4 and 8 week time points were performed using RM ANOVA (weight, blood glucose) and two-way ANOVA (IENF density, Von Frey, thermal, formalin Phase 1 and 2) followed by Fisher's PLSD. For correlations, populations were first examined for normal distribution using the Kolmogorov-Smirnov Normality Test. Populations with normal distributions were compared using the Pearson Product Moment Correlation; those that failed the normality test were compared using the Spearman Rank Order Correlation. Simple linear regression analyses were also performed to examine relationships between behavioral measures and innervation densities. All significance levels were set to 0.05. All data reported as mean +/- SEM.

4. Results and Figures

Wild-type vs. Heterozygous MrgD Mice

Although MrgD+/- mice were first reported to have no obvious behavioral or phenotypic abnormalities (Zylka et al. 2005), the MrgD allele has not been extensively studied with regard to its effect on animal behavior or the progression of nerve complications. Therefore, throughout these studies, MrgD+/+ and MrgD+/- littermates were tested alongside each other for each measure. There were no statistical differences between MrgD+/- and MrgD+/+ mice from the same experimental group and time point on any of the following measures: terminal weight, terminal glucose, baseline mechanical sensitivity, final mechanical sensitivity, thermal responses, and responses during the formalin test (data not

shown), indicating neither the transgene nor MrgD heterozygosity affect baseline behavioral measures, the development of diabetes, or the progression of diabetes-induced behavioral deficits.

IENF density in nondiabetic mice

Because virtually all epidermal fibers are either MrgD+ or CGRP+ (Zylka et al. 2005), using PGP9.5 immunostaining in conjuction with GFP expression allows for the extrapolation of peptidergic fibers. Thus, PGP+/GFP+ fibers were considered nonpeptidergic, while PGP+/GFP- fibers were considered peptidergic. Similar to Zylka et al. (2005), we observed distinct morphologies among PGP+/GFP+ and PGP+/GFP- fiber terminations in nondiabetic MrgD +/- mice (**Figure VIII-1**). PGP+/GFP+ fibers predominantly coursed straight through underlying strata, then exhibited a tortuous, meandering pattern prior to terminating among keratinocytes of the stratum granulosum (**Figure VIII-1B**). In contrast, PGP+/GFP- fibers coursed directly and terminated in the stratum basalis or spinosum (**Figure VIII-1C**). Occasional intertwining of PGP+/GFP+ and PGP+/GFP- fibers was observed.

Quantitation of the total number of epidermal fibers (PGP+/GFP+ and PGP+/GFP- fibers) revealed an average of 51.7 +/- 1.86 and 57.4 +/- 2.91 fibers/mm at 4 and 8 weeks post vehicle, respectively (12 and 16 weeks of age; **Figure VIII-2**). When divided into peptidergic and nonpeptidergic subtypes, the nonpeptidergic (PGP+/GFP+) fibers represented 74.1% of the total fiber population (38.4 +/- 1.36 fibers/mm) at 4 weeks post-vehicle. In contrast, PGP+/GFP- presumptive peptidergic

Figure VIII-1: PGP+/GFP+ (nonpeptidergic) and PGP+/GFP- (peptidergic) fibers are present in nondiabetic MrgD+/- mice

IENFs in hind paw footpad skin from nondiabetic 12-week old MrgD+/- mice. **(A)** IENFs immunostained for PGP9.5, representing all epidermal fibers and including both subpopulations. **(B)** GFP+ fibers representing nonpeptidergic IENFs. **(C)** Merged view. Arrows indicate PGP+/GFP- presumptive peptidergic IENFs (red).

Figure VIII-1

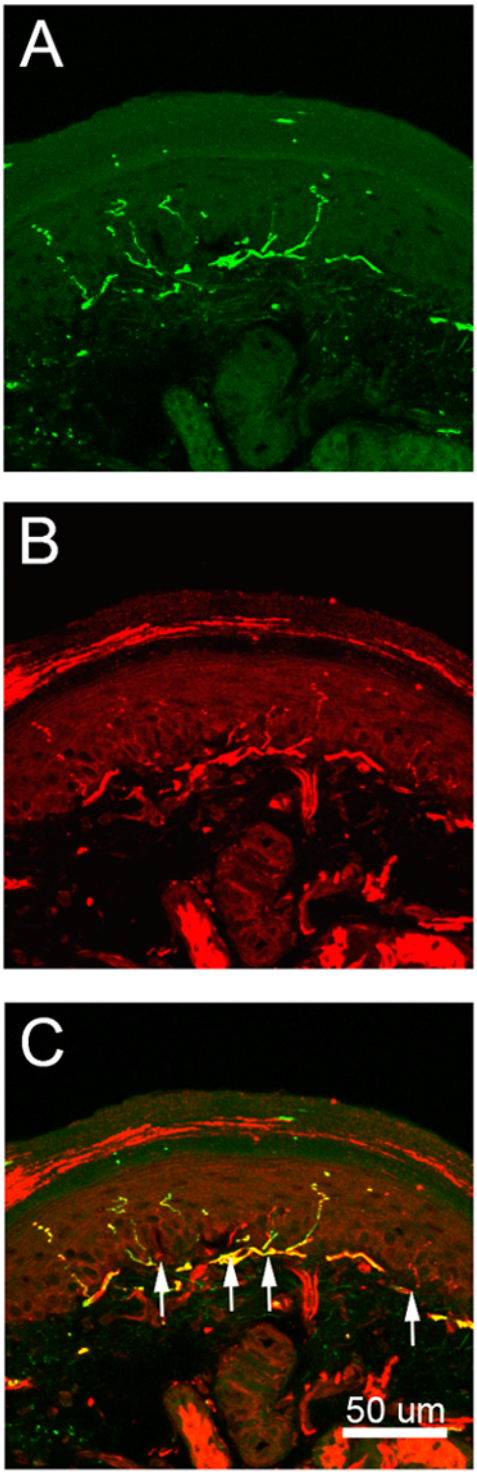

Figure VIII-2: Fiber subtypes and total number of fibers/mm is similar at 12 and 16 weeks of age in nondiabetic mice

Proportions of fiber subtypes in nondiabetic MrgD+/- mice at 4 and 8 weeks post-vehicle (12 and 16 weeks of age, respectively). At 4 weeks post-vehicle, the composition of epidermal fibers was 74.1% nonpeptidergic and 25.9% peptidergic. Similarly, at 8 weeks post-vehicle, 75.5% of epidermal fibers were nonpeptidergic and 24.5% were peptidergic. Data plotted as mean +/- SEM.

Figure VIII-2

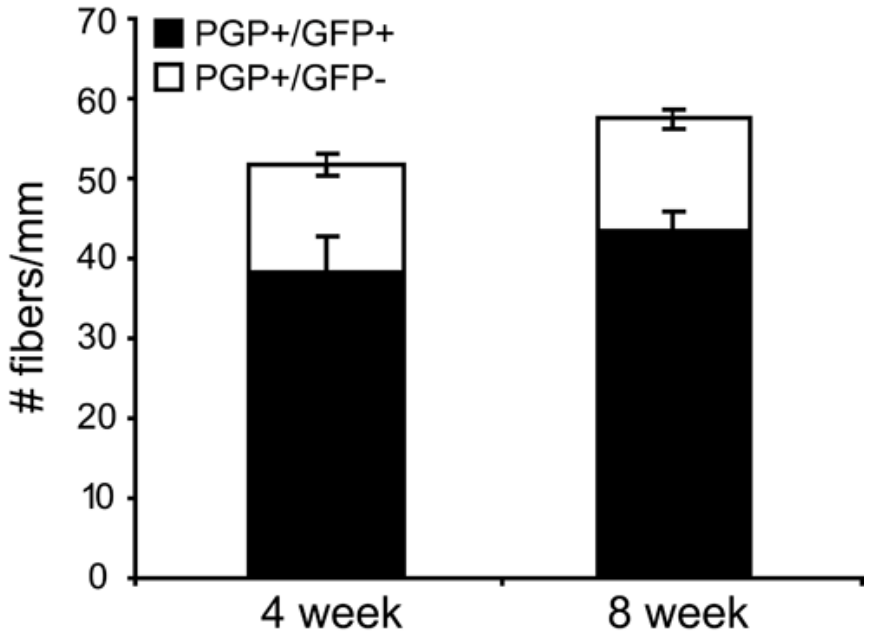

fibers constituted only 25.9% of the total (13.4 +/- 1.32 fibers/mm). The proportions were similar 8 weeks post-vehicle, with 75.5% nonpeptidergic (43.4 +/- 2.30 fibers/mm) and 24.5% peptidergic (14.1 +/- 1.18 fibers/mm; **Figure VIII-2**). No significant differences were found between 4 and 8 weeks in the number of fibers/mm, either in total or in subpopulations.

STZ-Induced Diabetes

Typical of this murine model and type 1 diabetes, STZ-injected mice exhibited polydipsia, polyuria, and weight loss. Nondiabetic mice increased in weight by 9.8% and 16.8% over the course of the study, whereas diabetic mice lost 12.9% and 7.4% of their body weight (4 and 8 week post-STZ, respectively; **Tables VIII-1 and 2**). Blood glucose levels of diabetic mice were significantly higher than nondiabetic mice at all time points examined (**Tables VIII-1 and 2**).

Progressive loss of IENF density in diabetic mice

As a likely consequence of chronic hyperglycemia, the dermis and epidermis in diabetic mice often appeared less compact and the dermal/epidermal junction basement membrane appeared less precise in diabetic mice. In addition, PGP+ fibers in diabetic mice often appeared thinner and shorter compared to fibers in nondiabetic mouse skin. Moreover, long fibers extending to the superficial epidermis were generally less prevalent in diabetic skin (**Figure VIII-3A, B, C, D**).

Table VIII-1: Weight and blood glucose levels of MrgD mice: 4 weeks post-STZ

		Week 0	Week 2	Week 4
Nondiabetic				
	Weight	24.0 +/- 0.71	23.6 +/- 0.65	26.4 +/- 0.79
	Glucose	NM	6.6 +/- 0.20	6.8 +/- 0.39
Diabetic				
	Weight	23.6 +/- 0.73	19.1* +/- 0.72	20.6* +/- 1.12
	Glucose	NM	23.9** +/- 1.42	24.7** +/- 1.52

Weight and blood glucose levels of nondiabetic and diabetic MrgD+/- mice from the 4-week time point at weeks 0, 2, and 4 post-STZ. Weight is in grams; glucose levels are mmol/L. Data represented as means +/- standard error of mean. NM = not measured. * $p < 0.05$ vs nondiabetic mice, ** $p < 0.0001$ vs nondiabetic mice

Table VIII-2: Weight and blood glucose levels of MrgD mice: 8 weeks post-STZ

		Week 0	Week 2	Week 4	Week 6	Week 8
Nondiabetic						
	Weight	23.8 +/- 0.57	24.5 +/- 0.64	24.5 +/- 0.65	26.4 +/- 0.76	27.8 +/- 1.01
	Glucose	NM	6.1 +/- 0.26	6.6 +/- 0.20	6.8 +/- 0.46	7.6 +/- 0.55
Diabetic						
	Weight	22.7 +/- 0.47	19.0** +/- 0.90	19.8* +/- 1.22	19.1**+/- 1.21	21.0* +/- 1.27
	Glucose	NM	22.9** +/- 1.14	19.8**+/- 0.96	22.3**+/- 0.81	24.7**+/- 1.25

Weight and blood glucose levels of nondiabetic and diabetic MrgD +/- mice from the 8-week time point at weeks 0, 2, 4, 6, and 8 post-STZ. Weight is in grams; glucose levels are mmol/L. Data represented as means +/- standard error of mean. NM = not measured. * $p < 0.05$ vs nondiabetic mice, ** $p < 0.0001$ vs nondiabetic mice

Figure VIII-3: IENFs are reduced in diabetic mice

Merged images of PGP immunostaining (red) and GFP expression (green) in hind paw footpad skin from nondiabetic and diabetic MrgD+/- mice. Arrows indicate PGP+/GFP- presumptive peptidergic fibers. **(A, C):** PGP+/GFP+ and PGP+/GFP- IENFs in nondiabetic (A) and diabetic (C) mice 4 weeks post-STZ. PGP+/GFP- fibers are reduced in diabetic mice at this time point. **(B, D):** PGP+/GFP+ and PGP+/GFP- IENFs in nondiabetic (B) and diabetic (D) mice 8 weeks post-STZ. Both PGP+/GFP- and PGP+/GFP+ fibers are reduced in diabetic mice at this time point.

Figure VIII-3

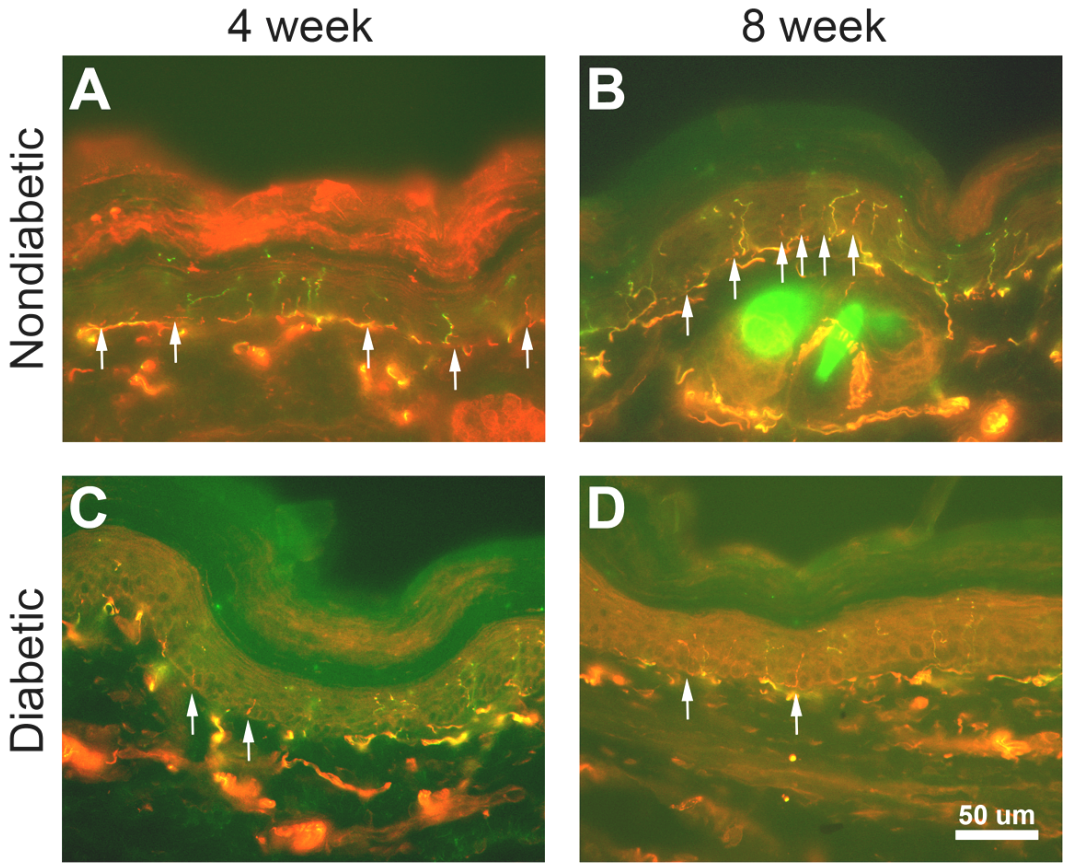

At 4 weeks post-STZ, the total number of PGP+ fibers/mm (representing all epidermal fibers) was 51.7 +/- 1.86 and 47.8 +/- 4.08 in skin from nondiabetic and diabetic mice, respectively, representing a nonsignificant 7.5% loss of overall epidermal innervation in diabetic mice ($p = 0.3810$; **Figure VIII-3A, C, 4A**). Evaluation of both axonal subtypes revealed that at this early time point, nonpeptidergic fibers did not decrease in diabetic (39.9 +/- 4.31 fibers/mm) compared to nondiabetic (38.4 +/- 1.36) mice ($p = 0.7291$; **Figure VIII-2A, C, 4B).** In contrast, peptidergic fibers were decreased by 40.6% in skin from diabetic (7.9 +/- 1.00 fibers/mm) compared to nondiabetic mice (13.4 +/- 1.32 fibers/mm; $p = 0.0045$; **Figure VIII-3A, C, 4C**).

At 8 weeks post-STZ, a significant loss in total epidermal innervation was evident in diabetic mice, with a 36.5% decrease in the total number of PGP+ fibers/mm in diabetic (36.5 +/-2.75) compared to nondiabetic mice (57.4 +/-2.91; $p < 0.0001$; **Figure VIII-3B, D, 4A**). In contrast to 4 weeks, however, both fiber subpopulations contributed to the overall loss at this later time point. Nonpeptidergic innervation was significantly decreased from 43.4 +/- 2.30 to 28.6 +/- 2.36 PGP+/GFP+ fibers/mm ($p = 0.0003$; **Figure VIII-3B, D, 4B**), a 34.1% decrease in diabetic compared to nondiabetic mice. The reduction in peptidergic innervation was similar to levels observed at 4 weeks post-STZ. At 8 weeks post-STZ, peptidergic fibers were reduced by 43.8% in diabetic mice, from 14.1 +/- 1.18 PGP+/GFP- fibers/mm in nondiabetic mice to 7.9 +/- 1.00 in diabetic mice ($p = 0.0011$; **Figure VIII-3B, D, 4C**).

Figure VIII-4: Loss of IENFs is subpopulation-specific early in the progression of diabetes

Quantification of total PGP+ (A), nonpeptidergic PGP+/GFP+ (B), and peptidergic PGP+/GFP- (C) IENFs in hind paw footpad skin from nondiabetic and diabetic MrgD+/- mice at 4 and 8 weeks post-STZ. **(A)** There were no significant differences in the total number of epidermal PGP+ fibers at 4 weeks post-STZ; however, at 8 weeks the total number of fibers/mm was reduced in diabetic mice. **(B)** Nonpeptidergic PGP+/GFP+ fibers remained unchanged 4 weeks post-STZ, but were reduced 8 weeks post-STZ. **(C)** The number of peptidergic PGP+/GFP- fibers/mm was reduced at the early 4 week post-STZ time point. This reduction was maintained at 8 weeks post-STZ. Data plotted as mean +/- SEM. * $p < 0.05$ vs. nondiabetic mice of the same time point, ** $p < 0.0001$ vs. nondiabetic mice of the same time point

Figure VIII-4

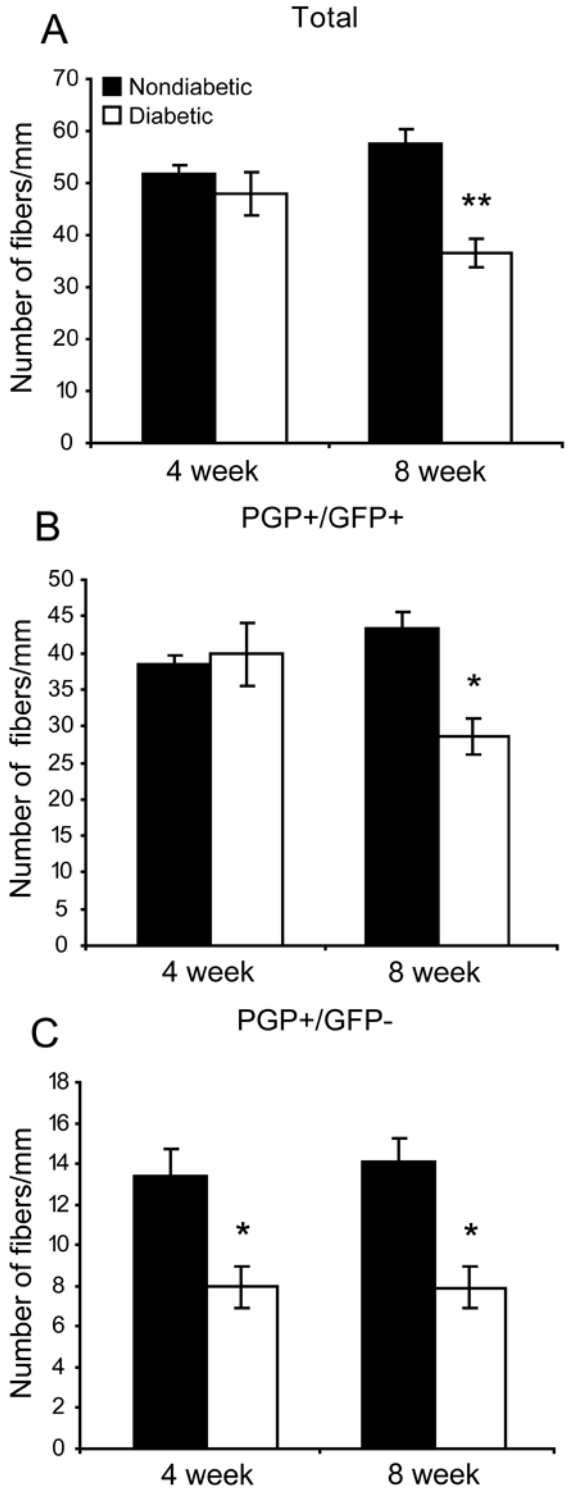

Overall, only PGP+/GFP- peptidergic fibers were lost 4 weeks post-STZ. This loss was not mirrored by PGP+/GFP+ fibers, which remained stable at this timepoint, nor was it reflected in a loss of total innervation. PGP+/GFP+ fibers were not decreased until 8 weeks post-STZ, at which time a loss in overall epidermal innervation was evident.

Diabetes-induced deficits in behavioral responses to noxious stimuli

Baseline Mechanical Sensitivity

To establish baseline mechanical sensitivity, heterozygous mice from all groups were tested prior to STZ-injection (at 8 weeks of age) for withdrawal responses to a 1.4 g Von Frey monofilament. There were no effects of either time point ($p = 0.1843$) or experimental group ($p = 0.3105$) on the average percent withdrawal of 6 applications to the hind paw footpad, indicating all groups had comparable mechanical sensitivity at 8 weeks of age upon entering the study (data not shown).

Reduction in Cutaneous Sensitivity Following Diabetes Induction

Mechanical

Consistent with previous studies using this model (Christianson et al. 2003b; Wright et al. 2004), diabetic mice displayed reduced percent paw withdrawals to monofilament application compared to nondiabetic mice at both 4 weeks and 8 weeks post-STZ (**Figure VIII-5A**). At 4 weeks post-STZ, diabetic mice responded with a

withdrawal an average of 34.7% +/- 6.23 of the time, significantly less than nondiabetic mice (62.6% +/- 4.90; p = 0.0021). Similarly, at 8 weeks post-STZ, the percent withdrawal response was 62.7% +/- 4.60 in nondiabetic and 45.2% +/- 5.04 in diabetic mice (p = 0.0198). Importantly, two-way ANOVA revealed a significant effect of experimental group (nondiabetic vs. diabetic; p = 0.0001) but not time point (4 vs. 8 weeks post-STZ; p = 0.3239), indicating the behavioral deficits at 4 weeks did not worsen with the diabetes progression. At 4 weeks post-STZ, percent withdrawal was not significantly correlated with the number of PGP+/GFP+ nonpeptidergic fibers/mm (p = 0.157; **Figure VIII-5B**). By contrast, correlation with PGP+/GFP- peptidergic fibers was moderately positive (p = 0.0251; **Figure VIII-5C**). By 8 weeks post-STZ, both PGP+/GFP+ (p = 0.0009) and PGP+/GFP- (p = 0.0013) fibers were strongly positively correlated with percent withdrawal (data not shown).

Thermal

Diabetic mice also demonstrated an increased latency in the time to withdrawal from a radiant heat source supplied by a thermal analgesiometer (Hargreaves apparatus) at both 4 and 8 weeks post-STZ (**Figure VIII-6A**). The latencies of nondiabetic mice were 9.0 s +/- 0.50 and 9.4 s. +/- 0.62 at 4 and 8 weeks post-STZ, respectively. Diabetic mice latencies were longer compared to nondiabetic mice, both at 4 weeks post-STZ (13.8 s +/- 0.89; p = 0.0001) and 8 weeks post-STZ (15.4 s +/- 1.01; p < 0.0001). Similar to measures of mechanical sensitivity, there was no effect of time on thermal latencies (p = 0.2257), suggesting the early loss of

Figure VIII-5: Behavioral responses to mechanical stimuli were suppressed in diabetic animals at 4 weeks post-STZ and correlated with peptidergic innervation.

(A) Behavioral responses to noxious mechanical stimuli in nondiabetic and diabetic MrgD+/- mice 4 and 8 weeks post-STZ. The percent withdrawal from a 1.4 g monofilament was reduced at 4 weeks of diabetes; this reduction was maintained and did not worsen by 8 weeks post-STZ. Data plotted as mean +/- SEM. **(B)** Mean percent withdrawal did not correlate with the number of PGP+/GFP+ epidermal fibers. **(C)** Correlation with the number of PGP+/GFP- fibers revealed a moderate, positive relationship. r = Pearson product moment correlation coefficient. b = slope of the linear regression line. The solid line represents the linear regression line and dotted lines represent 95% confidence intervals. Filled circles represent average values for individual animals. * $p < 0.05$

Figure VIII-5

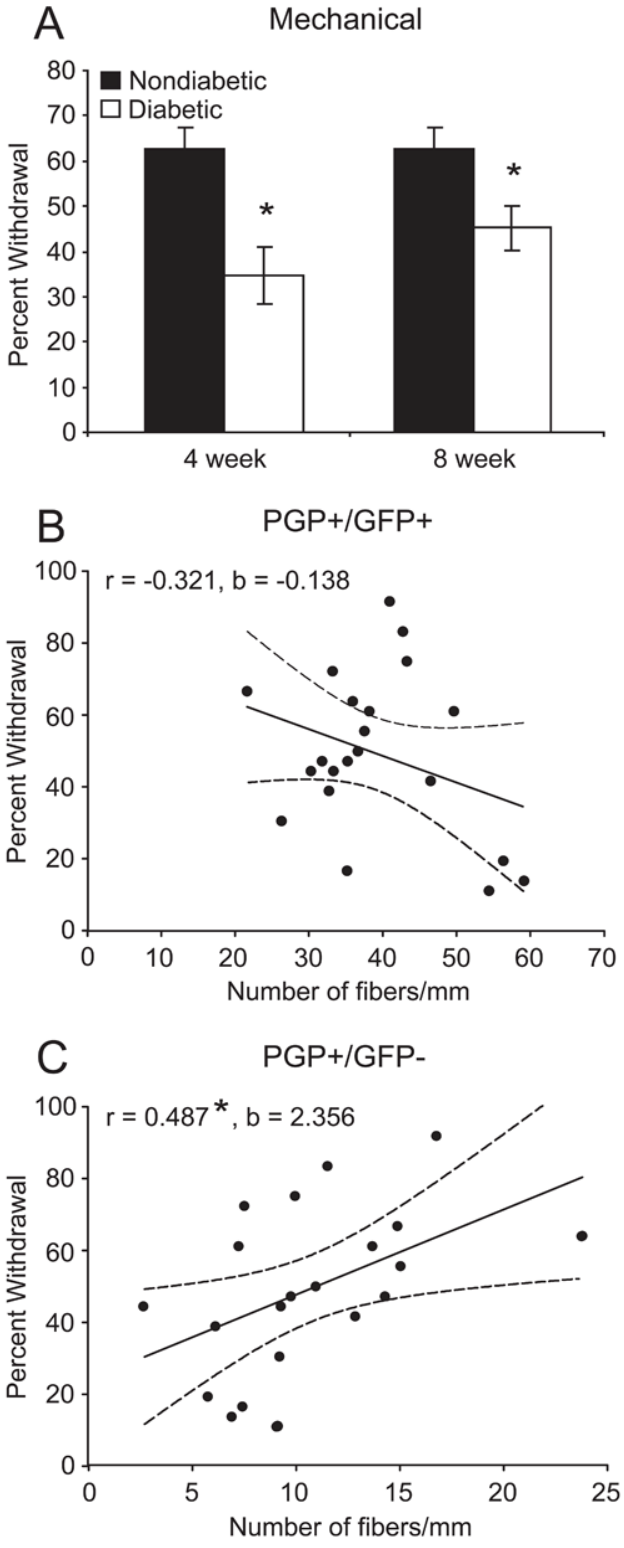

Figure VIII-6: Behavioral responses to noxious thermal stimuli were delayed in diabetic animals 4 weeks post-STZ and correlated with peptidergic innervation.

(A) The latency to withdrawal from a thermal heat source was longer in diabetic compared to nondiabetic MrgD+/- animals 4 weeks post-STZ and to a similar degree 8 weeks post-STZ. Data plotted as mean +/- SEM. **(B)** Paw withdrawal latencies did not show a significant correlation with PGP+/GFP+ innervation. **(C)** Paw withdrawal latencies were moderately, negatively correlated with PGP+/GFP- innervation. r = Pearson product moment correlation coefficient. b = slope of the linear regression line. The solid line represents the linear regression line and dotted lines represent 95% confidence intervals. Filled circles represent average values for individual animals. * $p < 0.05$

Figure VIII-6

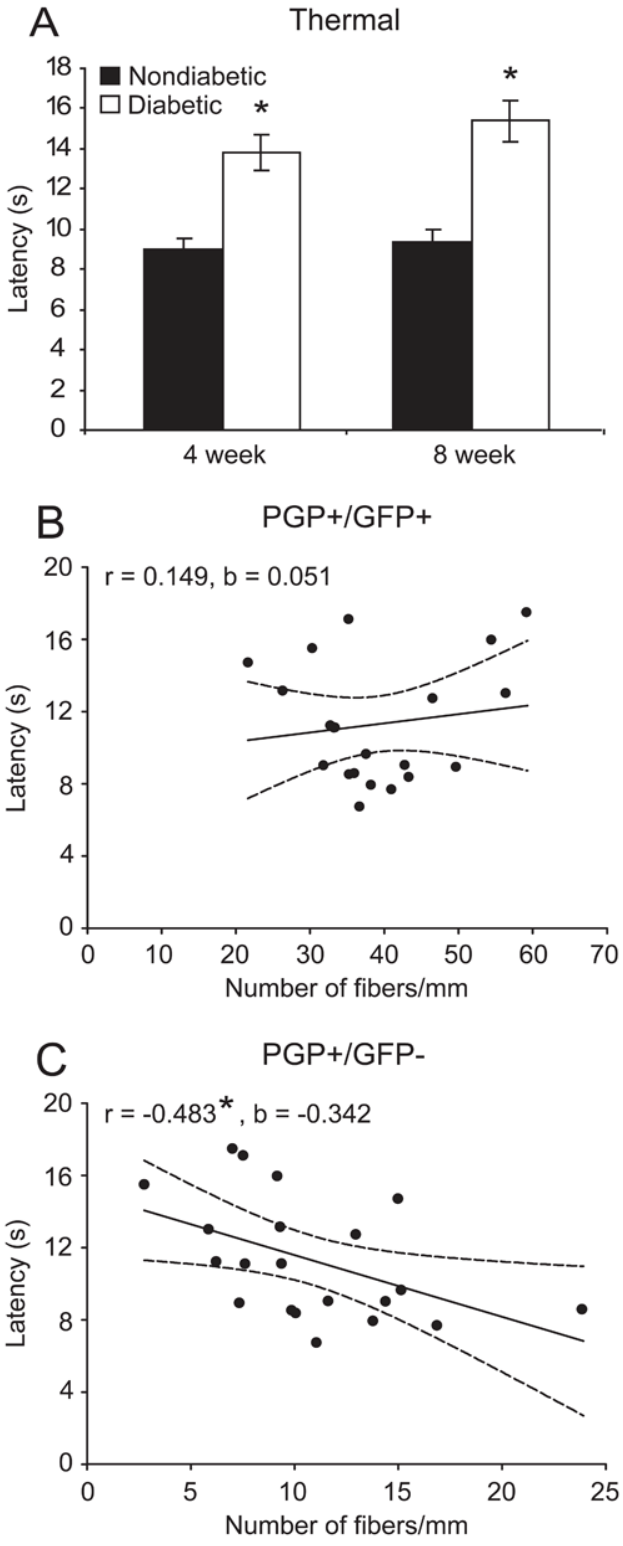

thermal sensitivity did not progress with time from 4 to 8 weeks post-STZ. At 4 weeks post-STZ, thermal latencies were negatively correlated with PGP+/GFP- ($p = 0.0267$), but not PGP+/GFP+ ($p = 0.5200$), innervation (**Figure VIII-6B, C**). By 8 weeks post-STZ, thermal latencies showed a strong, negative correlation with both fiber types (PGP+/GFP+: $p = 0.0005$; PGP+/GFP-: $p = 0.0083$; data not shown).

Formalin

The time devoted to the formalin-injected hind paw was recorded during the acute (Phase 1; **Figure VIII-7**) and inflammatory (Phase 2; **Figure VIII-8**) stages of the formalin test. Similar to mechanical and thermal hyposensitivity, early reductions in chemogenic sensitivity were apparent at 4 weeks and then sustained at 8 weeks post-STZ in both phases of the formalin test.

During Phase 1, behavioral responses of diabetic mice were significantly reduced compared to nondiabetic mice at 4 ($p = 0.0301$) and 8 ($p = 0.0016$) weeks post-STZ. Nondiabetic mice devoted 142.5 +/- 33.20 and 177.5 +/- 27.28 seconds to the injected foot at 4 and 8 weeks, respectively, and diabetic mice 64.3 s +/- 14.38 and 64.3 s +/- 9.29 (**Figure VIII-7A**). There was no statistical effect of time point. Phase 1 behavioral responses were significantly correlated with PGP+/GFP- ($p = 0.0171$; **Figure VIII-7C**) innervation at 4 weeks post-STZ, but not with PGP+/GFP+ ($p = 0.1870$) innervation (**Figure VIII-7B**). Correlations with both fiber subtypes were significant at 8 weeks post-STZ (PGP+/GFP+: $p = 0.0056$; PGP+/GFP-: $p = 0.0190$; data not shown).

Figure VIII-7: Phase 1 behavioral responses during the formalin test were suppressed in diabetic animals beginning 4 weeks post-STZ and were correlated with peptidergic innervation.

(A) At 4 weeks post-STZ, the amount of time devoted to the injected foot was decreased during the first 10 minutes of the formalin test in diabetic compared to nondiabetic MrgD+/- mice. This reduction was maintained 8 weeks post-STZ but did not worsen. Data plotted as mean +/- SEM. **(B)** Phase 1 behavioral responses were not correlated with PGP+/GFP+ innervation. **(C)** A strong positive correlation was observed between Phase 1 responses and the number of PGP+/GFP- fibers. r = Spearman rank order correlation coefficient. b = slope of the linear regression line. The solid line represents the linear regression line and dotted lines represent 95% confidence intervals. Filled circles represent average values for individual animals. * $p < 0.05$

Figure VIII-7

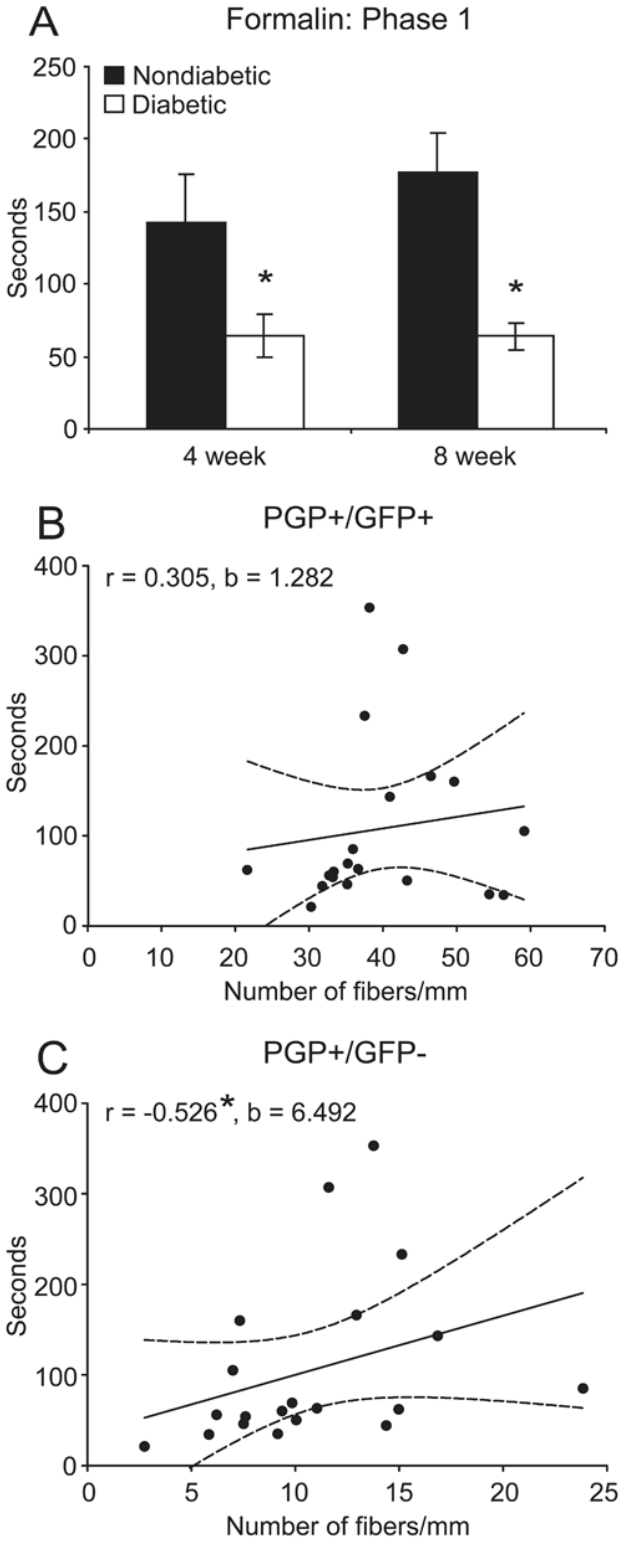

Figure VIII-8: Phase 2 formalin responses were reduced in diabetic animals 4 weeks post-STZ and were correlated with both peptidergic and nonpeptidergic innervation

(A) At 4 weeks post-STZ, diabetic mice exhibited reduced behavioral responses during Phase 2 of the formalin test. This reduction was maintained 8 weeks post-STZ. Data plotted as mean +/- SEM. **(B)** Interestingly, responses during Phase 2 of the formalin test were negatively correlated with PGP+/GFP+ innervation. **(C)** A strong positive correlation between Phase 2 responses and the number of PGP+/GFP- fibers was observed. r = Pearson product moment correlation coefficient. b = slope of the linear regression line. The solid line represents the linear regression line and dotted lines represent 95% confidence intervals. Filled circles represent average values for individual animals. * $p < 0.05$

Figure VIII-8

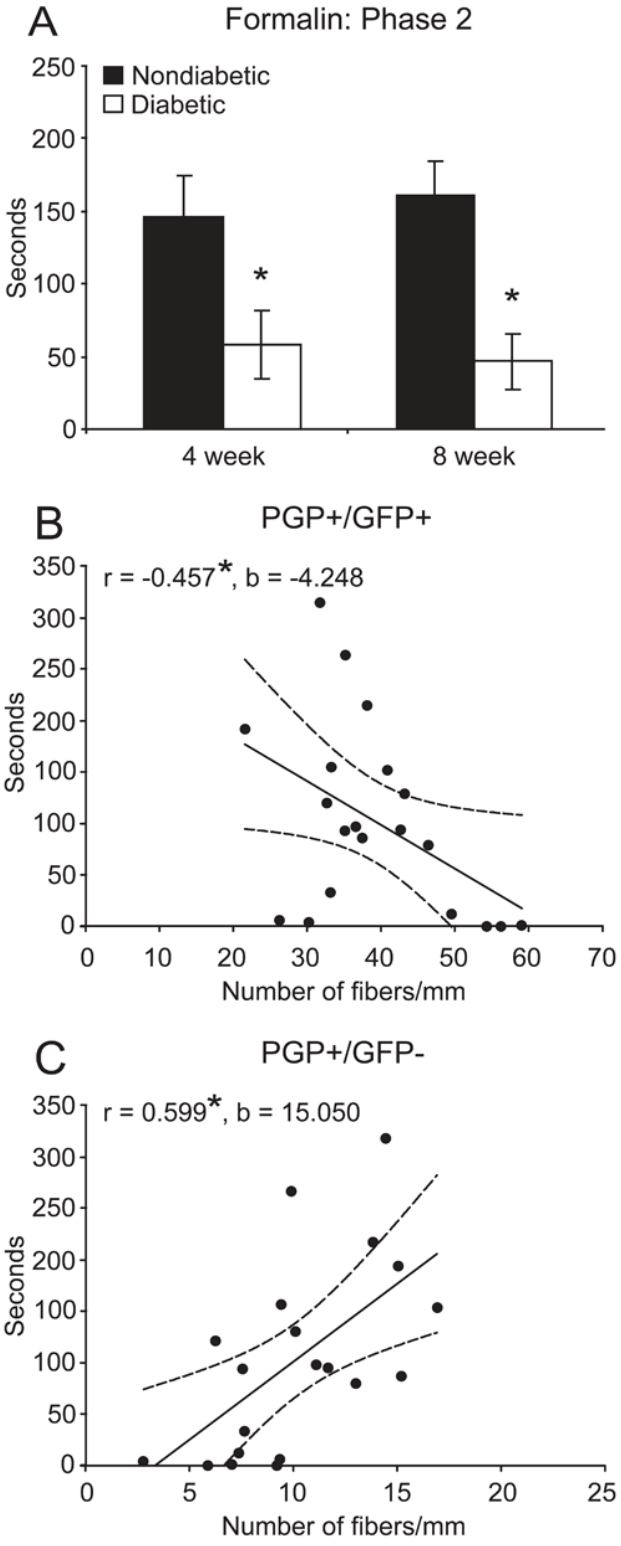

Behavioral responses during Phase 2 were decreased in diabetic (58.3 s +/- 23.60, 46.4 s +/- 18.79) compared to nondiabetic (146.4 s +/- 28.58, 160.6 s +/- 23.70) mice at both 4 ($p = 0.0288$) and 8 ($p = 0.0017$) weeks post-STZ, respectively (**Figure VIII-8A**). Again, there was no statistical effect of time point on Phase 2 behavioral responses to formalin ($p = 0.9617$), suggesting stability of the behavioral changes following their appearance 4 weeks after diabetes induction. Interestingly, at the 4 week time point, Phase 2 behavioral responses were negatively correlated with PGP+/GFP+ fibers ($p = 0.0427$; **Figure VIII-8B**). In contrast, a strong positive correlation was seen with PGP+/GFP- fibers ($p = 0.0052$; **Figure VIII-8C**). Both correlations were strong and in the positive direction 8 weeks post-STZ (PGP+/GFP+: $p = 0.0002$; PGP+/GFP-: $p = 0.0072$; data not shown).

In summary, behavioral deficits in mechanical, thermal, and chemogenic sensitivity emerged at 4 weeks post-STZ and did not worsen by 8 weeks post-STZ. At the 4 week time point, PGP+/GFP- peptidergic innervation was a better predictor of behavioral responses than PGP+/GFP+ nonpeptidergic innervation.

5. Discussion

As a consequence of the growing prevalence of diabetes throughout the world, symptoms associated with peripheral nerve damage are increasing but remain difficult to treat. In order to develop more efficacious therapeutics, we still require a better understanding of the spectrum of mechanisms underlying these conditions. Here, we evaluated axonal loss in an insensate dying back neuropathy with regard to nociceptor

subtypes and changes in cutaneous sensitivity. Results from these studies reveal a preferential loss of peptidergic fibers early in the disease progression that mirrored the temporal appearance of reduced nociceptive sensitivity. These results suggest that differential vulnerability and loss of nociceptor subtypes may play a role in the phenotype of neural symptoms that develop in patients with peripheral nerve damage.

Nociceptive subpopulations in murine epidermis

The relative exclusivity among MrgD-GFP and CGRP-expressing DRG neurons (Zylka et al. 2005) provides a unique opportunity to assess C-fiber subtypes at the level of the free nerve ending in the epidermis. This approach, compared to previous techniques using antibody staining for multiple neuropeptide markers, provides a simplistic and more reliable method to visualize fiber subtypes and avoids confounds associated with neuropeptide modulation (Brewster et al. 1994; Rittenhouse et al. 1996; Troger et al. 1999; Adeghate et al. 2006) or phenotypic switching (Hammond et al. 2004; Basbaum & Woolf 1999, Woolf and Ma 2007). Our findings of a 75:25% distribution of nonpeptidergic to peptidergic fibers differ slightly from those of Zylka et al (60:40; 2005), perhaps due to our extensive back-crossing onto a pure C57BL/6 background. Nonetheless, the anatomical differences in morphologies and termination zones between these fiber subpopulations, first reported by Zylka and colleagues (2005) and repeated here, suggest truly distinct populations and support future investigations into their functional roles.

Early diabetes-induced IENF loss is subpopulation-specific

Previous approaches to address the functionality of nociceptor subtypes have used a variety of approaches including selective knock-down (Vulchanova et al. 2001; Vierck et al. 2003) or mice null mutant for subpopulation-specific genes (Stucky et al. 2002; Lindfors et al. 2006). The current study is unique in that it appears to be the first to demonstrate a dichotomy in the loss of nociceptor subpopulations resulting from a progressive disease state, and suggests the peptidergic subpopulation may have increased sensitivity to metabolic and oxidative stresses on peripheral axons. Whether this sensitivity is indicative of an overall vulnerability of peptidergic neurons, a hallmark of diabetic neuropathy, or a phenomenon specific to insensate Type 1 diabetes in C57BL/6 mice is still unclear.

Regardless, we have shown that a selective loss is possible, but how a differential loss of fiber subtypes affects sensory function remains to be determined. It is plausible to suggest that a selective subtype loss disrupting the overall balance of peripheral input into the dorsal horn could have significant implications for settings of pain in addition to the insensate model explored here. Several putative mechanisms to address include the anatomical rearrangement of central projections in the dorsal horn, the hyperexcitability and sensitization of remaining peripheral fibers of the affected subpopulation as a compensation, or hyperexcitability and sensitization of the remaining, unaffected, subpopulation. As an example, uninjured afferents have been implicated in mechanical hyperalgesia in neuropathic settings via the upregulation of neuropeptides, neurotrophic factors, and signal transduction proteins

(Ringkamp and Meyer 2005). Although the model studied here results in cutaneous hypoalgesia and the selective loss of peptidergic fibers, it could be that the nature of the disease or injury (neuropathic vs. inflammatory) or the mechanism of damage influence the outcome (painful vs. insensate) of this imbalance. Investigating whether similar imbalances in peripheral input exist in painful models of diabetic neuropathy or in other disease states will be important in future studies.

It is important to note that 4 weeks following diabetes induction, peptidergic fibers were significantly reduced, yet the total number of epidermal fibers was unchanged. This is due to the fact that the peptidergic fibers contribute only a small percentage of the total epidermal population, and changes in this population only subtly change total numbers. However, this does not preclude the fact that these small changes may be functionally relevant. Previous studies have reported an onset of behavioral deficits prior to quantifiable intraepidermal fiber loss (Chen et al. 2005; Beiswenger et al. 2007; Obrosova et al. 2007a; Wright et al. 2007). Our results suggest a subpopulation-specific loss masked in the total could account for sensory threshold changes and should be considered in future studies.

Behavioral deficits parallel and correlate with losses in peptidergic innervation

Recently, Crozier et al. (2007) proposed that MrgD activation by its natural ligand, beta-alanine, increases the excitability and signaling of DRG neurons by inhibiting KCNQ/M-type potassium channel currents. Our findings demonstrate a lack of differences in behavioral responses between wildtype and heterozygous MrgD

mice and suggest that, at the very least, biallelic expression of MrgD in nonpeptidergic nociceptors is not required for sensitivity to noxious mechanical, thermal, or chemogenic stimuli. Homozygotes will need to be further evaluated to determine the role, if any, of MrgD function in pain transmission.

The unique molecular, anatomical, and developmental differences between nonpeptidergic and peptidergic DRG neurons suggest they also have functional differences or may communicate divergent information. Indeed, the nature of the input provided by the two primary subpopulations of nociceptors has been the subject of many studies. Nonpeptidergic neurons have longer-duration action potentials and may lead to more reliable transmitter release from terminals (Stucky & Lewin 1999). Nonpeptidergic and peptidergic neurons may differ in their expression of sodium channels, particularly NaV1.8 and NaV1.9 (Fang et al. 2005; Fang et al. 2006). Moreover, nonpeptidergic neurons may be more responsive to ATP via P2X3 expression (Bradbury et al. 1998; Snider and McMahon 1998), but peptidergic neurons are the primary responders to protons and capsaicin (Dirajlal et al. 2003). Although ablation of nonpeptidergic neurons results in transient decreases in thermal and mechanical nociceptive sensitivity (Vulchanova et al. 2001), peptidergic neurons display greater heat sensitivity (Stucky and Lewin 1999). In addition, substance-P-specific ablation significantly attenuates escape responses from nociceptive thermal stimuli (Vierck et al. 2003) and reduces mechanical and thermal hypersensitivity induced by capsaicin, formalin, or nerve injury (Mantyh et al. 1997; Nichols et al. 1999). Finally, nonpeptidergic and peptidergic neurons differ in their vulnerability to

and recovery from spinal nerve ligation (Hammond et al. 2004) and dorsal rhizotomy (Belyantseva and Lewin 1999). Perhaps most revealing was the finding by Braz et al. (2005) that the central neural circuit originated by nonpeptidergic DRG neurons projects to regions of the brain (globus pallidus, amygdala, ventromedial nucleus of the hypothalamus, and bed nucleus of the stria terminalis) that are associated with motivational/affective components of pain, rather than regions accessed by circuits originating with peptidergic neurons and associated with sensory/discriminative aspects of pain.

Our previous work with this model consistently reveals the emergence of behavioral deficits around 4 weeks following diabetes induction (Christianson et al. 2003b, Wright et al., 2004; Johnson et al., 2007). In this study, the behavioral deficits we observed in diabetic mice 4 weeks following diabetes induction were concomitant with the reduction in peptidergic innervation, suggesting the loss of peptidergic fibers may be important in the loss of sensitivity. Furthermore, correlations between behavioral responses and peptidergic innervation at this timepoint were moderate to strong, while correlations with nonpeptidergic innervation were not significant. These behavioral deficits, once present, were maintained as the disease progressed and did not worsen during periods in which nonpeptidergic fibers were degenerating, suggesting that the reduced epidermal innervation by nonpeptidergic axons does not contribute significantly to changes in withdrawal-related cutaneous sensitivity of the animal. These findings support those of Braz et al. (2005) and may indicate that peptidergic input is largely responsible for the discrimination of pain sensation, with

nonpeptidergic input serving only to modulate the principal information provided by the peptidergic. It is reasonable to hypothesize that with nonpeptidergic fibers dominating the input from the periphery, the animals' sensation of the stimulus may have been vague, dampened, or diffused.

This idea that small reductions in the peptidergic axonal number can manifest as significant changes in nociresponsive behaviors is supported by our own previous studies in this same model in which NGF was delivered intrathecally to diabetic mice (Christianson et al. 2003b). These studies revealed that deficits in mechanical and formalin sensitivity were improved by 2 weeks of NGF administration; however, NGF did not statistically increase total PGP-positive axonal innervation of the skin. Based on our current observations that the NGF-responsive population comprises such a small percent of the total skin innervation, it is not surprising that NGF did not change the overall innervation because any subpopulation-specific increases were masked by the large numbers of nonpeptidergic axons.

Belyantseva and Lewin (1999) reported dramatic differences in the ability of peptidergic and nonpeptidergic DRG neurons to regenerate centrally following dorsal rhizotomy, with peptidergic afferents vigorously sprouting into denervated segments compared to poor sprouting by nonpeptidergic afferents. The suggestion that peptidergic afferents are "primed" to better respond during nerve injury, perhaps via higher constitutive GAP43 expression (Verge et al. 1990; Schreyer et al. 1991), is consistent with a model wherein peptidergic inputs provide the primary, discriminative sensory input and require an increased capacity to respond in order to

maintain precise sensory information. A greater plasticity by peptidergic neurons could explain our previous data demonstrating differences in the amount of damage to peptidergic and nonpeptidergic spinal terminals in the STZ-diabetes model (Akkina et al. 2001). In the dorsal horn, peptidergic axons appeared relatively intact whereas nonpeptidergic axons underwent significant damage. The persistence of peptidergic central projections could instead reflect sprouting of these afferents in response to diabetes-induced stress. If the peptidergic subpopulation were vulnerable to metabolic stressors and damaged earlier, then compensatory mechanisms could lead to this sprouting response. Such mechanisms could include target derived neurotrophic support, since increased levels of NGF mRNA has been reported in the footpad skin of diabetic mice (Christianson et al. 2003a) and in the lateral calf muscles of diabetic human patients (Diemel et al. 1999). Experiments to preclude this central overcompensation may prevent the development of chronic pain and shed light on mechanisms that lead to painful versus insensate neuropathy in diabetic patients.

In conclusion, the MrgD-GFP+/- mice provide a new tool to assess subpopulation-specific changes in the composition of epidermal nerve fibers in diabetes and other settings of peripheral nerve damage. Our results add a new layer to the growing differences between peptidergic and nonpeptidergic C-fibers and reveal that these subtypes differ in their sensitivity to metabolic and oxidative stress associated with diabetes. These approaches should lead to improved studies of fiber-type changes in neuropathic and inflammatory pain, as well as sensory loss.

IX. Chapter Five:

Quantitative measures of sensory nerve function and cutaneous nerve fiber density in patients with diabetic neuropathy

1. Abstract

In this study, we evaluated the relationship between specific measures of sensory nerve function and cutaneous nerve fiber density in human patients with diabetic neuropathy. Nondiabetic (n=10) and diabetic (n=19) subjects were evaluated for small nerve fiber function using common neuropathy scales, quantitative sensory testing, and nerve conduction recordings. Additionally, intraepidermal nerve fiber (IENF) and myelinated dermal nerve fiber (MDNF) densities were quantified using PGP9.5 and NF-H immunostaining in 3 mm skin punch biopsies from the distal right lateral calf. In diabetic patients, all sensory measures tested were significantly abnormal compared to nondiabetic controls. Additionally, IENF and MDNF densities were reduced by approximately 65%. The specificity and sensitivity of IENF for detecting neuropathy was 78.9% and 80.0%, respectively; for MDNF density, 84.2% and 90.0%. IENF density was significantly correlated with scores on the MNSI patient questionnaire (MNSI-Pt), heat pain and vibration detection thresholds, and sural and tibial nerve amplitudes. Significant correlations were found between MDNF density and scores on the MNSI-Pt and health professional evaluation (MNSI-HP) and the MDNS; heat pain and vibratory detection thresholds; amplitudes of sural, tibial, and peroneal nerves; latency of the sural nerve; and conduction velocities of tibial and peroneal nerves. Neither IENF nor MDNF densities were correlated with cold detection thresholds. Results from this study extend the validation of IENF density and introduce the utility of MDNF density in assessing diabetic neuropathy.

2. Introduction

In the previous three studies, behavioral deficits resulting from diabetes-induced neuropathy in mice have been examined in relation to cutaneous innervation. While much can learned from studies such as these, modeling human disease in other species is inherently problematic, especially a length-dependent axonal syndrome in an animal with axons at least 10 times shorter than those of humans. The answers to questions begun in the human must ultimately return and be tested there. Consequently, in this study we have continued our investigations into the relationship between neuropathic symptoms and peripheral innervation by examining nerve fibers in skin biopsies of human diabetic patients. Specifically, we have evaluated the relationship between epidermal and dermal nerve fiber densities and quantitative measures of sensory nerve function.

Assessing cutaneous innervation in skin biopsies provides advantages other methods lack. QST assessments of sensory thresholds reveal nerve dysfunction and can even address the type of nerve affected (small vs. large), but cannot indicate whether denervation has occurred or whether fibers are simply damaged but still intact. Adding amplitude measures, particularly of the sural sensory nerve, can further clarify this question, as amplitude is reflective of the number of axons present. However, although small fibers outnumber large fibers by 8:1 in cutaneous sensory nerves (Griffin et al. 2001), electrophysiological measures predominantly expose large rather than small fiber deficits, and this tool cannot indicate the level of small versus large fiber functional loss. Directly examining nerve fibers from skin biopsies

is a much more illuminating approach. To date, skin biopsy has allowed for the direct examination of epidermal fibers in numerous studies exploring small fiber deficits and neuropathies. A particular question has been how well epidermal nerve fiber density reflects the somatosensory status of human patients, and whether the assessment of epidermal nerve fibers in skin biopsies can be validated as an indicator of the presence, type, and severity of neuropathy. Here, we have continued this validation and have also validated an additional measure, the quantification of dermal myelinated nerve fibers. Dermal innervation has been studied very little with regard to neuropathy-induced sensory dysfunction, but its addition to the study of cutaneous innervation allows for the examination of relationships with measures of large fiber dysfunction. We believe the combination of epidermal and dermal nerve fiber quantification in skin biopsies, especially when used in conjunction with QST and electrophysiology, provide a comprehensive tool for the evaluation and study of diabetic neuropathy.

3. Experimental Procedures

Subjects

Diabetic neuropathy subjects were recruited from the patient population at the University of Kansas Medical Center Neuromuscular Clinics between August 2004 and December 2007. Nondiabetic control subjects with no signs or symptoms of central or peripheral nerve disease were recruited at the University of Kansas Medical Center and consisted of university and hospital employees, their relatives, and

community volunteers. No subjects received monetary compensation for study participation. The research and human subjects protocol was approved by the institutional research ethics committee, and written informed consent was obtained from all subjects before inclusion in the study. Exclusion criteria included skin or clotting conditions that would preclude a biopsy or previous diagnosis of non-diabetic neuropathy. Subjects underwent careful clinical neurological history and examination (reflexes, distal strength and vibration sense, position sense, touch and pinprick pain). Nondiabetic control subjects had normal results at clinical neurological examination. All subjects were tested in relation to neuropathic signs using the Michigan Neuropathy Screening Instrument, both the patient version (MNSI-Pt) and the health professional evaluation (MNSI-HP), and the Michigan Diabetic Neuropathy Score (MDNS).

Electrophysiological Measures

Electrophysiological examinations of the peroneal, tibial, and sural nerves were performed in a standard manner using a Neuromax 1004 machine (Xltek, Ontario, Canada) and disposable surface electrodes. The surface temperature of the limbs were maintained at >32 °C (>30.5 °C in the foot). Amplitude, latency, and conduction velocity were measured.

Quantitative Sensory Testing

QST was performed using a TSA-2001 Neurosensory Analyzer Model TSA-II

with the Vibratory Sensory Analyzer VSA-3000 Option. Prior to testing, subjects received standardized instructions. Heat pain detection thresholds were obtained using a limits paradigm in which the patient halted the temperature increase when an uncomfortable sensation was perceived. A reaction time artifact is built in to this measurement, and an average of six stimuli yielded the detection threshold. Thermal thresholds were examined on the dorsum of the right foot using a thermode (30 mm x 30 mm). The adaptation temperature was set at 30-32 °C, and the rate of temperature change ranged from 0.3 °C/sec. and 4.0 °C/sec. Temperature limits were set at 50 °C and 0 °C. For cooling detection thresholds, a constant stimulus staircase algorithm was used that is independent of reaction time. In this paradigm, a coarse step is used initially until the first 'yes' response is achieved. Subsequently, stimuli are decreased by intermediate steps until a 'no' response is given. The subsequent stimuli are increased or decreased by the fine search step, and the direction changes according to the response: increasing for 'no', decreasing for 'yes'. Four negative responses are required after a fine search has begun to terminate the test. Step sizes used were 2.0, 1.0 and 0.2 °C, and the mean of all results during the fine step search stage yielded the detection threshold. Vibratory detection thresholds were examined on the plantar surface of the great toe with the vibratory pin pressing the toe with a consistent pressure of 50 g. A limits paradigm was used in which the vibration amplitude increased until the patient detected and halted the stimulus. The rate of vibratory change varied between 0.1 and 4.0 μm/sec. The mean of six stimuli yielded the detection threshold.

Skin biopsy

The punch skin biopsies were performed using a 3 mm disposable circular punch (Miltex, York, PA) after injection of 2% lidocaine under sterile technique. No suture was used. Biopsies were obtained from the distal part of the right lateral ankle, 8 cm above the lateral malleolus. The skin was directly placed in freshly prepared Zamboni's fixative (pH 7.4) on ice for one hour, rinsed in fresh PBS for 2 days, and then placed in 30% sucrose for cryoprotection for 1 day. Tissue was frozen in Tissue Tek on dry ice and stored at -80 °C until sectioning. Sections of 50 µm were cut perpendicular to the epidermis at -20 °C and stored at -20 °C until immunostaining. Slides were coded in order to carry out analyses in a blinded fashion.

Cutaneous Innervation

Immunohistochemistry

After thawing 5 min. at room temperature, slide-mounted tissue was encircled with a Pap Pen to create a hydrophobic ring (Research Products International). Tissue sections were covered with a blocking solution (0.5% porcine gelatin, 1.5% normal goat serum, 0.5% Triton-X, Superblock buffer (Pierce, Rockford, IL) for 1 hr. at room temperature. For epidermal innervation, a rabbit anti-PGP 9.5 primary antibody (1:400; Ultraclone, Cambridge, UK) and a goat anti-rabbit secondary antibody (Alexa 555; 1:2000; Molecular Probes, Eugene, OR) were used to label all axons in the skin. For myelinated dermal innervation, a rabbit anti-Neurofilament-H primary antibody ([#AB1991], 1:500; Chemicon, Temecula, CA) and a goat anti-

rabbit secondary antibody (Alexa 555; 1:2000; Molecular Probes) were used to visualize all myelinated axons in the dermis. Primaries were diluted in blocking solution and sections incubated overnight at 4°C in a humidified tray. For visualization, sections were washed 3 x 5 min. with PBS followed by incubation for 1 hr with secondary antibodies diluted in PBS. Following three washes with PBS, slides were coverslipped and viewed using fluorescence microscopy.

Epidermal Axon Quantification

Intraepidermal nerve fiber (IENF) density was quantified according to recently published guidelines (Lauria et al. 2005). Three randomly chosen tissue sections were quantified from each biopsy, with at least 150 μm between sections. For each section, three frames of view at 40X magnification were randomly chosen for quantification, and the length of the dermal/epidermal junction in each frame was measured using NIH ImageJ. Only single PGP 9.5+ axons crossing the dermal-epidermal junction were counted, excluding secondary branching and nerve fragments not crossing the dermal-epidermal junction (Lauria et al. 2005). The number of IENF/mm in each of three frames of view was averaged for each section, and the average across all sections provided the mean IENF density for each biopsy.

Myelinated Dermal Axon Quantification

Myelinated dermal nerve fiber (MDNF) density was quantified in three randomly chosen tissue sections from each biopsy, with at least 150 μm between sections. For each section, 3 frames of view at 20X magnification were randomly chosen for quantification. For each frame of view, the dermal area occupied by NF-

H+ immunoreactivity within 100 μm of the dermal-epidermal junction was calculated as a percent of the total area measured using NIH ImageJ. The percent area occupied by NF-H+ immunoreactivity in each of 3 frames of view was summed for each section, as the three frames of view typically spanned the full length of the biopsy section. The average of three sections was used to calculate the mean percent area for each biopsy. The average of all biopsies in a group (nondiabetic vs. diabetic) yielded group means.

Statistical Analysis

To determine whether data sets were normally distributed, the Kolmogorov-Smirnoff Normality Test was used on all measures. Data that passed the normality test were analyzed using parametric statistical tests, and data that failed were analyzed using nonparametric statistical tests.

Differences in mean IENF and MDNF densities were compared between nondiabetic and diabetic groups using an unpaired t-test or the Mann-Whitney Rank Sum test as appropriate. To assess innervation variability, the coefficient of variation (CoV) was calculated for IENF and MDNF density in individual biopsies. CoV was calculated as the standard deviation of three sections from one biopsy divided by the mean of the three sections and multiplied by 100 for each biopsy. The average of CoV measures from all biopsies in a group (nondiabetic vs. diabetic) yielded group CoV means for IENF or MDNF densities. Various cut-offs were explored for both IENFD and MDNFD densities to find a value with maximum sensitivity and

specificity. The final performance characteristics (sensitivity, specificity, efficiency, positive predictive value, negative predictive value) were obtained using the 25th percentile cutoff for IENF control data and the 5th percentile cutoff for MDNF control data.

Differences in mean MSNI-Pt, MNSI-HP, and MDNS scores; heat pain, cold and vibratory detection thresholds; sural nerve latency and amplitude; and peroneal and tibial nerve latencies, amplitudes, and conduction velocities were compared between nondiabetic and diabetic groups using unpaired t-tests or Mann-Whitney Rank Sum tests as appropriate.

Regression analyses were performed to examine the relationship between IENF or MDNF densities and various measures of sensory nerve function. Because age was shown to be significantly correlated with IENF density ($R = -0.409$, $p = 0.0276$ by Spearman's Rank Order Correlation), multiple linear regressions were performed in which IENF density and age were co-independent variables and the sensory measure of interest was the dependent variable. However, age was not correlated with MDNF density ($R = -0.267$, $p = 0.161$ by Pearson's Product Moment Correlation); therefore, simple linear regressions were used to examine the relationship between sensory measures of interest (dependent variable) and MDNF density (independent variable). The strength of correlations was defined as follows: 0.01 – 2.0: little to no correlation; 0.20 – 0.40: weak correlation; 0.40 – 0.60: moderate; 0.60 – 0.80: moderate-to-strong; 0.80 – 0.99: very strong.

4. Results and Figures

Demographic and Clinical Measures

The clinical profiles of the 29 subjects studied are shown in **Table IX-1**. Scores on all three neuropathy scales (MNSI-Pt, MNSI-HP, and MDNS) were significantly higher in diabetic compared to nondiabetic patients, indicating the presence of diabetes-induced neuropathy. To further define the neuropathy of this cohort, patient responses to individual questions on the MNSI-Pt are summarized in **Table IX-2**, and the percent of patients with each symptom is displayed for both nondiabetic and diabetic subjects. Not more than one nondiabetic subject responded positively for any given symptom. The most common item reported by diabetic subjects was muscle cramps (84.2% of diabetic patients), followed by previous diagnosis of neuropathy (78.9%), prickling sensations (73.7%), and burning pain (68.4%). The least common item reported was amputation (5.3%; 1 diabetic patient). Five MNSI-Pt questions related to positive (painful) symptoms (prickling, burning pain, painful feet while walking, allodynia, and increased sensitivity to touch); all diabetic subjects except for two reported experiencing at least one positive symptom, indicating this cohort largely consisted of subjects with painful neuropathy. Three questions related to insensate symptoms (numbness, thermal sensory loss, insensitivity of feet while walking), and 57.9% of diabetic subjects reported experiencing at least one of these symptoms. 100% of patients with an insensate symptom also reported at least one painful symptom; 64.7% of patients reporting a painful symptom expressed at least one insensate symptom.

Table IX-1: Clinical characteristics of nondiabetic and diabetic subjects

	Nondiabetic	Diabetic
Number of subjects	10	19
Male	3	9
Female	7	10
Age (years):		
Median (min/max)	38 (23/58)	56 (39/83)
Symptom duration (years):		
Median (min/max)	N/A	2 (0/10)
MDNS-Pt	0.40 +/- 0.163	5.05 +/- 0.604**
MDNS-HP	0.05 +/- 0.050	3.63 +/- 0.608**
MDNS	0.10 +/- 0.100	8.26 +/- 1.843**

Clinical characteristics of nondiabetic and diabetic subjects. MDNS-Pt, MDNS-HP, and MDNS scores were significantly higher in diabetic compared to nondiabetic subjects. ** $p < 0.0001$ compared to nondiabetic subjects.

Table IX-2: Presence or absence of MNSI-Pt symptoms in nondiabetic and diabetic patients

Symptom (in legs or feet)	Number of patients with symptom (%)	
	Nondiabetic	**Diabetic**
Muscle cramps	1 (10)	16 (84.2)
Previous neuropathy diagnosis	0 (0)	15 (78.9)
Prickling	0 (0)	14 (73.7)
Burning pain	0 (0)	13 (68.4)
Nocturnal worsening	0 (0)	11 (57.9)
Numbness	0 (0)	10 (52.6)
Painful feet when walking	0 (0)	9 (47.4)
Weakness	0 (0)	7 (36.8)
Skin changes (dryness, cracking)	1 (10)	5 (27.8)
Allodynia	0 (0)	4 (21.1)
Thermal sensory loss	1 (10)	3 (16.7)
Increased sensitivity to touch	0 (0)	3 (15.8)
Open sore on foot	1 (10)	3 (15.8)
Insensitivity of feet when walking	1 (10)	3 (15.8)
Amputation	0 (0)	1 (5.3)

The number and percent of patients in each group reporting individual symptoms from the MNSI-Pt. Data expressed as number of patients (percent of patients) in each group.

Epidermal and dermal cutaneous innervation in nondiabetic and diabetic subjects

We used immunohistochemistry to visualize epidermal and dermal innervation in skin-punch biopsies taken from the distal calf of nondiabetic and diabetic patients. PGP9.5 ubiquitously labels all axons, and we used PGP9.5-immunoreactivity to visualize epidermal fibers (**Figure IX-1A, B**), which exclusively consist of unmyelinated c-fibers and an occasional Aδ fiber. These fibers are nociceptors. Individual PGP9.5+ fibers separated from nerve fasicles at the dermal-epidermal junction and penetrated the epidermis, coursing fairly straight among keratinocytes. Limited branching was observed (approximately one branch node every third fiber, data not shown). Fibers in biopsies from diabetic patients often appeared thin and spidery and occasionally contained large swellings, which have been shown to be indicative of further neuropathy worsening (Lauria et al. 2003). Diabetic fibers generally appeared to be fewer rather than shorter, but no fiber length measurements were recorded. Quantitation of intraepidermal nerve fiber (IENF) density revealed an average of 15.5 +/- 2.69 fibers per mm of dermal-epidermal junction in nondiabetic subjects. IENF density was reduced by 65.0% in diabetic patients (5.4 +/- 1.54 fibers/mm; $p < 0.05$; **Figure IX-2A**).

Neurofilament-H (NF-H) is the heavy chain subunit (200 kDa) of neurofilaments, which are type IV intermediate filaments found in myelinated axons. We used antibodies against NF-H to visualize myelinated dermal innervation. Myelinated fibers in the dermis coursed along within mixed nerve fascicles and then extended superficially as small fascicles or individual fibers, many of which

Figure IX-1: IENF and MDNF in nondiabetic and diabetic human subjects

(A,B) PGP9.5-immunoreactive intraepidermal nerve fibers in distal leg biopsies from nondiabetic (A) and diabetic (B) subjects. PGP9.5+ fibers are reduced in diabetic compared to nondiabetic subjects. **(C,D)** NFH-immunoreactive myelinated dermal nerve fibers in distal leg biopsies from nondiabetic (C) and diabetic (D) subjects. Fewer NFH+ fibers were evident in diabetic compared to nondiabetic subjects. Scale bar equals 100 μm for each panel. Arrows indicate immunoreactive nerve fibers.

Figure IX-1

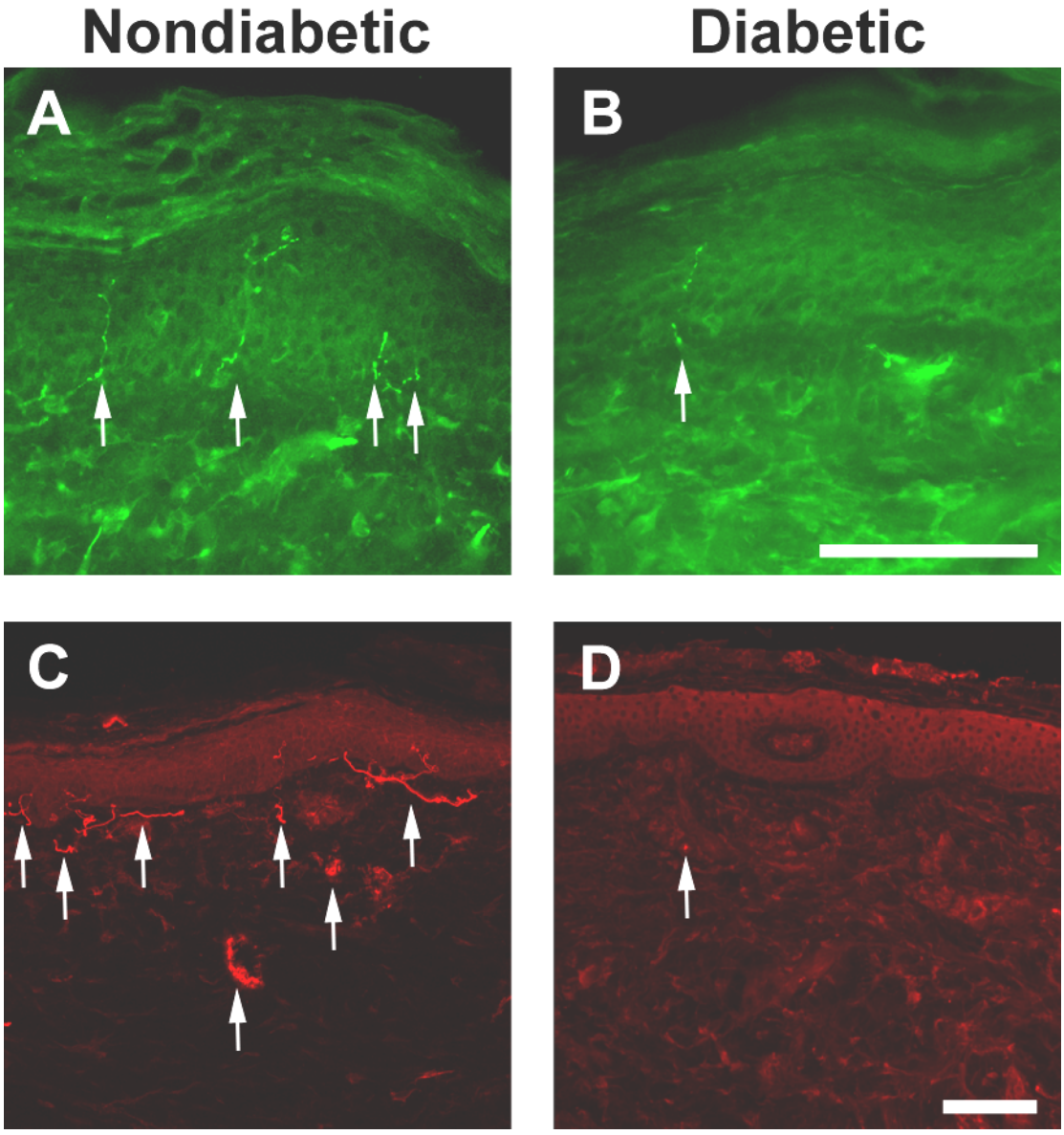

Figure IX-2: Cutaneous innervation is reduced in diabetic patients

(A) Intraepidermal nerve fiber density in biopsies from nondiabetic (closed circles) and diabetic (open circles) subjects. The number of fibers/mm was reduced in diabetic compared to nondiabetic subjects ($p < 0.05$). **(B)** Myelinated dermal nerve fiber density in biopsies from nondiabetic (closed circles) and diabetic (open circles) subjects. The percent area occupied by NF-H staining was reduced in diabetic compared to nondiabetic subjects ($p < 0.05$). Bar = mean value for each group.

Figure IX-2

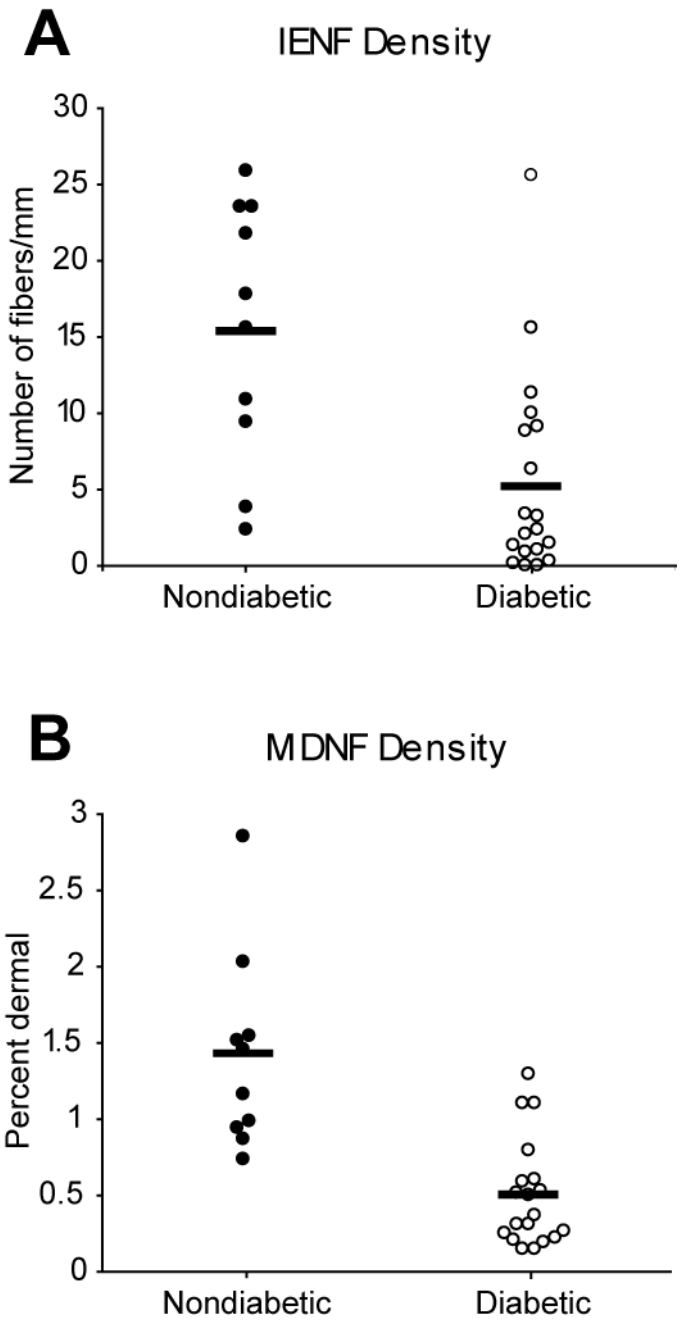
A
IENF Density
Number of fibers/mm
30
25
20
15
10
5
0
Nondiabetic
Diabetic
B
MDNF Density
Percent dermal
3
2.5
2
1.5
1
0.5
0
Nondiabetic
Diabetic

terminated at the dermal/epidermal border. Similar to IENF, myelinated dermal nerve fiber (MDNF) density was markedly reduced in diabetic compared to nondiabetic subjects (**Figure IX-1C, D; 2B**). The percent area occupied by dermal staining was 1.41% +/- 0.203 in nondiabetic subjects and 0.50% +/- 0.80 in diabetic subjects ($p < 0.05$; **Figure 2B**), a 64.6% reduction in MDNF density.

The coefficient of variation (CoV (%) = SD/mean x 100) was calculated for each diabetic and nondiabetic biopsy as an indicator of the amount of innervation variability. For IENF density, biopsies from diabetic patients had a mean CoV of 79.8%, which is 6.3 times more variable than biopsies from nondiabetic patients (12.7%; **Figure IX-3A**). For MDNF density, the CoV of diabetic biopsies (41.3%) was 2.4 times more variable than nondiabetic biopsies (17.6%; **Figure IX-3B**). Overall, these data suggest the innervation of diabetic biopsies is highly variable, both for the group as whole and within individual biopsies. For nondiabetic biopsies, dermal innervation is more variable than epidermal innervation; but for diabetic biopsies, dermal innervation is less variable than epidermal.

Using a cut-off value of 9.4 fibers/mm, the sensitivity of IENF density in discriminating diabetic from nondiabetic subjects was 78.9%, and the specificity in discriminating nondiabetic from diabetic patients was 80%. For MDNF density, using a cut-off value of 0.80%, the sensitivity was 84.2% and the specificity 90.0%. A summary of these and other performance characteristics is given in **Table IX-3**. Overall, the highest sensitivity, specificity, efficiency, positive predictive value, and

Figure IX-3: IENF and MDNF innervation variability in nondiabetic and diabetic biopsies

Coefficient of variation (CoV) of individual biopsies from nondiabetic (closed circles) and diabetic (open circles) patients. **(A)** Biopsies from diabetic patients have increased variability in IENF density compared to biopsies from nondiabetic patients. **(B)** Biopsies from diabetic patients also have increased variability in MDNF density compared to biopsies from nondiabetic patients. Circles represent one biopsy. Bar = mean CoV for each group.

Figure IX-3

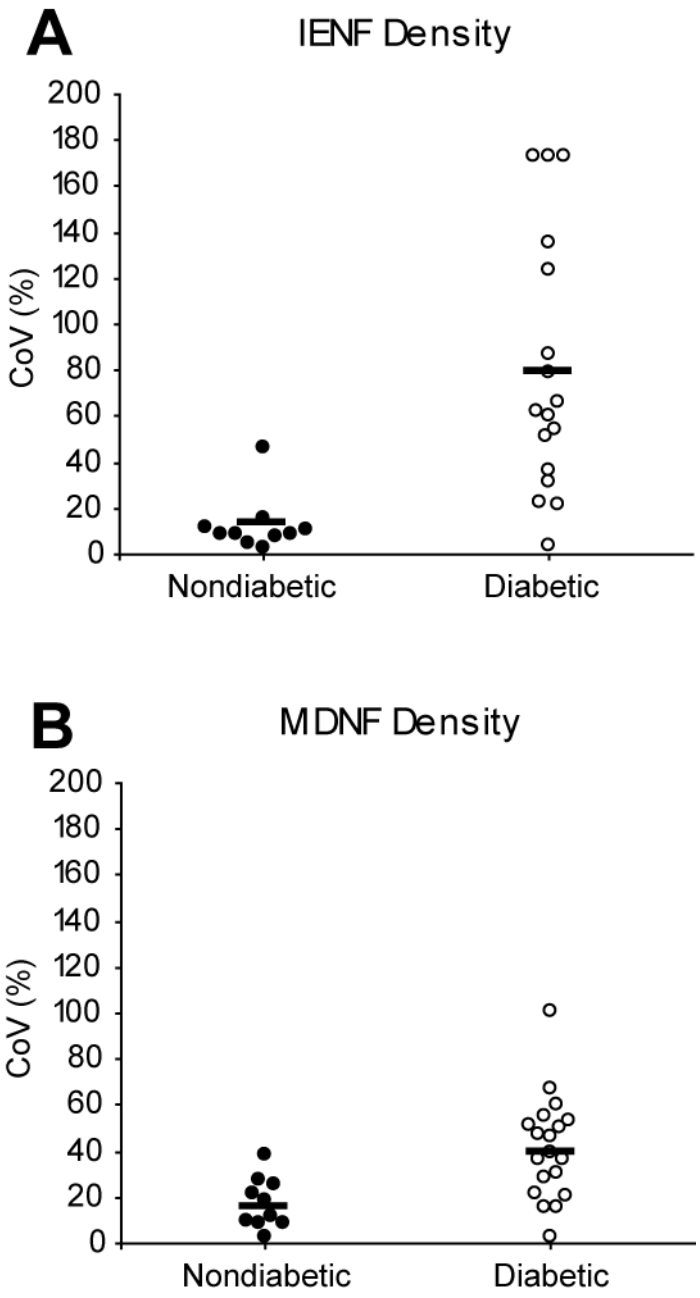
A
IENF Density
CoV (%)
200
180
160
140
120
100
80
60
40
20
0
Nondiabetic
Diabetic
B
MDNF Density
CoV (%)
200
180
160
140
120
100
80
60
40
20
0
Nondiabetic
Diabetic

Table IX-3: Performance Characteristics of IENF and MDNF densities

	Cutoff	Sensitivity	Specificity	Efficiency	Positive Predictive Value (%)	Negative Predictive Value (%)
IENF	9.4 fibers/mm	78.9	80.0	79.3	83.3	63.6
MDNF	0.80%	84.2	90.0	86.2	94.1	75.0

Sensitivity (percentage true positive), specificity (percentage true negative), efficiency (percentage correctly classified), positive predictive value (percentage below cut-off point who truly have neuropathy), and negative predictive value (percentage above cut-off point who truly do not have neuropathy) of IENF and MDNF densities (McArthur et al. 1998).

negative predictive value for diabetic vs. nondiabetic patients were obtained with MDNF density.

Quantitative measures of sensory nerve function

Quantitative sensory testing

Detection thresholds for heat pain, cold, and vibration were assessed in nondiabetic and diabetic subjects. Thresholds for heat pain and vibration detection were determined using a limits algorithm, and thresholds for cold detection used a staircase levels algorithm. Overall, diabetic patients had abnormal sensory thresholds. The heat pain threshold temperatures of diabetic subjects (48.16 °C +/- 0.567) were significantly higher than those of nondiabetic subjects (45.70 °C +/- 0.894; $p < 0.05$; **Figure IX-4A**), indicating a higher temperature deviation from baseline was required for heat pain detection. A bigger drop in temperature from baseline was also required before cold sensation was perceived by diabetic compared to nondiabetic subjects; diabetic patients had reduced cold detection threshold temperatures (22.96 °C +/- 2.213 versus 29.88 °C +/- 0.676; $p < 0.05$; **Figure IX-4B**). For vibration sensation, the average detection threshold was significantly higher in diabetics (62.80 μm +/- 10.225) compared to nondiabetic controls (6.07 μm +/- 2.229; $p < 0.05$; **Figure IX-4C**).

Electrophysiological testing

Nerve conduction studies (amplitude, latency, and nerve conduction velocity) were performed on sural, tibial, and peroneal nerves in both groups of subjects.

Figure IX-4: Measures of sensory nerve function in nondiabetic and diabetic subjects

Sensory thresholds and sensory nerve amplitude of nondiabetic (closed circles) and diabetic (open circles) subjects. **(A)** Heat pain threshold temperatures of diabetic patients were significantly higher than those of nondiabetic control subjects. **(B)** Cold detection threshold temperatures were significantly reduced in diabetic compared to nondiabetic subjects. **(C)** Diabetic patients had significantly higher vibratory detection thresholds compared to nondiabetic subjects. **(D)** Amplitudes of the sural nerve, a purely sensory nerve, were significantly reduced in diabetic compared to nondiabetic subjects. Bar = mean value for each group.

Figure IX-4

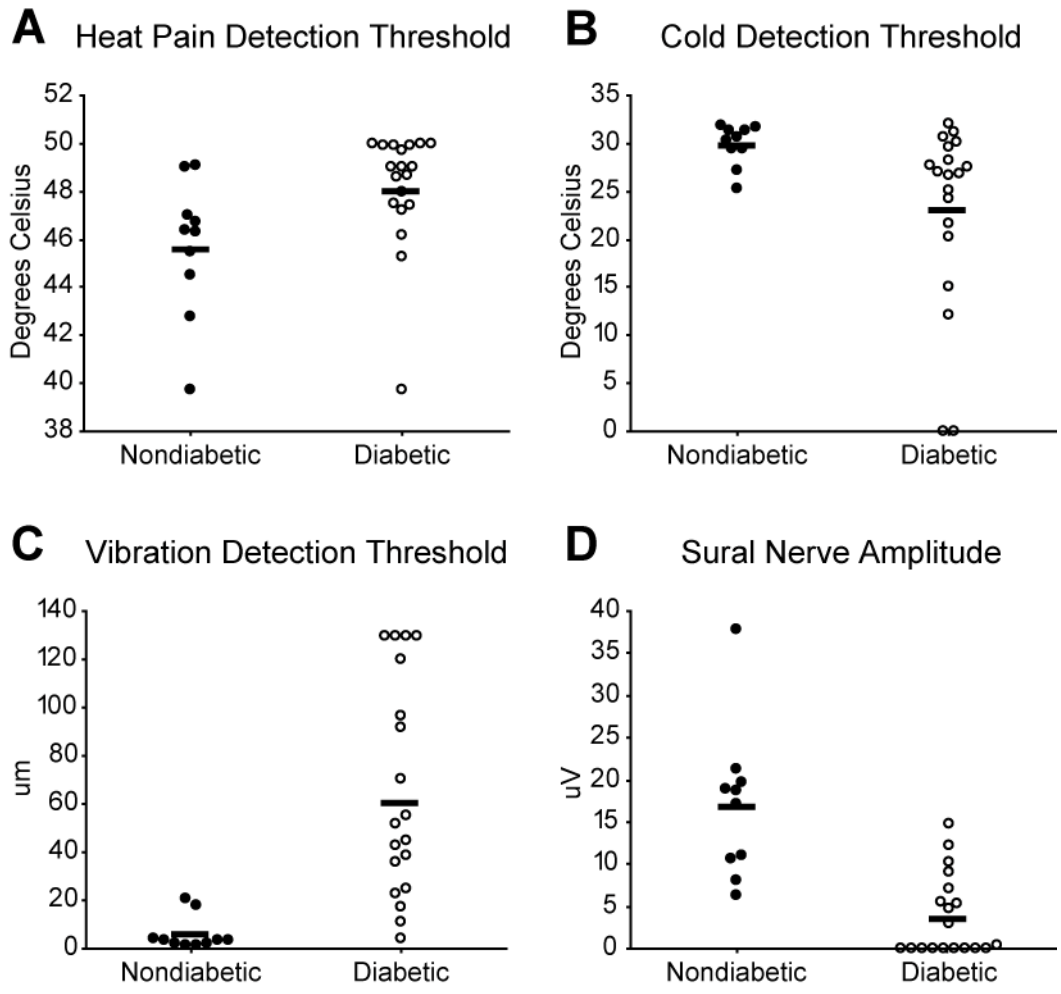
A
Heat Pain Detection Threshold
Degrees Celsius
52
50
48
46
44
42
40
38
Nondiabetic
Diabetic
B
Cold Detection Threshold
Degrees Celsius
35
30
25
20
15
10
5
0
Nondiabetic
Diabetic
C
Vibration Detection Threshold
um
140
120
100
80
60
40
20
0
Nondiabetic
Diabetic
D
Sural Nerve Amplitude
uV
40
35
30
25
20
15
10
5
0
Nondiabetic
Diabetic

Nerve dysfunction was obviously present in diabetic nerves. For example, nerve amplitude is an indicator of the total number of axons present in the nerve, and in diabetic compared to nondiabetic subjects, amplitude was significantly decreased in the peroneal (2.80 mV +/- 0.691 versus 5.58 mV +/- 0.534; $p < 0.05$), tibial (5.62 mV +/- 1.223 versus 12.85 mV +/- 1.784; $p < 0.05$) and sural (3.81 μV +/- 1.107 versus 16.98 μV +/- 2.869; $p < 0.05$; **Figure IX-4D**) nerves. Furthermore, nerve latencies (time from nerve stimulus to nerve firing) were significantly longer in the peroneal (5.78 ms +/- 0.421 versus 4.34 ms +/- 0.235; $p < 0.05$) and sural (6.96 ms +/- 0.684 versus 3.90 ms +/- 0.137; $p = 0.0767$), but not tibial (4.94 ms +/- 0.441 versus 3.97 ms +/- 0.119; $p > 0.05$), nerves of diabetic compared to nondiabetic subjects. Conduction velocity was significantly slower in diabetic compared to nondiabetic subjects for both the peroneal (34.49 m/s +/- 3.343 versus 49.43 m/s +/- 1.515; $p < 0.0001$) and the tibial (33.50 m/s +/- 3.592 versus 50.69 m/s +/- 2.075; $p < 0.0001$) nerves.

Correlation of IENF and MDNF densities with measures of sensory nerve function

To investigate whether the degree of cutaneous innervation paralleled sensory deficits, regression analyses were performed between each measure of sensory nerve function and IENF or MDNF density (**Table IX-4**). Simple linear regression analysis was used to examine relationships with MDNF density. Correlations with IENF density were further refined by multiple linear regression to account for the significant association between age and IENF density.

Table IX-4: Correlation of IENF and MDNF densities with measures of sensory nerve function

	IENF			MDNF		
	r	β	p-value	r	β	p-value
Neuropathy Scales						
MNSI - Pt	0.632	-2.073	0.0014*	0.600	-2.932	0.0006*
MNSI - HP	0.572	-0.105	0.0628	0.586	-2.531	0.0008*
MDNS	0.530	-0.265	0.0980	0.480	-5.710	0.0084*
QST						
Heat Pain Threshold	0.524	-0.164	0.0084*	0.626	-2.772	0.0003*
Cold Threshold	0.659	-0.216	0.1736	0.201	2.690	0.2967
Vibratory threshold	0.630	-2.263	0.0150*	0.552	-40.371	0.0019*
Electrophysiology						
Sural Amplitude	0.762	0.595	0.0003*	0.514	7.333	0.0043*
Sural Latency	0.490	-0.053	0.3758	0.493	-2.191	0.0066*
Tibial Amplitude	0.517	0.303	0.0299*	0.658	6.612	0.0001*
Tibial Latency	0.335	0.020	0.5852	0.137	-0.350	0.4800
Tibial CV	0.525	0.550	0.0956	0.415	10.130	0.0253*
Peroneal Amplitude	0.485	0.065	0.3054	0.389	1.789	0.0373*
Peroneal Latency	0.462	0.031	0.3935	0.317	-0.840	0.0936
Peroneal CV	0.511	0.433	0.1481	0.384	8.455	0.0400*

Linear correlations between measures of sensory nerve function and IENF or MDNF density. Correlations with IENF density were controlled for age (multiple linear regression analysis with IENF density and age as independent variables). As no association between age and MDNF density was found, simple linear regression analyses were sufficient. CV = conduction velocity; r = correlation coefficient; β = regression coefficient (slope of linear regression line). * $p < 0.05$ indicates the independent variable (IENF or MDNF density) can be used to predict the dependent variable (sensory measure of interest)

After controlling for age, significant moderate linear correlations with IENF density were found for heat pain thresholds and tibial nerve amplitudes. Moderate-to-strong correlations were found with MNSI-Pt scores, vibratory detection thresholds, and sural nerve amplitudes. The correlation between IENF density and sural nerve amplitudes was the strongest of the study (0.762). Interestingly, the moderate correlations with the other neuropathy scores (MNSI-HP and MDNS) were not significant; in addition, no significant association was found between IENF density and cold detection thresholds.

MDNF density was significantly associated with all three neuropathy scores, moderately with the MDNS and the MNSI-HP and moderate-to-strongly with the MNSI-Pt. Significant correlations were also found with heat pain thresholds (moderate-to-strong) and vibratory detection thresholds (moderate), but not cold detection thresholds. MDNF density correlated with more electrophysiological measures than IENF density, including sural nerve amplitude (moderate) and latency (moderate), tibial nerve amplitude (moderate-to-strong) and conduction velocity (moderate), and peroneal nerve amplitude (weak) and conduction velocity (weak).

5. Discussion

The validity of skin biopsy in assessing the extent of cutaneous innervation has resulted in cutaneous nerve fiber density becoming a widely used indicator of neuropathy. Here, we evaluated the relationship between various measures of sensory nerve function and cutaneous innervation, both epidermal and dermal. Our

study aimed to further validate IENF density and introduce the utility of MDNF density in assessing diabetic neuropathy.

Clinical characteristics of the cohort

In this study, although gender- and age-matching efforts were made, the control cohort was significantly younger than the diabetics. For the most part the literature shows no age-related decrease in IENF density (McArthur et al. 1998; Vlckova-Moravcova et al. 2008). However, we found an association between age and IENF (but not MDNF) density. This was somewhat accounted for by including age as a covariate in regression analyses with IENF density, but patient recruitment in future studies should include efforts to preclude this confound.

Diabetic subjects in this study were confirmed as neuropathic based on their increased MNSI-Pt, MNSI-HP, and MDNS scores. However, these global scores do not define the type of neuropathy (insensate versus painful), nor do they reveal the symptoms experienced by patients. Therefore, individual items on the MNSI patient questionnaire were examined. This analysis revealed our cohort largely consisted of patients with painful symptoms, indicating interpretation of our results should be limited to painful diabetic neuropathy. Mixed results have been shown with regard to the degree of cutaneous innervation and the presence of painful neuropathic symptoms. Pain has been associated in some studies with intact fiber innervation (Rowbotham and Fields 1996) and in others with decreased fiber density (Lauria et al. 2003); one study found that the relationship depends on the severity of neuropathy

(Sorensen et al. 2006a). Unfortunately, the power of the current study was not sufficient to determine whether IENF or MDNF densities were different between subjects with and without individual painful MNSI-Pt symptoms. Additional subjects are currently being recruited, and further publications will address the utility of IENF and MDNF densities in discriminating between painful and insensate neuropathy.

Interestingly, although painful neuropathy symptoms included allodynia, diabetic patients in this study had reduced, not elevated, sensory detection thresholds. Dysfunction of both small (heat pain, cold) and large (vibration) fibers was demonstrated. Similar findings for patients with pain have been reported by numerous other studies (Shun et al. 2004; Sorensen et al. 2006a and b; Vlckova-Moravcova et al. 2008), and it has been shown that abnormalities in sensory thresholds as measured by QST are not predictive of pain (Sorensen et al. 2006b). It seems that although sensory thresholds reflect the degree of sensory nerve fiber damage and dysfunction, they are not a reliable indicator of the somatosensory status of the patient. Furthermore, deficits in sensory thresholds do not necessarily implicate damage to fibers as a mechanism of pain (Rowbotham and Fields 1996). It must be noted that allodynic or hyperalgesic responses could have been muted by any pain medications taken by diabetic subjects with painful neuropathy.

Cutaneous Innervation

Our findings of reduced IENF densities in diabetic patients echo numerous previous studies. However, although one previous publication has examined sub-

epidermal nerve plexus density in painful neuropathy, the current study is the first to demonstrate specific reductions in myelinated dermal nerve fibers in DN subjects.

The epidermal and dermal innervation of individual biopsies was strikingly more variable in diabetic compared to nondiabetic subjects as measured by coefficients of variation. This variability is a novel finding and likely indicates a degree of innervation patchiness in diabetic biopsies that could be due to select regions of dying-back denervation or regions of hyperinnervation interspersed with regions of denervation. Regardless, how the regions of intact fibers behave when adjacent regions have denervated should be explored as a potential mechanism of pain in the presence of reduced overall peripheral input. Hyperinnervation could result from a last-gasp overproliferation of dying fibers, improper reinnervation of denervating fibers, or an increased branching response. An attractive mechanism, especially in light of results from Chapter VIII, is that a selective subpopulation-specific dying back accounts for the imbalance and patchiness in biopsy innervation, with remaining, unaffected fibers overproliferating or leading to pain sensations through some other means. These potential mechanisms merit future study and should be particularly examined with regard to painful versus insensate neuropathy.

Our sensitivity and specificity values for IENF density are in agreement with previous reports and demonstrate the high diagnostic validity of IENF density for the assessment of diabetic neuropathy. Here, we add MDNF density as another reliable tool for such assessments. Interestingly, the sensitivity and specificity of MDNF density resulted in even higher diagnostic validity than IENF density, suggesting the

evaluation of dermal innervation can be a valuable tool in predicting and evaluating the presence and severity of neuropathy.

IENF and MDNF densities also differed in the degree to which they correlated with various measures of sensory nerve function. Overall, the reduction in both IENF and MDNF densities predicted deficits in some, but not all, measures examined here, and MDNF density correlated with a greater number of measures. The finding that MDNF density correlated with more neuropathy scales than did IENF density implies it is a better predictor of the presence of neuropathy as we measure it in the clinic today. This disparity could also indicate the MNSI-HP and the MDNS include more items assessing large fiber function than the MNSI-Pt.

For sensory thresholds, both IENF and MDNF densities were associated with heat pain and vibration detection, indicating both density measures can predict small and large fiber dysfunction. Interestingly, neither IENF nor MDNF densities correlated with cold detection thresholds, supporting about half of previous reports in a body of literature that is quite mixed with regard to cold sensation and cutaneous innervation. One previous study reported associations with cold sensation in insensate, but not painful patients (Sorensen et al. 2006b). Another report reasoned that relationships between cold sensation and IENF density are found predominantly in studies that evaluate differences between two or more neuropathic groups, rather than studies that include nondiabetic controls (Vlckova-Moravcova et al. 2008). As our study included both a nondiabetic control group and a diabetic cohort largely

consisting of painful subjects, it is perhaps not surprising we found no correlation with cold sensation. Another explanation is that cold sensation is related less to fiber density and more to expression of various receptor molecules important in cold detection (i.e. TRPM8, TRPA1), or to the presence/absence of nerve fiber subpopulations responsible for transmitting specifically cold sensation.

Although both IENF and MDNF densities correlated well with amplitude of the purely sensory sural nerve, as expected, MDNF density additionally correlated with measures of larger, mixed nerves, suggesting it may predict motor fiber deficits as well as large sensory fiber deficits. The lack of correlation with IENF densities suggests electrophysiological measures are not useful in predicting small fiber deficits.

Finally, it is worth noting that all linear correlations between cutaneous innervation and sensory measures were classified as only moderate to moderate-to-strong. Furthermore, based on R^2 values, the greatest amount of variation that could be accounted for by IENF or MDNF density was 58.1% (sural nerve amplitude and IENF density). Thus, other factors must be at work in determining neuropathy scores, sensory thresholds, and electrophysiological recordings. Putative mechanisms to be addressed include the effects of central pain pathways, tissue growth factor expression, nerve fiber branching, pain molecular mediator expression, and subpopulation-specific losses in nerve density.

Overall, this study has corroborated and extended earlier studies with regard to IENF density, as well as introducing MDNF density as a novel tool that can expand the assessment of diabetic neuropathy. Compared to IENF density, evaluation of MDNF density provided added sensitivity and specificity in neuropathy diagnosis, demonstrated less innervation variability in biopsies from diabetic subjects, and correlated better with neuropathy scales and electrophysiological measures. Furthermore, MDNF density can inform on aspects of large fiber complications not revealed by IENF density; for example, studies are currently underway to assess whether myelinated dermal innervation can predict proprioceptive deficits in patients with advanced diabetic neuropathy. Combining IENF and MDNF density measures allows for the concomitant evaluation of small and large fiber complications of diabetes, and the added value of assessing MDNF density should secure its place in the arsenal of tools used to assess diabetic neuropathy.

IX. Chapter Six:

Conclusions

Diabetes-induced nerve damage results in cutaneous denervation, nerve conduction slowing, suppressed regenerative responses, and debilitating sensory symptoms. The increasing prevalence of diabetic neuropathy and the importunate treatment difficulties justify continued study into the mechanisms underlying the disease and the exploration of animal models useful for assessing its complications. One persistent question, in particular, is the focus of this work: how well can the sensory symptoms of diabetic neuropathy be predicted by the disease hallmark, reduced cutaneous innervation? Reductions in cutaneous nerve fiber density are consistently found in both human patients and rodent models of diabetes. The field has exploited this fact, and nerve density measures are increasingly utilized in the diagnosis of neuropathy and have even been proposed as a benchmark for the efficacy of treatments. But the extent to which cutaneous innervation reflects somatosensory status remains a question.

The purpose of this study was to elucidate the relationship between cutaneous nerve fiber density and the presence of neuropathy and its accompanying symptoms, both in animal models and human patients. Part of this goal, by necessity, included validating established animal models and clinical neuropathy measures.

1. Diabetes-induced hypoalgesia is paralleled by attenuated stimulus-induced spinal Fos expression in diabetic mice

This study was originally undertaken to establish the validity of the behavioral data we were obtaining from STZ-induced diabetic C57BL/6 mice, which indicated

an insensate neuropathy. By examining Fos expression in the spinal dorsal horn neurons, and thus indirectly observing the level of peripheral activity, we sought to establish that the behavioral reductions were not artifactual but truly the result of decreased peripheral input. Results from this study demonstrated that: 1) STZ-injected C57BL/6 mice are indeed a model of insensate neuropathy, as evidenced by reduced activation of spinal second order neurons by peripheral afferents. 2) Diabetes-induced losses in pain sensitivity parallel reductions in peripheral input. 3) Improvements in peripheral innervation are not reflected by improvements in nociceptive sensitivity.

2. Selective deficits in nocifensive behavior despite normal cutaneous axon innervation in leptin receptor null mutant (*db/db*) mice

To assess *db/db* type 2 diabetic mice as a model for peripheral neuropathy, we evaluated behavioral responses to noxious stimuli and quantified epidermal and dermal innervation of the hind paw. The principle findings of this study include: 1) Leptin receptor-deficient mice develop selective deficits in nociceptive sensitivity, but are not an explicit model of diabetes-induced distal nerve fiber loss. 2) Behavioral deficits can occur in the absence of quantifiable cutaneous fiber loss.

3. Early loss of peptidergic intraepidermal nerve fibers in an STZ-induced mouse model of insensate diabetic neuropathy

In order to understand the consequences of diabetes on specific subpopulations of nerve fibers, diabetic transgenic MrgD mice expressing GFP in cutaneous nonpeptidergic c-fibers were evaluated for nociceptive sensitivity and subpopulation-specific epidermal innervation. Results from this study revealed several important findings: 1) MrgD mice are an excellent tool for studying subpopulation-specific effects of diabetes or other nerve diseases. 2) Nerve fiber subpopulations can be differentially vulnerable to metabolic disease. Peptidergic fibers are selectively lost early in the progression of STZ-induced insensate diabetic neuropathy in MrgD mice. 3) Diabetes-induced behavioral deficits are more closely associated with the peptidergic, rather than the nonpeptidergic, subpopulation, underscoring the importance of peptidergic fibers in pain sensation.

4. Quantitative sensory measures of small nerve fiber function and cutaneous nerve fiber density in patients with diabetic neuropathy

To continue the validation of nerve fiber quantification in human skin biopsies for assessing diabetic neuropathy, diabetic and nondiabetic subjects were recruited and tested for measures of sensory nerve fiber function and evaluated for cutaneous nerve fiber density. Principle findings include: 1) IENF density is highly sensitive and specific for diagnosing diabetic neuropathy. 2) MDNF density is a novel measure of cutaneous innervation in humans with greater sensitivity and specificity than IENF density and can be used to assess large fiber complications of diabetic neuropathy. 3) IENF and MDNF densities correlate with some, but not all measures

of sensory nerve fiber function, and cannot account for more than 60% of the variability in any given neuropathic symptom.

Serendipitously, in our investigations we have validated or introduced the use of several tools for assessing diabetic neuropathy. For example, STZ-induced diabetic C57BL/6 mice are now confirmed as having reduced peripheral input and progressive somatosensory deficits, and they can be used to study the mechanisms, complications, and treatment of insensate diabetic neuropathy. Of particular interest is comparing this model with STZ-injected A/J mice, which we have recently discovered develop increased behavioral sensitivity to noxious stimuli. Exploring mechanisms underlying the development of insensate versus painful neuropathy in these type 1 models and in the type 2 *db/db* and *ob/ob* mice is the focus of future research. Such mechanisms include differences in insulin support, AGE accumulation and levels of oxidative stress during the progression of diabetic neuropathy.

Secondly, we have demonstrated *db/db* mice develop a relatively limited insensate neuropathy without overt fiber loss. Investigating what causes nerve dysfunction in the absence of dying back could implicate mechanisms developing early in the progression of diabetic neuropathy and may identify treatment strategies to slow or halt the disease before overt axonal degeneration occurs.

Thirdly, MrgD mice have proven useful in establishing the existence subpopulation-specific vulnerabilities in diabetic neuropathy and can now be used to

explore treatment mechanisms targeted at the peptidergic subpopulation. Furthermore, not only can this mechanism possibly explain the development of behavioral deficits in advance of quantifiable overall fiber loss in some diabetic animal models, these studies have also set the stage for future investigations into the role of subpopulation-specific losses in the generation of pain or painless symptoms. It could be that the nature of the disease or injury or the mechanism of damage influence the outcome (painful vs. insensate) of this imbalance. Investigating whether similar imbalances in peripheral input exist in painful models of diabetic neuropathy or in other disease states will be important in future studies, particularly in humans. We are currently exploring whether such a selective fiber imbalance exists in human diabetic painful or painless patients, a task quite limited by the availability of antibodies against subpopulation-specific markers and the greater overlap of nociceptive subpopulations in human skin. Finally, these mice can be used to explore the mechanisms that render these peptidergic and nonpeptidergic subpopulations differentially vulnerable to diabetes. Differences in regenerative capacities, expression of insulin receptors or insulin receptor substrates, oxidative stress responses, and cutaneous trophic factor production are all mechanisms which could identify molecules worthy of investigation.

Finally, we have validated the clinical use of myelinated dermal nerve fiber density in assessing the presence and sensory symptoms of diabetic neuropathy. Furthermore, MDNF can prove useful in evaluating specifically large-fiber complications. For example, studies are currently underway in which the relationship

between myelinated innervation and proproceptive and balance deficits is being explored.

Collectively, these studies demonstrate there are subtle disconnects in the degree to which nerve fiber density indicates pain sensitivity. Cutaneous innervation appears to correlate nicely with signs of sensory dysfunction as it is developing, but not in all cases (*db/db* mice), and the Fos study here and other previous studies (McArthur et al. 2000) have shown this relationship may be altered when treatments are tested to improve either aspect. As an outcome measure, cutaneous innervation may not correlate with the restoration of sensation or cessation of pain. Furthermore, while it appears established that loss of fibers can predict sensory dysfunction as measured by electrophysiological and sensory threshold testing, these are merely indicators that nerve damage exists, and not read-outs of pain per se. There appears to be a difference in evoked pain sensitivity as measured by QST and spontaneous pain sensations experienced by patients, as both can be present in an individual. Therefore, ascertaining whether a particular treatment improved fiber innervation or sensory thresholds is meaningless unless accompanied by some measure of patient symptom report. Future studies should be directed toward addressing this question and determining the ability of cutaneous nerve fiber density to predict pain or lack of pain in human subjects. Furthermore, cutaneous nerve fiber density should not be depended upon in isolation as an outcome measure of treatment efficacy unless this relationship can be established.

XI. Chapter Seven:

References

Abbadie C, Lombard MC, Morain F, Besson JM. Fos-like immunoreactivity in the rat superficial dorsal horn induced by formalin injection in the forepaw: effects of dorsal rhizotomies. Brain Res 1992;578(1-2):17-25.
Abbadie C, Taylor BK, Peterson MA, Basbaum AI. Differential contribution of the two phases of the formalin test to the pattern of c-fos expression in the rat spinal cord: studies with remifentanil and lidocaine. Pain 1997;69(1-2):101-110.
Adeghate E, Rashed H, Rajbandari S, Singh J. Pattern of distribution of calcitonin gene-related Peptide in the dorsal root ganglion of animal models of diabetes mellitus. Ann N Y Acad Sci 2006;1084:296-303.
Akkina SK, Patterson CL, Wright DE. GDNF rescues nonpeptidergic unmyelinated primary afferents in streptozotocin-treated diabetic mice. Exp Neurol 2001;167(1):173-182.
Apfel SC, Arezzo JC, Brownlee M, Federoff H, Kessler JA. Nerve growth factor administration protects against experimental diabetic sensory neuropathy. Brain Res 1994;634(1):7-12.
Apfel SC, Schwartz S, Adornato BT, Freeman R, Biton V, Rendell M, Vinik A, Giuliani M, Stevens JC, Barbano R, Dyck PJ. Efficacy and safety of recombinant human nerve growth factor in patients with diabetic polyneuropathy: A randomized controlled trial. rhNGF Clinical Investigator Group. JAMA 2000;284(17):2215-2221.
Argoff CE, Cole BE, Fishbain DA, Irving GA. Diabetic peripheral neuropathic pain: clinical and quality-of-life issues. Mayo Clin Proc 2006;81(4 Suppl):S3-11.
Basbaum AI, Woolf CJ. Pain. Curr Biol 1999;9(12):R429-431.
Beiswenger K, Calcutt N, Mizisin AP. The time course of structural and functional changes in epidermal nerves of a mouse model of type 1 diabetes. J Peripher Nerv Syst 2007;12(S1):8.
Belmadani S, Palen DI, Gonzalez-Villalobos RA, Boulares HA, Matrougui K. Elevated epidermal growth factor receptor phosphorylation induces resistance artery dysfunction in diabetic db/db mice. Diabetes 2008.
Belyantseva IA, Lewin GR. Stability and plasticity of primary afferent projections following nerve regeneration and central degeneration. Eur J Neurosci 1999;11(2):457-468.
Berryman AM, Maritim AC, Sanders RA, Watkins JB, 3rd. Influence of treatment of diabetic rats with combinations of pycnogenol, beta-carotene, and alpha-lipoic acid on parameters of oxidative stress. J Biochem Mol Toxicol 2004;18(6):345-352.
Berti-Mattera LN, Eichberg J. Phospholipid metabolism and protein phosphorylation in sciatic nerve from genetically diabetic (db/db) mouse. Diabetes 1988;37(12):1703-1707.
Bevan P. Insulin signalling. J Cell Sci 2001;114(Pt 8):1429-1430.
Bianchi R, Buyukakilli B, Brines M, Savino C, Cavaletti G, Oggioni N, Lauria G, Borgna M, Lombardi R, Cimen B, Comelekoglu U, Kanik A, Tataroglu C, Cerami A, Ghezzi P. Erythropoietin both protects from and reverses

experimental diabetic neuropathy. Proc Natl Acad Sci U S A 2004;101(3):823-828.
Bianchi R, Marelli C, Marini P, Fabris M, Triban C, Fiori MG. Diabetic neuropathy in db/db mice develops independently of changes in ATPase and aldose reductase. A biochemical and immunohistochemical study. Diabetologia 1990;33(3):131-136.
Bitar MS, Al-Saleh E, Al-Mulla F. Oxidative stress--mediated alterations in glucose dynamics in a genetic animal model of type II diabetes. Life Sci 2005;77(20):2552-2573.
Bon K, Wilson SG, Mogil JS, Roberts WJ. Genetic evidence for the correlation of deep dorsal horn Fos protein immunoreactivity with tonic formalin pain behavior. J Pain 2002;3(3):181-189.
Boucek P. Advanced Diabetic Neuropathy: A Point of no Return? Rev Diabet Stud 2006;3(3):143-150.
Bradbury EJ, Burnstock G, McMahon SB. The expression of P2X3 purinoreceptors in sensory neurons: effects of axotomy and glial-derived neurotrophic factor. Mol Cell Neurosci 1998;12(4-5):256-268.
Braz JM, Nassar MA, Wood JN, Basbaum AI. Parallel "pain" pathways arise from subpopulations of primary afferent nociceptor. Neuron 2005;47(6):787-793.
Brewster WJ, Diemel LT, Leach RM, Tomlinson DR. Reduced sciatic nerve substance P and calcitonin gene-related peptide in rats with short-term diabetes or central hypoxaemia co-exist with normal messenger RNA levels in the lumbar dorsal root ganglia. Neuroscience 1994;58(2):323-330.
Brozinick JT, Jr., Berkemeier BA, Elmendorf JS. "Actin"g on GLUT4: membrane & cytoskeletal components of insulin action. Curr Diabetes Rev 2007;3(2):111-122.
Cain DM, Khasabov SG, Simone DA. Response properties of mechanoreceptors and nociceptors in mouse glabrous skin: an in vivo study. J Neurophysiol 2001;85(4):1561-1574.
Calcutt NA. Experimental models of painful diabetic neuropathy. J Neurol Sci 2004;220(1-2):137-139.
Calcutt NA, Jolivalt CG, Fernyhough P. Growth factors as therapeutics for diabetic neuropathy. Curr Drug Targets 2008;9(1):47-59.
Calcutt NA, Jorge MC, Yaksh TL, Chaplan SR. Tactile allodynia and formalin hyperalgesia in streptozotocin-diabetic rats: effects of insulin, aldose reductase inhibition and lidocaine. Pain 1996;68(2-3):293-299.
Calcutt NA, Stiller C, Gustafsson H, Malmberg AB. Elevated substance-P-like immunoreactivity levels in spinal dialysates during the formalin test in normal and diabetic rats. Brain Res 2000;856(1-2):20-27.
Cameron NE, Gibson TM, Nangle MR, Cotter MA. Inhibitors of advanced glycation end product formation and neurovascular dysfunction in experimental diabetes. Ann N Y Acad Sci 2005;1043:784-792.

Carson KA, Bossen EH, Hanker JS. Peripheral neuropathy in mouse hereditary diabetes mellitus. II. Ultrastructural correlates of degenerative and regenerative changes. Neuropathol Appl Neurobiol 1980;6(5):361-374.
Casellini CM, Vinik AI. Clinical manifestations and current treatment options for diabetic neuropathies. Endocr Pract 2007;13(5):550-566.
Cesena RM, Calcutt NA. Gabapentin prevents hyperalgesia during the formalin test in diabetic rats. Neurosci Lett 1999;262(2):101-104.
Chalk C, Benstead TJ, Moore F. Aldose reductase inhibitors for the treatment of diabetic polyneuropathy. Cochrane Database System Reviews (Online) 2007(4):CD004572.
Chattopadhyay M, Krisky D, Wolfe D, Glorioso JC, Mata M, Fink DJ. HSV-mediated gene transfer of vascular endothelial growth factor to dorsal root ganglia prevents diabetic neuropathy. Gene Ther 2005;12(18):1377-1384.
Chattopadhyay M, Mata M, Goss J, Wolfe D, Huang S, Glorioso JC, Fink DJ. Prolonged preservation of nerve function in diabetic neuropathy in mice by herpes simplex virus-mediated gene transfer. Diabetelogia 2007;50(7):1550-1558.
Chen H, Charlat O, Tartaglia LA, Woolf EA, Weng X, Ellis SJ, Lakey ND, Culpepper J, Moore KJ, Breitbart RE, Duyk GM, Tepper RI, Morgenstern JP. Evidence that the diabetes gene encodes the leptin receptor: identification of a mutation in the leptin receptor gene in db/db mice. Cell 1996;84(3):491-495.
Chen SR, Pan HL. Hypersensitivity of spinothalamic tract neurons associated with diabetic neuropathic pain in rats. J Neurophysiol 2002;87(6):2726-2733.
Chen YS, Chung SS, Chung SK. Noninvasive monitoring of diabetes-induced cutaneous nerve fiber loss and hypoalgesia in thy1-YFP transgenic mice. Diabetes 2005;54(11):3112-3118.
Chiang MC, Lin YH, Pan CL, Tseng TJ, Lin WM, Hsieh ST. Cutaneous innervation in chronic inflammatory demyelinating polyneuropathy. Neurology 2002;59(7):1094-1098.
Choi JS, Dib-Hajj SD, Waxman SG. Differential slow inactivation and use-dependent inhibition of Nav1.8 channels contribute to distinct firing properties in IB4+ and IB4- DRG neurons. J Neurophysiol 2007;97(2):1258-1265.
Chong MS, Hester J. Diabetic painful neuropathy: current and future treatment options. Drugs 2007;67(4):569-585.
Christianson JA, Riekhof JT, Wright DR. Restorative effects of neurotrophin treatment on diabetes-induced cutaneous axon loss in mice. Exp Neurol 2003;179(2):188-199.
Christianson JA, Ryals JM, Johnson MS, Dobrowsky RT, Wright DE. Neurotrophic modulation of myelinated cutaneous innervation and mechanical sensory loss in diabetic mice. Neuroscience 2007;145(1):303-313.
Christianson JA, Ryals JM, McCarson KE, Wright DE. Beneficial actions of neurotrophin treatment on diabetes-induced hypoalgesia in mice. J Pain 2003;4(9):493-504.
Chua SC Jr, Chung WK, Wu-Peng XS, Zhang Y, Liu SM, Tartaglia L, Leibel RL.

Phenotypes of mouse diabetes and rat fatty due to mutations in the OB (leptin) receptor. Science 1996;271(5251):994–996.
Ciruela A, Dixon AK, Bramwell S, Gonzalez MI, Pinnock RD, Lee K. Identification of MEK1 as a novel target for the treatment of neuropathic pain. Br J Pharmacol 2003;138(5):751-756.
Crozier RA, Ajit SK, Kaftan EJ, Pausch MH. MrgD activation inhibits KCNQ/M-currents and contributes to enhanced neuronal excitability. J Neurosci 2007;27(16):4492-4496.
Daulhac L, Mallet C, Courteix C, Etienne M, Duroux E, Privat AM, Eschalier A, Fialip J. Diabetes-induced mechanical hyperalgesia involves spinal mitogen-activated protein kinase activation in neurons and microglia via N-methyl-D-aspartate-dependent mechanisms. Mol Pharmacol 2006;70(4):1246-1254.
Diemel LT, Cai F, Anand P, Warner G, Kopelman PG, Fernyhough P, Tomlinson DR. Increased nerve growth factor mRNA in lateral calf skin biopsies from diabetic patients. Diabet Med 1999;16(2):113-118.
Dirig DM, Salami A, Rathbun ML, Ozaki GT, Yaksh TL. Characterization of variables defining hindpaw withdrawal latency evoked by radiant thermal stimuli. J Neurosci Methods 1997;76(2):183-191.
Dirajlal S, Pauers LE, Stucky CL. Differential response properties of IB(4)-positive and -negative unmyelinated sensory neurons to protons and capsaicin. J Neurophysiol 2003;89(1):513-524.
Dobretsov M, Ghaleb AH, Romanovsky D, Pablo CS, Stimers JR. Impaired insulin signaling as a potential trigger of pain in diabetes and prediabetes. Int Anesthesiol Clin 2007;45(2):95-105.
Dobrowsky RT, Rouen S, Yu C. Altered neurotrophism in diabetic neuropathy: spelunking the caves of peripheral nerve. J Pharmacol Exp Ther 2005;313(2):485-491.
Dong F, Ren J. Fitness or fatness--the debate continues for the role of leptin in obesity-associated heart dysfunction. Curr Diabetes Rev 2007;3(3):159-164.
Dong F, Zhang X, Yang X, Esberg LB, Yang H, Zhang Z, Culver B, Ren J. Impaired cardiac contractile function in ventricular myocytes from leptin-deficient ob/ob obese mice. J Endocrinol 2006;188(1):25-36.
Drel VR, Mashtalir N, Ilnytska O, Shin J, Li F, Lyzogubov VV, Obrosova IG. The leptin-deficient (ob/ob) mouse: a new animal model of peripheral neuropathy of type 2 diabetes and obesity. Diabetes 2006;55(12):3335-3343.
Ebenezer GJ, Hauer P, Gibbons C, McArthur JC, Polydefkis M. Assessment of epidermal nerve fibers: a new diagnostic and predictive tool for peripheral neuropathies. J Neuropathol Exp Neurol 2007;66(12):1059-1073.
Eckersley L, Ansselin AD, Tomlinson DR. Effects of experimental diabetes on axonal and Schwann cell changes in sciatic nerve isografts. Brain Res Mol Brain Res 2001;92(1-2):128-137.
Fang X, Djouhri L, McMullan S, Berry C, Okuse K, Waxman SG, Lawson SN. trkA is expressed in nociceptive neurons and influences electrophysiological

properties via Nav1.8 expression in rapidly conducting nociceptors. J Neurosci 2005;25(19):4868-4878.
Fang X, Djouhri L, McMullan S, Berry C, Waxman SG, Okuse K, Lawson SN. Intense isolectin-B4 binding in rat dorsal root ganglion neurons distinguishes C-fiber nociceptors with broad action potentials and high Nav1.9 expression. J Neurosci 2006;26(27):7281-7292.
Freshwater JD, Svensson CI, Malmberg AB, Calcutt NA. Elevated spinal cyclooxygenase and prostaglandin release during hyperalgesia in diabetic rats. Diabetes 2002;51(7):2249-2255.
Gabra BH, Benrezzak O, Pheng LH, Duta D, Daull P, Sirois P, Nantel F, Battistini B. Inhibition of type 1 diabetic hyperalgesia in streptozotocin-induced Wistar versus spontaneous gene-prone BB/Worchester rats: efficacy of a selective bradykinin B1 receptor antagonist. J Neuropathol Exp Neurology 2005;64(9):782-789.
Gandhi R, Ryals JM, Wright DE. Neurotrophin-3 reverses chronic mechanical hyperalgesia induced by intramuscular acid injection. J Neurosci 2004;24(42):9405-9413.
Garris DR, Garris BL. Estrogenic restoration of functional pancreatic islet cytoarchitecture in diabetes (db/db) mutant C57BL/KsJ mice: relationship to estradiol localization, systemic glycemia, and persistent hyperinsulinemia. Cell Tissue Res 2005;319(2):231-242.
Genuth S. Insights from the diabetes control and complications trial/epidemiology of diabetes interventions and complications study on the use of intensive glycemic treatment to reduce the risk of complications of type 1 diabetes. Endocr Pract 2006;12 Suppl 1:34-41.
Gibran NS, Jang YC, Isik FF, Greenhalgh DG, Muffley LA, Underwood RA, Usui ML, Larsen J, Smith DG, Bunnett N, Ansel JC, Olerud JE. Diminished neuropeptide levels contribute to the impaired cutaneous healing response associated with diabetes mellitus. J Surg Res 2002;108(1):122-128.
Greer JJ, Ware DP, Lefer DJ. Myocardial infarction and heart failure in the db/db diabetic mouse. Am J Physiol Heart Circ Physiol. 2006;290(1):H146-H153.
Griffin JW, McArthur JC, Polydefkis M. Assessment of cutaneous innervation by skin biopsies. Curr Opin Neurol. 2001;14(5):655-659
Hammond DL, Ackerman L, Holdsworth R, Elzey B. Effects of spinal nerve ligation on immunohistochemically identified neurons in the L4 and L5 dorsal root ganglia of the rat. J Comp Neurol 2004;475(4):575-589.
Herrmann DN, McDermott MP, Henderson D, Chen L, Akowuah K, Schifitto G; North East AIDS Dementia (NEAD) Consortium. Epidermal nerve fiber density, axonal swellings and QST as predictors of HIV distal sensory neuropathy. Muscle Nerve 2004;29(3):420-427.
Herrmann DN, Griffin JW, Hauer P, Cornblath DR, McArthur JC. Epidermal nerve fiber density and sural nerve morphometry in peripheral neuropathies. Neurology 1999;53(8):1634-1640.

Hirai A, Yasuda H, Joko M, Maeda T, Kikkawa R. Evaluation of diabetic neuropathy through the quantitation of cutaneous nerves. J Neurol Sci 2000;172(1):55-62.
Hogan P, Dall T, Nikolov P. Economic costs of diabetes in the US in 2002. Diabetes care 2003;26(3):917-932.
Huang TJ, Sayers NM, Verkhratsky A, Fernyhough P. Neurotrophin-3 prevents mitochondrial dysfunction in sensory neurons of streptozotocin-diabetic rats. Exp Neurol 2005;194(1):279-283.
Hunt SP, Mantyh PW. The molecular dynamics of pain control. Na Rev Neurosci 2001;2(2):83-91.
Hunt SP, Pini A, Evan G. Induction of c-fos-like protein in spinal cord neurons following sensory stimulation. Nature 1987;328(6131):632-634.
Hunt SP, Rossi J. Peptide- and non-peptide-containing unmyelinated primary afferents: the parallel processing of nociceptive information. Philos Trans Royal S Lond B Biol Sci 1985;308(1136):283-289.
Hylden JL, Wilcox GL. Intrathecal morphine in mice: a new technique. Eur J Pharmacol 1980;67(2-3):313-316.
Iizuka S, Suzuki W, Tabuchi M, Nagata M, Imamura S, Kobayashi Y, Kanitani M, Yanagisawa T, Kase Y, Takeda S, Aburada M, Takahashi KW. Diabetic complications in a new animal model (TSOD mouse) of spontaneous NIDDM with obesity. Exp Anim 2005;54(1):71-83.
Jaffey PB, Gelman BB. Increased vulnerability to demyelination in streptozotocin diabetic rats. J Comp Neurol 1996;373(1):55-61.
Johnson MS, Ryals JM, Wright DE. Diabetes-induced chemogenic hypoalgesia is paralleled by attenuated stimulus-induced fos expression in the spinal cord of diabetic mice. J Pain 2007;8(8):637-649.
Kamei J, Hitosugi H, Kasuya Y. Formalin-induced nociceptive responses in diabetic mice. Neurosci Lett 1993;149(2):161-164.
Kamei J, Ohhashi Y, Aoki T, Kasuya Y. Streptozotocin-induced diabetes in mice reduces the nociceptive threshold, as recognized after application of noxious mechanical stimuli but not of thermal stimuli. Pharmacol Biochem Behav 1991;39(2):541-544.
Kamei J, Zushida K, Morita K, Sasaki M, Tanaka S. Role of vanilloid VR1 receptor in thermal allodynia and hyperalgesia in diabetic mice. Eur J Pharmacol 2001;422(1-3):83-86.
Kamenov Z, Higashino H, Todorova M, Kajimoto N, Suzuki A. Physiological characteristics of diabetic neuropathy in sucrose-fed Otsuka Long-Evans Tokushima fatty rats. Methods Find Exp Clinical Pharmacol 2006;28(1):13-18.
Kennedy JM, Zochodne DW. The regenerative deficit of peripheral nerves in experimental diabetes: its extent, timing and possible mechanisms. Brain 2000;123 (Pt 10):2118-2129.
Kennedy JM, Zochodne DW. Impaired peripheral nerve regeneration in diabetes mellitus. J Peripher Nerv Syst 2005;10(2):144-157.

Kennedy WR, Wendelschafer-Crabb G, Johnson T. Quantitation of epidermal nerves in diabetic neuropathy. Neurology 1996;47(4):1042-1048.
Kido Y, Nakae J, Accili D. Clinical review 125: The insulin receptor and its cellular targets. J Clin Endocrinol Metab 2001;86(3):972-979.
Kolavennu V, Zeng L, Peng H, Wang Y, Danesh FR. Targeting of RhoA/ROCK signaling ameliorates progression of diabetic nephropathy independent of glucose control. Diabetes 2008;57(3):714-723.
Koltzenburg M, Stucky CL, Lewin GR. Receptive properties of mouse sensory neurons innervating hairy skin. J Neurophysiol 1997;78(4):1841-1850.
Konrad RJ, Mikolaenko I, Tolar JF, Liu K, Kudlow JE. The potential mechanism of the diabetogenic action of streptozotocin: inhibition of pancreatic beta-cell O-GlcNAc-selective N-acetyl-beta-D-glucosaminidase. Biochem J 2001;356(Pt 1):31-41.
Ktorza A, Bernard C, Parent V, Penicaud L, Froguel P, Lathrop M, Gauguier D. Are animal models of diabetes relevant to the study of the genetics of non-insulin-dependent diabetes in humans? Diabetes Metab 1997;23(Suppl 2):38-46.
Kuzumoto Y, Kusunoki S, Kato N, Kihara M, Low PA. Effect of the aldose reductase inhibitor fidarestat on experimental diabetic neuropathy in the rat. Diabetologia 2006;49(12):3085-3093.
Lauria G, Cornblath DR, Johansson O, McArthur JC, Mellgren SI, Nolano M, Rosenberg N, Sommer C. EFNS guidelines on the use of skin biopsy in the diagnosis of peripheral neuropathy. Eur J Neurol 2005a;12(10):747-758.
Lauria G, Lombardi R. Skin biopsy: a new tool for diagnosing peripheral neuropathy. BMJ 2007;334(7604):1159-1162.
Lauria G, Lombardi R, Borgna M, Penza P, Bianchi R, Savino C, Canta A, Nicolini G, Marmiroli P, Cavaletti G. Intraepidermal nerve fiber density in rat foot pad: neuropathologic-neurophysiologic correlation. J Peripher Nerv Syst 2005b;10(2):202-208.
Lauria G, Morbin M, Lombardi R, Borgna M, Mazzoleni G, Sghirlanzoni A, Pareyson D. Axonal swellings predict the degeneration of epidermal nerve fibers in painful neuropathies. Neurology. 2003;61(5):631-6.
Leinninger GM, Feldman EL. Insulin-like growth factors in the treatment of neurological disease. Endocr Dev 2005;9:135-159.
Leinninger GM, Vincent AM, Feldman EL. The role of growth factors in diabetic peripheral neuropathy. J Peripher Nerv Syst 2004;9(1):26-53.
Li F, Abatan OI, Kim H, Burnett D, Larkin D, Obrosova IG, Stevens MJ. Taurine reverses neurological and neurovascular deficits in Zucker diabetic fatty rats. Neurobiol Dis 2006;22(3):669-676.
Lindfors PH, Voikar V, Rossi J, Airaksinen MS. Deficient nonpeptidergic epidermis innervation and reduced inflammatory pain in glial cell line-derived neurotrophic factor family receptor alpha2 knock-out mice. J Neurosci 2006;26(7):1953-1960.

Low PA, Benrud-Larson LM, Sletten DM, Opfer-Gehrking TL, Weigand SD, O'Brien PC, Suarez GA, Dyck PJ. Autonomic symptoms and diabetic neuropathy: a population-based study. Diabetes Care 2004;27(12):2942-2947.
Low PA, Dotson RM. Symptomatic treatment of painful neuropathy. JAMA 1998;280(21):1863-1864.
Malmberg AB, Chen C, Tonegawa S, Basbaum AI. Preserved acute pain and reduced neuropathic pain in mice lacking PKCgamma. Science 1997;278(5336):279-283.
Mantyh PW, Rogers SD, Honore P, Allen BJ, Ghilardi JR, Li J, Daughters RS, Lappi DA, Wiley RG, Simone DA. Inhibition of hyperalgesia by ablation of lamina I spinal neurons expressing the substance P receptor. Science 1997;278(5336):275-279.
McArthur JC, Stocks EA, Hauer P, Cornblath DR, Griffin JW. Epidermal nerve fiber density: normative reference range and diagnostic efficiency. Arch Neurol 1998;55(12):1513-1520.
McArthur JC, Yiannoutsos C, Simpson DM, Adornato BT, Singer EJ, Hollander H, Marra C, Rubin M, Cohen BA, Tucker T, Navia BA, Schifitto G, Katzenstein D, Rask C, Zaborski L, Smith ME, Shriver S, Millar L, Clifford DB, Karalnik IJ. A phase II trial of nerve growth factor for sensory neuropathy associated with HIV infection. AIDS Clinical Trials Group Team 291. Neurology 2000 54(5):1080-1088.
McCall WD, Tanner KD, Levine JD. Formalin induces biphasic activity in C-fibers in the rat. Neurosci Lett 1996;208(1):45-48.
McCarthy AM, Spisak KO, Brozinick JT, Elmendorf JS. Loss of cortical actin filaments in insulin-resistant skeletal muscle cells impairs GLUT4 vesicle trafficking and glucose transport. Am J Physiol Cell Physiol 2006;291(5):C860-868.
McHugh JM, McHugh WB. Diabetes and peripheral sensory neurons: what we don't know and how it can hurt us. AACN Clin Issues 2004;15(1):136-149.
Metz TO, Alderson NL, Thorpe SR, Baynes JW. Pyridoxamine, an inhibitor of advanced glycation and lipoxidation reactions: a novel therapy for treatment of diabetic complications. Arch Biochem Biophys 2003;419(1):41-49.
Molliver DC, Radeke MJ, Feinstein SC, Snider WD. Presence or absence of TrkA protein distinguishes subsets of small sensory neurons with unique cytochemical characteristics and dorsal horn projections. J Comp Neurol 1995;361(3):404-416.
Molliver DC, Snider WD. Nerve growth factor receptor TrkA is down-regulated during postnatal development by a subset of dorsal root ganglion neurons. J Comp Neurol 1997;381(4):428-438.
Molliver DC, Wright DE, Leitner ML, Parsadanian AS, Doster K, Wen D, Yan Q, Snider WD. IB4-binding DRG neurons switch from NGF to GDNF dependence in early postnatal life. Neuron 1997;19(4):849-861.
Morgado C, Tavares I. C-fos expression at the spinal dorsal horn of streptozotocin-induced diabetic rats. Diabetes Metab Res Rev 2007;23(8):644-652.

Murray CW, Porreca F, Cowan A. Methodological refinements to the mouse paw formalin test. An animal model of tonic pain. J Pharmacol Methods 1988;20(2):175-186.
Nagy JI, Hunt SP. Fluoride-resistant acid phosphatase-containing neurones in dorsal root ganglia are separate from those containing substance P or somatostatin. Neuroscience 1982;7(1):89-97.
Navarro X, Sutherland DE, Kennedy WR. Long-term effects of pancreatic transplantation on diabetic neuropathy. Ann Neurol 1997;42(5):727-736.
Nichols ML, Allen BJ, Rogers SD, Ghilardi JR, Honore P, Luger NM, Finke MP, Li J, Lappi DA, Simone DA, Mantyh PW. Transmission of chronic nociception by spinal neurons expressing the substance P receptor. Science 1999;286(5444):1558-1561.
Norido F, Canella R, Zanoni R, Gorio A. Development of diabetic neuropathy in the C57BL/Ks (db/db) mouse and its treatment with gangliosides. Exp Neurol 1984;83(2):221-232.
Obrosova IG, Ilnytska O, Lyzogubov VV, Pavlov IA, Mashtalir N, Nadler JL, Drel VR. High-fat diet induced neuropathy of pre-diabetes and obesity: effects of "healthy" diet and aldose reductase inhibition. Diabetes 2007;56(10):2598-2608.
Obrosova IG, Xu W, Lyzogubov VV, Ilnytska O, Mashtalir N, Vareniuk I, Pavlov IA, Zhang J, Slusher B, Drel VR. PARP inhibition or gene deficiency counteracts intraepidermal nerve fiber loss and neuropathic pain in advanced diabetic neuropathy. Free Radic Biol Med 2008;44(6):972-981.
Pan CL, Lin YH, Lin WM, Tai TY, Hsieh ST. Degeneration of nociceptive nerve terminals in human peripheral neuropathy. Neuroreport 2001;12(4):787-792.
Pan CL, Tseng TJ, Lin YH, Chiang MC, Lin WM, Hsieh ST. Cutaneous innervation in Guillain-Barré syndrome: pathology and clinical correlations. Brain 2003;126(Pt. 2):386-397.
Paré M, Albrecht PJ, Noto CJ, Bodkin NL, Pittenger GL, Schreyer DJ, Tigno XT, Hansen BC, Rice FL. Differential hypertrophy and atrophy among all types of cutaneous innervation in the glabrous skin of the monkey hand during aging and naturally occurring type 2 diabetes. J Comp Neurol 2007;501(4):543-567.
Pertovaara A, Wei H, Kalmari J, Ruotsalainen M. Pain behavior and response properties of spinal dorsal horn neurons following experimental diabetic neuropathy in the rat: modulation by nitecapone, a COMT inhibitor with antioxidant properties. Exp Neurol 2001;167(2):425-434.
Piercy V, Banner SE, Bhattacharyya A, Parsons AA, Sanger GJ, Smith SA, Bingham S. Thermal, but not mechanical, nociceptive behavior is altered in the Zucker Diabetic Fatty rat and is independent of glycemic status. J Diabetes Complications 1999;13(3):163-169.
Pitel S, Raccah D, Gerbi A, Pieroni G, Vague P, Coste TC. At low doses, a gamma-linolenic acid-lipoic acid conjugate is more effective than docosahexaenoic acid-enriched phospholipids in preventing neuropathy in diabetic rats. J Nutri 2007;137(2):368-372.

Pittenger GL, Ray M, Burcus NI, McNulty P, Basta B, Vinik AI. Intraepidermal nerve fibers are indicators of small-fiber neuropathy in both diabetic and nondiabetic patients. Diabetes Care 2004;27(8):1974-1979.
Polydefkis M, Hauer P, Sheth S, Sirdofsky M, Griffin JW, McArthur JC. The time course of epidermal nerve fibre regeneration: studies in normal controls and in people with diabetes, with and without neuropathy. Brain 2004;127(Pt 7):1606-1615.
Pop-Busui R, Sima A, Stevens M. Diabetic neuropathy and oxidative stress. Diabetes Metab Res Rev 2006;22(4):257-273.
Presley RW, Menetrey D, Levine JD, Basbaum AI. Systemic morphine suppresses noxious stimulus-evoked Fos protein-like immunoreactivity in the rat spinal cord. J Neurosci 1990;10(1):323-335.
Puig S, Sorkin LS. Formalin-evoked activity in identified primary afferent fibers: systemic lidocaine suppresses phase-2 activity. Pain 1996;64(2):345-355.
Purves TD, Tomlinson DR. Diminished transcription factor survival signals in dorsal root ganglia in rats with streptozotocin-induced diabetes. Ann N Y Acad Sci 2002;973:472-476.
Quattrini C, Tavakoli M, Jeziorska M, Kallinikos P, Tesfaye S, Finnigan J, Marshall A, Boulton AJ, Efron N, Malik RA. Surrogate markers of small fiber damage in human diabetic neuropathy. Diabetes 2007;56(8):2148-2154.
Quattrini C, Tesfaye S. Understanding the impact of painful diabetic neuropathy. Diabetes Metab Res Rev 2003;19 Suppl 1:S2-8.
Ringkamp M, Meyer RA. Injured versus uninjured afferents: Who is to blame for neuropathic pain? Anesthesiology 2005;103(2):221-223.
Rittenhouse PA, Marchand JE, Chen J, Kream RM, Leeman SE. Streptozotocin-induced diabetes is associated with altered expression of peptide-encoding mRNAs in rat sensory neurons. Peptides 1996;17(6):1017-1022.
Romanovsky D, Cruz NF, Dienel GA, Dobretsov M. Mechanical hyperalgesia correlates with insulin deficiency in normoglycemic streptozotocin-treated rats. Neurobiol Dis 2006;24(2):384-394.
Rowbotham MC, Fields HL. The relationship of pain, allodynia and thermal sensation in post-herpetic neuralgia. Brain 1996;119 (Pt 2):347-354.
Said G. Diabetic neuropathy--a review. Nature clinical practice 2007;3(6):331-340.
Schmader KE. Epidemiology and impact on quality of life of postherpetic neuralgia and painful diabetic neuropathy. Clin J Pain 2002;18(6):350-354.
Schreyer DJ, Skene JH. Fate of GAP-43 in ascending spinal axons of DRG neurons after peripheral nerve injury: delayed accumulation and correlation with regenerative potential. J Neurosci 1991;11(12):3738-3751.
Shun CT, Chang YC, Wu HP, Hsieh SC, Lin WM, Lin YH, Tai TY, Hsieh ST. Skin denervation in type 2 diabetes: correlations with diabetic duration and functional impairments. Brain 2004;127(Pt 7):1593-1605.
Sima AA, Robertson DM. Peripheral neuropathy in mutant diabetic mouse [C57BL/Ks (db/db)]. Acta Neuropathol 1978;41(2):85-89.

Singleton JR, Smith AG, Bromberg MB. Increased prevalence of impaired glucose tolerance in patients with painful sensory neuropathy. Diabetes Care 2001a;24(8):1448-1453.
Singleton JR, Smith AG, Bromberg MB. Painful sensory polyneuropathy associated with impaired glucose tolerance. Muscle Nerve 2001b;24(9):1225-1228.
Sinnreich M, Taylor BV, Dyck PJ. Diabetic neuropathies. Classification, clinical features, and pathophysiological basis. Neurologist 2005;11(2):63-79.
Smith AG, Russell J, Feldman EL, Goldstein J, Peltier A, Smith S, Hamwi J, Pollari D, Bixby B, Howard J, Singleton JR. Lifestyle intervention for pre-diabetic neuropathy. Diabetes Care 2006;29(6):1294-1299.
Smith AG, Singleton JR. Idiopathic neuropathy, pre-diabetes and the metabolic syndrome. J Neurol Sci 2006;242(1-2):9-14.
Smith AG, Singleton JR. Impaired Glucose Tolerance and Neuropathy. Neurologist 2008;14(1):23-29.
Snider WD, McMahon SB. Tackling pain at the source: new ideas about nociceptors. Neuron 1998;20(4):629-632.
Song KH, Lee WJ, Koh JM, Kim HS, Youn JY, Park HS, Koh EH, Kim MS, Youn JH, Lee KU, Park JY. alpha-Lipoic acid prevents diabetes mellitus in diabetes-prone obese rats. Biochem Biophys Res Comm 2005;326(1):197-202.
Sorensen L, Molyneaux L, Yue DK. Insensate versus painful diabetic neuropathy: the effects of height, gender, ethnicity and glycaemic control. Diabetes Res Clin Pract 2002;57(1):45-51.
Sorensen L, Molyneaux L, Yue DK. The level of small nerve fiber dysfunction does not predict pain in diabetic Neuropathy: a study using quantitative sensory testing. Clin J Pain 2006a;22(3):261-265.
Sorensen L, Molyneaux L, Yue DK. The relationship among pain, sensory loss, and small nerve fibers in diabetes. Diabetes Care 2006b;29(4):883-887.
Stucky CL, Lewin GR. Isolectin B(4)-positive and -negative nociceptors are functionally distinct. J Neurosci 1999;19(15):6497-6505.
Stucky CL, Rossi J, Airaksinen MS, Lewin GR. GFR alpha2/neurturin signalling regulates noxious heat transduction in isolectin B4-binding mouse sensory neurons. J Physiol 2002;545(Pt 1):43-50.
Sullivan KA, Lentz SI, Roberts JL, Jr., Feldman EL. Criteria for creating and assessing mouse models of diabetic neuropathy. Curr Drug Targets 2008;9(1):3-13.
Sumner CJ, Sheth S, Griffin JW, Cornblath DR, Polydefkis M. The spectrum of neuropathy in diabetes and impaired glucose tolerance. Neurology 2003;60(1):108-111.
Suzuki Y, Sato J, Kawanishi M, Mizumura K. Lowered response threshold and increased responsiveness to mechanical stimulation of cutaneous nociceptive fibers in streptozotocin-diabetic rat skin in vitro--correlates of mechanical allodynia and hyperalgesia observed in the early stage of diabetes. Neurosci Res 2002;43(2):171-178.

Takeshita N, Yamaguchi I. Insulin attenuates formalin-induced nociceptive response in mice through a mechanism that is deranged by diabetes mellitus. The J Pharmacol Exp Therapeutics 1997;281(1):315-321.
Tamura Y, Monden M, Suzuki H, Yamada M, Koyama K, Shiomi H. Beneficial action of 2,4,4-trimethyl-3-(15-hydroxypentadecyl)-2-cyclohexen-1-one, a novel long-chain fatty alcohol, on diabetic hypoalgesia and neuropathic hyperalgesia. J Pharmacol Sci 2006;102(2):248-252.
Tesfaye S, Kempler P. Painful diabetic neuropathy. Diabetologia 2005;48(5):805-807.
The Diabetes Control and Complications Trial Research Group. The effect of intensive diabetes therapy on the development and progression of neuropathy. Ann Int Med 1995;122(8):561-568.
Thomas PK. Diabetic neuropathy: mechanisms and future treatment options. J Neurol Neurosurg Psychiatry 1999;67(3):277-279.
Tomiyama M, Furusawa K, Kamijo M, Kimura T, Matsunaga M, Baba M. Upregulation of mRNAs coding for AMPA and NMDA receptor subunits and metabotropic glutamate receptors in the dorsal horn of the spinal cord in a rat model of diabetes mellitus. Brain Res Mol Brain Res 2005;136(1-2):275-281.
Tomlinson DR, Gardiner NJ. Glucose neurotoxicity. Nature reviews 2008;9(1):36-45.
Toth C, Brussee V, Zochodne DW. Remote neurotrophic support of epidermal nerve fibres in experimental diabetes. Diabetelogia 2006;49(5):1081-1088.
Traub RJ, Mendell LM. The spinal projection of individual identified A-delta- and C-fibers. J Neurophysiol 1988;59(1):41-55.
Troger J, Humpel C, Kremser B, Kralinger M, Teuchner B, Kunze C, Philipp W, Kieselbach G. The effect of streptozotocin-induced diabetes mellitus on substance P and calcitonin gene-related peptide expression in the rat trigeminal ganglion. Brain Res 1999;842(1):84-91.
Umapathi T, Tan WL, Loke SC, Soon PC, Tavintharan S, Chan YH. Intraepidermal nerve fiber density as a marker of early diabetic neuropathy. Muscle Nerve 2007;35(5):591-598.
Underwood RA, Gibran NS, Muffley LA, Usui ML, Olerud JE. Color subtractive-computer-assisted image analysis for quantification of cutaneous nerves in a diabetic mouse model. J Histochem 2001;49(10):1285-1291.
Vareniuk I, Pavlov IA, Drel VR, Lyzogubov VV, Ilnytska O, Bell SR, Tibrewala J, Groves JT, Obrosova IG. Nitrosative stress and peripheral diabetic neuropathy in leptin-deficient (ob/ob) mice. Exp Neurol 2007;205(2):425-436.
Verge VM, Tetzlaff W, Richardson PM, Bisby MA. Correlation between GAP43 and nerve growth factor receptors in rat sensory neurons. J Neurosci 1990;10(3):926-934.
Vierck CJ, Jr., Kline RH, Wiley RG. Intrathecal substance p-saporin attenuates operant escape from nociceptive thermal stimuli. Neuroscience 2003;119(1):223-232.
Vincent AM, Edwards JL, Sadidi M, Feldman EL. The antioxidant response as a drug target in diabetic neuropathy. Curr Drug Targets 2008;9(1):94-100.

Vincent AM, Feldman EL. New insights into the mechanisms of diabetic neuropathy. Rev Endocr Metab Disord 2004;5(3):227-236.
Vincent AM, Russell JW, Low P, Feldman EL. Oxidative stress in the pathogenesis of diabetic neuropathy. Endocr Rev 2004;25(4):612-628.
Vinik A, Ullal J, Parson HK, Casellini CM. Diabetic neuropathies: clinical manifestations and current treatment options. Nat Clin Pract Endocrinol Metab 2006;2(5):269-281.
Vinik AI, Park TS, Stansberry KB, Pittenger GL. Diabetic neuropathies. Diabetologia 2000;43(8):957-973.
Vitadello M, Filliatreau G, Dupont JL, Hassig R, Gorio A, Di Giamberardino L. Altered axonal transport of cytoskeletal proteins in the mutant diabetic mouse. J Neurochem 1985;45(3):860-868.
Vlckova-Moravcova E, Bednarik J, Dusek L, Toyka KV, Sommer C. Diagnostic validity of epidermal nerve fiber densities in painful sensory neuropathies. Muscle Nerve 2008;37(1):50-60.
Vulchanova L, Olson TH, Stone LS, Riedl MS, Elde R, Honda CN. Cytotoxic targeting of isolectin IB4-binding sensory neurons. Neuroscience 2001;108(1):143-155.
Walwyn WM, Matsuka Y, Arai D, Bloom DC, Lam H, Tran C, Spigelman I, Maidment NT. HSV-1-mediated NGF delivery delays nociceptive deficits in a genetic model of diabetic neuropathy. Exp Neurology 2006;198(1):260-270.
Wang XL, Zhang HM, Chen SR, Pan HL. Altered synaptic input and GABAB receptor function in spinal superficial dorsal horn neurons in rats with diabetic neuropathy. J Physiol 2007;579(Pt. 3):849-861.
Wang Z, Dohle C, Friemann J, Green BS, Gleichmann H. Prevention of high- and low-dose STZ-induced diabetes with D-glucose and 5-thio-D-glucose. Diabetes 1993;42(3):420-428.
Watson RT, Pessin JE. Intracellular organization of insulin signaling and GLUT4 translocation. Recent Prog Horm Res 2001;56:175-193.
Wellmer A, Misra VP, Sharief MK, Kopelman PG, Anand P. A double-blind placebo-controlled clinical trial of recombinant human brain-derived neurotrophic factor (rhBDNF) in diabetic polyneuropathy. J Peripher Nerv Syst 2001;6(4):204-210.
Woolf CJ, Ma Q. Nociceptors--noxious stimulus detectors. Neuron 2007;55(3):353-364.
Wright DE, Johnson MS, Arnett MG, Smittkamp SE, Ryals JM. Selective changes in nocifensive behavior despite normal cutaneous axon innervation in leptin receptor-null mutant (db/db) mice. J Peripher Nerv Syst 2007;12(4):250-261.
Wright DE, Ryals JM, McCarson KE, Christianson JA. Diabetes-induced expression of activating transcription factor 3 in mouse primary sensory neurons. J Peripher Nerv Syst. 2004;9(4):242-54.
Wu G, Ringkamp M, Hartke TV, Murinson BB, Campbell JN, Griffin JW, Meyer RA. Early onset of spontaneous activity in uninjured C-fiber nociceptors after injury to neighboring nerve fibers. J Neurosci 2001;21(8):RC140.

Wu G, Ringkamp M, Murinson BB, Pogatzki EM, Hartke TV, Weerahandi HM, Campbell JN, Griffin JW, Meyer RA. Degeneration of myelinated efferent fibers induces spontaneous activity in uninjured C-fiber afferents. J Neurosci 2002;22(17):7746-7753.

Yagihashi S, Yamagishi S, Wada R. Pathology and pathogenetic mechanisms of diabetic neuropathy: correlation with clinical signs and symptoms. Diabetes research and clinical practice 2007;77 Suppl 1:S184-189.

Yeomans DC, Pirec V, Proudfit HK. Nociceptive responses to high and low rates of noxious cutaneous heating are mediated by different nociceptors in the rat: behavioral evidence. Pain 1996;68(1):133-140.

Zhuang HX, Wuarin L, Fei ZJ, Ishii DN. Insulin-like growth factor (IGF) gene expression is reduced in neural tissues and liver from rats with non-insulin-dependent diabetes mellitus, and IGF treatment ameliorates diabetic neuropathy. J Pharmacol Exp Ther 1997;283(1):366-374.

Zochodne DW. Neurotrophins and other growth factors in diabetic neuropathy. Semin Neurol 1996;16(2):153-161.

Zylka MJ. Nonpeptidergic circuits feel your pain. Neuron 2005;47(6):771-772.